AD-A082 453 ALASKA UNIV FAIRBANKS INST OF MARINE SCIENCE F/G 4/1
DYNAMICS OF THE EXCHANGE OF CARBON DIOXIDE IN ARCTIC AND SUBARC--ETC(U)
1973 J J KELLEY N00014-67-A-0317-0001
UNCLASSIFIED NL

(15) N00014-67-A-0317-0001
N00014-67-A-0103-0007

(6) DYNAMICS OF THE EXCHANGE OF CARBON DIOXIDE IN ARCTIC AND SUBARCTIC REGIONS

(11) 1973

by

(10) John J. Kelley

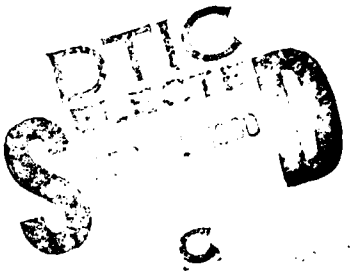

(12) 155

Institute of Marine Science
University of Alaska
Fairbanks, Alaska 99701

405785

NORTH MEADOW LAKE FIELD STATION
BARROW, ALASKA NOVEMBER, 1965

TABLE OF CONTENTS

LIST OF TABLES

LIST OF FIGURES

ABSTRACT

The dynamics of atmospheric carbon dioxide interaction with the ocean and land masses is manifested in subtle fluctuations and long-term trends. Measurements over the past 100 years indicate that there has been an increase in atmospheric carbon dioxide as a result of the industrial revolution. Theories have been formulated on how an increase in carbon dioxide might effect climatic change, but the validity of historical data collection remains uncertain.

A study was initiated in 1961 to accurately document the concentration and variation of carbon dioxide in the arctic atmosphere near Barrow, Alaska. Carbon dioxide in air was measured continuously by infrared analysis and the use of reference gases calibrated with precision in a cooperative program of CO_2 observations in Hawaii and the Antarctic.

Carbon dioxide is increasing at a rate of approximately 0.8 parts per million by volume per year in the arctic atmosphere, as well as in the tropics and the Antarctic. The seasonal variation for CO_2 in the air, greatest in the Arctic and very small in the Antarctic, is primarily a response to photosynthetic utilization of carbon dioxide by terrestrial plants in the northern hemisphere.

Tundra soils in the arctic regions of Alaska overlay permanently frozen ground. During the summer thaw period, the soil is a continual source of CO_2 to the atmosphere and vegetation. Carbon dioxide continues to be released during the rest of the year, however, when the ground is frozen and covered with snow, at temperatures too low for significant biological activity. The phenomena of gas evasion under conditions of freezing soil solution, confirmed by laboratory experimentations, has been attributed to thermally induced physical processes occurring in the spring, generating bursts of high CO_2 levels under the snow in a short time span when the tundra surface begins to warm.

PCO_2 was measured in an arctic lake and pond, which were supersaturated in carbon dioxide with respect to air throughout the period of open water. PCO_2 in the lake water under the ice in the fall and early winter exceeded 12,000 parts per million. In the surface water, PCO_2 was inversely related to wind speed and temperature but directly proportional to sediment

temperature. Calculated evasion rates based on *in situ* observations indicated an average transfer of approximately 0.34 mg CO_2 $cm^{-2}atm^{-1}min^{-1}$ to the atmosphere.

The distribution of carbon dioxide in arctic and subarctic surface seawater was measured in the Barents, Dara, Norwegian and Bering Seas and in the north Atlantic and Pacific Oceans. Lowest levels of PCO_2 undersaturation were observed in the Barents Sea (-160 parts per million).

The north-central and western Bering Sea was generally undersaturated in the late summer, at which time the eastern part was supersaturated. The western part of the north Pacific Ocean was also undersaturated in PCO_2, near equilibrium in the Gulf of Alaska. PCO_2 in the surface waters of the ice-covered Bering Sea and Arctic Ocean were supersaturated in PCO_2 during the winter. Open water constitutes as much as 11% of the pack ice during the winter and could be an important factor in the air-sea transfer of carbon dioxide in the Arctic. When the ice cover is absent for a significant period of time, as in open leads of polyni, CO_2 can be released from the seawater to the atmospheric reservoir.

Along the coastal areas of southwest Alaska, the surface water was highly undersaturated in carbon dioxide. This condition is attributed to biological uptake of CO_2 in nearshore areas. Proximity to land is associated with waters enriched in beneficial nutrients introduced through processes of land drainage and tidal mixing.

Continuous measurements of PCO_2 in the surface seawater was used to delineate the spatial extent of upwelling near the eastern Aleutian Islands. In the surface water near two passes, PCO_2 levels were in excess of 600 parts per million with high nutrient concentrations, high salinity, and low temperature and dissolved oxygen values. Based on maximum recorded CO_2 concentrations (over 600 parts per million), the source of the upwelled water was estimated to be from 200 m depth. From these observations of arctic and subarctic surface waters, it was possible to measure the range of CO_2 partial pressures, which indicate a seasonal variability that may alter the direction of the air-sea exchange of CO_2.

PREFACE

This work presents the results of nearly thirteen years of research on various aspects of carbon dioxide dynamics in the Arctic regions of North America. Much of the information presented here has been published in various scientific journals particularly the subjects in Chapters 3, 4 and 5. From the beginning of this research in 1960-61 the main emphasis has been on the interpretation of the variations and identification of sources and sinks for atmospheric carbon dioxide. Many years of data were required to elucidate the long term trend of CO_2 in the atmosphere and it is not too surprising to note that the results of many of the subprograms were published before the subject which is presented in Chapter 2 - Carbon Dioxide in the Arctic Atmosphere. The Barrow atmospheric carbon dioxide program ended in 1967, it took two more years to assimilate and publish all of the data as a report pending final analysis of all of the reference gases. Research in progress which is not described here is the results on the measurement of CO_2 exchange over the tundra vegetation by a micrometeorological exchange method.

During the course of this long investigation many people have been associated with various phases of the research. Their assistance and advice have been invaluable. Early stages of this work at the Department of Atmospheric Sciences, University of Washington, were encouraged by R. Adm. Charles Thomas (now deceased) and Professors P. E. Church and N. Unterleiner. Continued advice and support at the Institute of Marine Science was generously given by Professor D. W. Hood. I am particularly indebted to Professor C. D. Keeling, Scripps Institution of Oceanography, whose generous assistance and counsel made it possible to establish an accurate analytical base.

Grateful appreciation is given to Mr. Howard Parriott (now deceased) who assisted me in the development and construction of nearly all of the early instrumentation used throughout the investigations of CO_2 in the atmosphere and the sea. Mrs. M. Chaney and Mrs. M. Lorette, at the University of Washington and Mrs. L. Longerich at the University of Alaska provided invaluable assistance with the voluminous data analysis, laboratory and logistic support. My periodic collaboration with Drs. P. K. Park and L. Gordon at the Oregon State University and my collaboration with Dr.

P. Coyne has afforded much success in elucidating processes that govern the distribution and exchange of CO_2.

I am also grateful for the support received at sea aboard the USCG icebreakers *Eastwind, Burton Island* and *Northwind*, the NOAA oceanographic research vessel *Oceanographer* and the University of Alaska's research vessel R/V *Acona*. Particular acknowledgment is given to the Naval Arctic Research Laboratory, Barrow, Alaska, whose director and staff have generously supported nearly all phases of the investigations over the past decade. The success of this research at Barrow would not have been possible without the generous financial support and encouragement from Dr. Max Britton (Arctic Branch, O.N.R.) and Mr. R. McGregor (Arctic Branch, O.N.R.).

Financial support was obtained from the Office of Naval Research Contracts N00014-67-A-0103-0007, NR 307-252 (University of Washington), N00014-67-A-0317-0001 AB, NR 307-308 (University of Alaska), and National Science Foundation Grants GB 8274 and GA 33387 (Bering Sea), and GV 29343 (IBP-Tundra Biome).

I gratefully acknowledge the collaboration with Dr. S. Kanamori and the interest and kind consideration of Professor Y. Kitano, Water Research Laboratory of Nagoya University.

J. J. K.

University of Alaska
Fairbanks
1973

CHAPTER 1

INTRODUCTION

1.1 CO_2 and Climatic Change

Interest in the natural abundance and variations of carbon dioxide associated with theories that would explain world-wide climatic change are not new. More than 100 years ago, the British physicist John Tyndall (1861) made initial attempts to assess the importance of atmospheric CO_2 on the earth's heat balance. He attributed climatic temperature changes to variations in the amount of carbon dioxide in the atmosphere. Tyndall's theory explained that carbon dioxide controls the planet's temperature because carbon dioxide molecules in the air absorb sunlight and emit infrared radiation. By intercepting a part of the infrared radiation that is emitted by the earth's surface and reradiating it back toward the earth, the rate of surface cooling is diminished. At the same time the upper atmosphere is cooled. This radiation is most intense at wavelengths very close to the symmetrical principal absorption band (13-17 microns) of the carbon dioxide spectrum. When the carbon dioxide concentration is sufficiently high the weaker absorption bands become effective. The increased carbon dioxide in the atmosphere presumably would act as a blanket to prevent the escape of the trapped radiation into space. This condition has often been referred to as a "greenhouse" effect.

The Swedish physicist-chemist Arrhenius (1896, 1903) consolidated the theory of the influence of atmospheric carbon dioxide on the basis of extensive calculations. Chamberlin (1897, 1898, 1899), in a series of articles presenting in detail the geological implications of climatic change, further promoted the theory of climatic change.

Eventually, the CO_2 theory lost considerable favor when it was recognized that water vapor was also a strong absorber of infrared radiation (Brooks, 1951). A revival of the theory was given by Plass (1956) who showed that the influence of carbon dioxide on the infrared flux showed that if the carbon dioxide concentration doubles when the average temperature rises 3.6°C and if it falls to half of its present value then the

temperature would fall 3.8°C. Previous estimates of a temperature increase had yielded a higher value for a doubling of CO_2 (Arrhenius, 1896; 6°), and a lower value (Callendar, 1938; 2°), but were shown to be in error. The effect due to water vapor was assumed to be small. In addition, industrial processes and other human activities which release carbon dioxide to the atmosphere may have caused the temperature rise noted at the time of Plass' investigation. Recent recalculations of the role of carbon dioxide on temperature which take into account effects of clouds and water vapor (Kaplan, 1960; Möller, 1963), complex atmospheric interactions (Manabie and Strickler, 1964); Manabie and Wetherald, 1967), and aerosols (Rasool and Schneider, 1971) confirm that the addition of carbon dioxide in the atmosphere does increase the surface temperature, although the rates vary depending on the constraints put on the calculations.

Callendar (1958) indicated that direct measurements of atmospheric carbon dioxide reported since the late nineteenth century tended to show an increase in concentration. Some question existed as to whether the observed trend was statistically significant (Slocum, 1955; Bray, 1959).

1.2 Atmospheric CO_2 Monitoring Programs

Indirect estimates leading to increases in the atmospheric carbon dioxide inventory, based on anthropogenic sources, are discussed by Revelle and Suess (1957) and Bolin and Eriksson (1959). Thus, it soon became evident that it was important to systematically and accurately follow the course of carbon dioxide in the atmosphere primarily to ascertain whether or not carbon dioxide was increasing globally.

Prior to the International Geophysical Year (1956) the results of a great number of carbon dioxide measurements had been published, but it was difficult to find much regularity in these measurements. The mean yearly value from 1800 to 1955 covers a large range from greater than 600 ppm to less than 250 ppm by volume (Fonselius *et al.*, 1956). The highest values occur in the beginning of the 19th century. The scatter in early values probably reflects the technique of analysis available at that time. As techniques improved the scatter tended to decrease to about 300 ppm. Callendar (1938) used the mean values for CO_2 in the atmosphere of Western

Europe to investigate the effect that the industrial revolution may have had on carbon dioxide levels. He obtained a mean value of 294 ppm in the period 1865 to 1900 with no trend, and then an increase to about 322 ppm during the period from 1900 to 1935 (Callendar, 1940, 1949; Buch, 1939a, 1939b). In this last series of data, primarily from samples collected over the north Atlantic and Scandinavia, Buch (1934) and Fonselius and Koroleff (1955) used a comparable technique (Krogh and Brant-Rehberg, 1929) for the microdetermination of CO_2 in the air; a first step vitally needed for any trace gas baseline study.

Carbon dioxide in the atmosphere had been found to be significantly variable (Gelukauf, 1951), as reported by Keeling (1960). However, the degree of variability was much smaller than previously believed (Stepanova, 1952; Slocum, 1955; Fonselius *et al.*, 1956; Callendar, 1958; Bray, 1959).

Settlement of the problem of secular changes in atmospheric carbon dioxide would require a large volume of observational data distributed over an extensive region of space and time. A suitable opportunity to realize such a program presented itself in connection with the plans for a world-wide investigation of trace elements in the atmosphere which were drawn up on the initiative of C.-G. Rossby at the Institute of Meteorology, Stockholm. A resolution to begin these investigations internationally was approved at a conference in Stockholm (Eriksson, 1954) in 1954. A program was begun to monitor the content of carbon dioxide in air in Scandinavia on a regular basis.

The International Geophysical Year provided an opportunity to establish the secular trend of carbon dioxide at sites far removed from areas of industry or rapid development. In 1957 accurate continuous surface measurements of carbon dioxide in air began in Hawaii (Pales and Keeling, 1965) and Antarctica (Brown and Keeling, 1965). Continuous measurements of carbon dioxide relative to dry air were made by infrared analysis, described by Smith (1953), and a series of accurately controlled reference gases determined manometrically (Keeling, 1958) at the Scripps Institution of Oceanography. Continuous measurements of carbon dioxide by infrared analysis using the S.I.O. standards began near Barrow, Alaska in 1961 (Kelley, 1969). These observations continued with few interruptions until

1967 at Barrow and to the present time at Mauna Loa, Hawaii, with flask sampling continuing at the Soviet Pole to the present time.

During the I.G.Y. and post-I.G.Y. programs, measurements of carbon dioxide in the atmosphere were made from air sampled in flasks and later analyzed by infrared analysis and are summarized by Keeling *et al.*, 1968. The samples collected on ships and aircraft established the horizontal and vertical distribution of tropospheric carbon dioxide (Bolin and Keeling, 1963).

Two major features result from all of these observations. There is a seasonal oscillation and long term increase in atmospheric carbon dioxide. Carbon dioxide in the air, above the trade wind inversion at all latitudes between 15° and 25° over the Pacific Ocean, is representative of the observations made in Hawaii (Pales and Keeling, 1965; Keeling *et al.*, 1972). The seasonal oscillation reaches a maximum at sea level in the Arctic (Kelley, 1969). The amplitude diminishes south of Hawaii (Bolin and Keeling, 1963) and a carbon dioxide amplitude is slight in the lower stratosphere (Bolin and Bishof, 1970). The seasonal oscillation in the atmosphere is due to the release and assimilation of carbon dioxide by seasonal plant growth and soil, primarily in polar regions where plant growth is conspicuous, by well defined seasons (Junge and Czeplak, 1968). Owing to a larger land mass and extent of vegetation the oscillation is greater in the northern hemisphere. All of the data from the Antarctic, Hawaii and Arctic show an average annual increase in carbon dioxide concentration of about 0.8 ppm by volume dry air.

Previous observations of carbon dioxide in the high atmosphere had been made by collecting samples in flasks with later analysis by an infrared method. Kelley (1969a) employed direct measurement of carbon dioxide during April 1967 at various altitudes over the Western United States by mounting an infrared gas analyzer in a National Center for Atmospheric Research (NCAR) Beechcraft Queen-Air A-80. The flight path was chosen to include the heavily industrialized Pacific coastal areas and sparsely populated and lightly industrialized interior regions. The sampling elevation was chosen to be close to mid-atmospheric level (500 mb). The carbon dioxide concentration was observed to diminish by 2.2 ppm from the

west coast of the U.S. to north-central Colorado. The results of the analysis accord with monthly average values of the concentration of CO_2 in the atmosphere at 500 mb for the sector 125° to 155°W longitude, and 25° to 70°N latitude, reported from flask data by Bolin and Keeling (1963, Figure 6) for April 1960. Allowing for the annual rate of increase (Pales and Keeling, 1965), the average adjusted carbon dioxide concentration at 500 mb from 33° to 48°N latitude over the Pacific Ocean was 322.3 ppm for 1967. The results also agreed with continuous infrared analyses of carbon dioxide at Barrow, Alaska for April 1967 (323.4 ppm). The data indicate that the concentration of carbon dioxide for the western United States, northern Alaska, and the north Pacific Ocean are essentially the same during the month of April and established the possibility of making accurate routine baseline measurements of CO_2 from aircraft by infrared analysis.

Concurrent with the observations of carbon dioxide in the atmosphere conducted in the United States, were measurements made by Soviet scientists over land along the northern shores of the Black Sea (Bruevich and Liutsarev, 1961) and from the *Vityaz* over the Indian Ocean from 1958-1960 (Liutsarev and Bruevich, 1964). The equipment was essentially the same as that used by Krogh and Brandt Rehberg (1929) and did not produce separate determination with precision better than 4-5%. Some general conclusions could be made from the analysis of the air. The highest carbon dioxide concentration in the atmosphere over the Indian Ocean was observed in the northern tropical air mass. Reduction in carbon dioxide concentrations were sometimes noticed when crossing the fronts of air masses, possibly because of increased vertical exchange in the vicinity of the fronts.

1.3 CO_2 in the Surface Waters of the Sea

Chemical interaction between atmospheric carbon dioxide and the carbonate system was under investigation by the late 19th century. The importance of the ocean as a regulator of atmospheric carbon dioxide was pointed out by Schloesing (1872, 1880).

Although the oceans are ultimately capable of absorbing most of the carbon dioxide produced by man, they may not be able to keep pace with the rate of increase under present conditions.

Observations of the equilibrium partial pressure of carbon dioxide, PCO_2, with respect to air, is essential to understanding how the atmosphere and ocean exchange carbon dioxide. Keeling (1968), in a review of the literature, prepared charts showing the global distribution of PCO_2 in ocean waters. The sources for preparation of these charts covered a span of observations of over 60 years. All of the investigations (Krogh, 1904; Buch, 1939a, 1939b; and Wattenburg, 1933) employed a direct equilibration-titration technique developed by Krogh (1904). These early investigations of PCO_2 including later measurements based on pH and alkalinity were inadequate for observing small changes in PCO_2. With the advent of the I.G.Y. a program was begun to measure PCO_2 by infrared analysis similar to the atmospheric measurements (Takahashi, 1961; Ibert, 1963; Hood *et al.*, 1963; Keeling *et al.*, 1965; Keeling *et al.*, 1968). This method of analysis afforded much higher sensitivity, and large-scale patterns became discernible. The data mostly represent summer conditions and a latitudinal spread from tropical to temperate zones. The Pacific and Atlantic Oceans show belts of high PCO_2 relative to the atmosphere near the equator. In the Indian Ocean during the northern summer PCO_2 diminishes southward from India to 30°S with no high pressure belt near the equator. In the subtropical regions of all oceans PCO_2 tends to be low except in areas where coastal upwelling occurs.

Recent measurements of PCO_2, by infrared analysis in ocean surface waters, have been made in the Atlantic and Pacific Oceans. Rudolf (1971) shows that PCO_2 in the surface water is lower than PCO_2 in the overlying air layer on a transect from the Färoe Islands to Helgoland. The concentration of carbon dioxide in the air and surface ocean water was measured continuously during 1969 between 10°S and 60°N along a constant longitude of 30°S (Buchen, 1971). The data confirmed the latitudinal dependence of carbon dioxide of Atlantic surface water as observed by Wattenberg (Meteor Expedition, 1933) and charted by Keeling (1968). A seasonal trend in PCO_2, north of about 40°N latitude due to vertical mixing of the upper layers of the ocean, was associated with winter cooling of the surface waters. The data suggested that the amount of carbon dioxide in the water had only a minor influence over the meridional distribution of carbon dioxide in the atmosphere.

Akiyama *et al.* (1968) observed PCO_2 in the surface waters of the north Pacific Ocean (January to March, 1967) from measurements of pH, total alkalinity, temperature, and salinity. Values of PCO_2 changed locally from 250 to 400 ppm, with the highest values found in the coastal waters north of Luzon Island, in the area 130°E of the Philippines, and the equatorial region south of 10°N. Lower values were found in the middle latitudes of the open ocean along 137°E. Further observations of PCO_2 were continued in north Pacific ocean water (Akiyama, 1968, 1969a,b). Miyaki and Sugimura (1969) and Sugimura and Hirao (1970) measured carbon dioxide in surface waters and the atmosphere in the Pacific, the Indian and the Antarctic Ocean areas, by infrared analysis. The results showed that the partial pressure in the air was nearly constant (317-325 ppm), while that in the water changed widely (283-512 ppm). The highest values were found in the Antarctic Ocean and the lowest in the Kuroshio region. It was suggested that the high PCO_2 levels in the Antarctic seas were due to higher organic productivity and the vertical mixing between the surface and deep waters (upwelling). The lower PCO_2 found in the Kuroshio region was reputed to be due to the presence of a faint pycnocline and lower phytoplankton primary productivity.

Few data are available for the arctic and subarctic regions. Recent observations of the distribution of carbon dioxide in the surface waters of arctic and subarctic seas (Kelley, 1970; Gordon *et al.*, 1973) will be discussed in later chapters.

The advent of the GEOSECS (Geochemical Ocean Sections Study) provided a program for intensive intercalibration of various methods of analysis for carbon dioxide in surface waters of the ocean (Takahashi *et al.*, 1970), as well as a long term series of measurements of PCO_2 in the worlds oceans. Measurements were made by a pH-alkalinity method, titration method, total carbon dioxide extraction method, gas chromatic method, and PCO_2-total carbon dioxide method. The discrepancies between the results of various methods showed that direct measurements of PCO_2 were 3 to 5% lower than those calculated from pH-alkalinity measurements.

1.4 CO_2 in the Biosphere

Knowledge of the flow of carbon dioxide, within and across the biosphere, is necessary, to understand the variations in carbon dioxide that occur in that atmosphere and the oceans. Vegetation is a buffer of great importance to the CO_2 system. It absorbs and releases carbon dioxide between the atmosphere and the upper layers of the ocean and land. Biological productivity rises with increasing atmospheric carbon dioxide levels (Hutchinson, 1954), but it is difficult to assess the effect adequately because of lack of world-wide long-term observations of primary productivity. Rodin and Basilevic (1968) did, however, provide a very comprehensive set of data concerning the community metabolism of various vegetation types of the world. Included in this study were estimates of biomass (tons per hectare) separated into contributions from separate components of the plant, tree, or shrub. Should the terrestrial biomass be increasing due to the rise in atmospheric carbon dioxide, this may be offset by man's increased use of forest products, agricultural products, and requirements for living space, as well as a resulting deterioration of the biosphere by various forms of pollution. We are already using more than 40% of the total land surface and have reduced the total amount of organic matter in land vegetation by almost one third (SCEP, 1970).

As early as 1959 the possibility of organizing an international research effort was discussed. By 1964 the International Council of Scientific Unions (ICSU) created a Special Committee for the International Biological Program (SCIBP), which was charged with organizing a research effort for investigating the biological basis for productivity and human welfare. The IBP program became a collective venture incorporating many disciplines working under an integrated research concept. Investigations into the transport of carbon within an ecosystem was greatly enhanced.

The proximity of an IBP tundra biome program located on the coast of northern Alaska, where extensive atmospheric carbon dioxide measurements had been previously made (Kelley, 1969), afforded an opportunity to investigate the concentration and exchange of this gas within various components of an Arctic ecosystem. Carbon dioxide dynamics under the

snow, and its exchange across the tundra vegetation, lakes, and ponds, was investigated.

1.5 Purpose and Scope of this Work

Several problems emerged from the results of observations of carbon dioxide in the arctic atmosphere. Although the primary purpose of the original program was to document and follow any secular trend in CO_2 in the near surface atmosphere, it soon became evident that it would be possible to trace anomalous fluctuations in CO_2 to various components of the natural environment: the sea, the vegetation, the soil and tundra surface fresh water bodies. The following chapters will discuss the results of extensive investigations of the variations of carbon dioxide in the atmosphere, the sea, and the flow of carbon among various components of an Arctic ecosystem.

CHAPTER 2

CARBON DIOXIDE IN THE ARCTIC ATMOSPHERE

2.1 Introduction

Important to the evaluation of secular and seasonal trends was the method of measurement and calibration. It was known at the beginning of this investigation that analytical accuracy and precision must be better than 1 ppm by volume if long term trends were to be reliably documented. Furthermore, some plan of research has to be resolved whereby the data collected at one location could be compared with that taken at another with high integrity over a time span of many years. Because of the effects of vegetation, soil, possible pollution plumes and sporadic influx of CO_2 rich air, a continuous measuring program was desirable. Previous analysis of CO_2 in air, by methods similar to those of Krogh and Brandt-Rehberg (1929), where discrete samples of air were collected and brought back to the laboratory for chemical analysis, were totally inadequate for the investigation. Non-dispersive analysis of CO_2 in air, by an infrared technique, was preferable. At the inception of the Arctic atmospheric CO_2 program, observations by continuous infrared analysis were already in progress at Mauna Loa Hawaii and in the Antarctic (Pales and Keeling, 1965, Brown and Keeling, 1965). Non-dispersive infrared analyzers were available, and one was acquired for installation at a remote site near Point Barrow, Alaska (Figure 1) with support from the U.S. Navy at the Arctic Research Laboratory. An accurate and stable means of calibrating the analyzer was required and several commercial sources of reference gases were available, none of which were adequate. This situation has not changed appreciably today. Accurate sets of manometrically determined reference gases were, however, made available by Dr. C. D. Keeling at the Scripps Institution of Oceanography, La Jolla, California. A decision was made to cooperate with the Scripps (S.I.O.) program, and observations began at the Barrow observatory in July 1961.

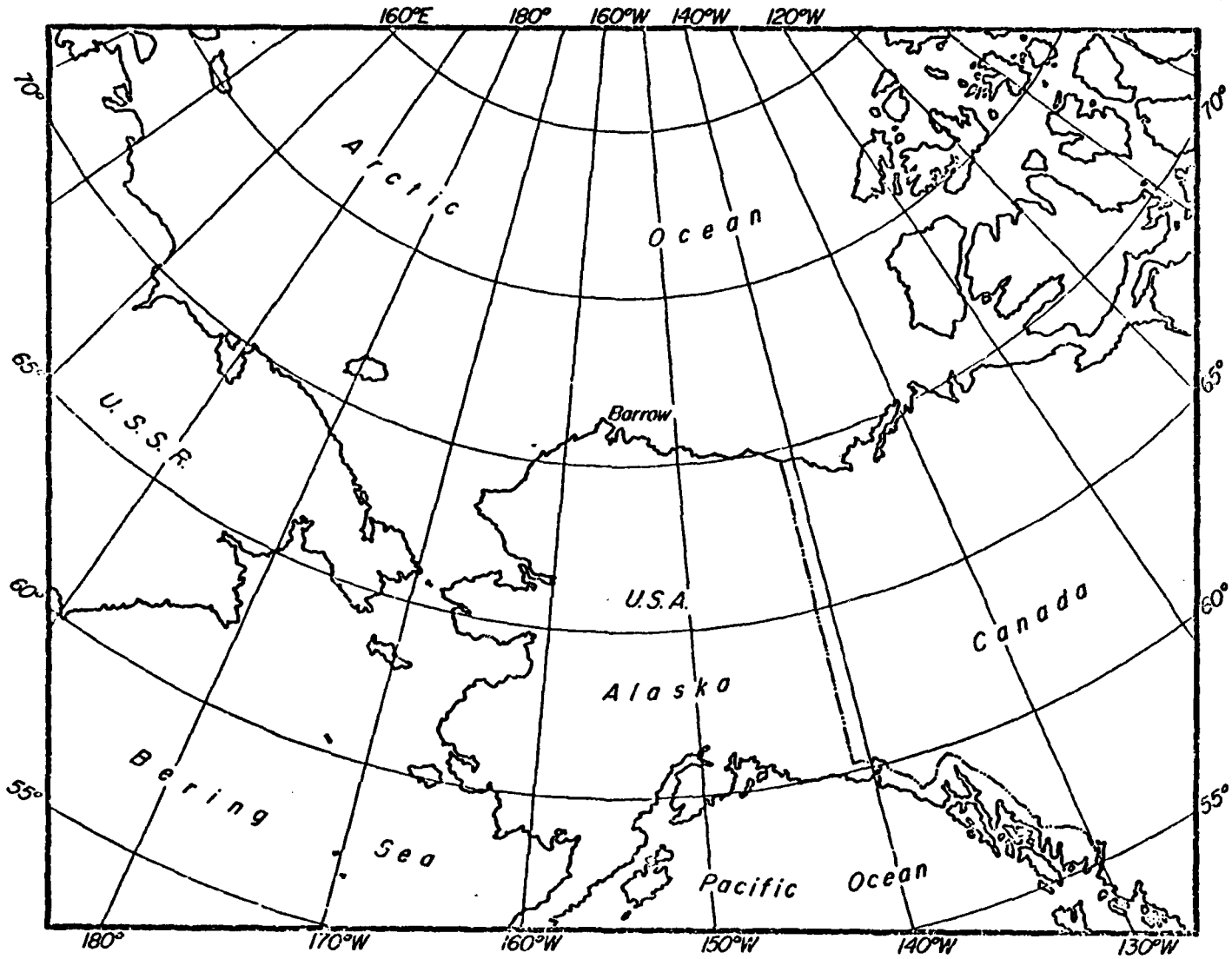

Figure 1. Location of Barrow, Alaska.

2.2 The Observing Site

The sampling site was located on the coast approximately 1.5 km northeast of the Arctic Research Laboratory and maintenance camp. Since the prevailing wind was from the east the site offered an excellent opportunity to utilize camp power, and to be generally upwind of sources of CO_2 generated by human activity. Observations continued until a storm damaged the station in October 1963. The program was discontinued from October 1963 until December 1965, during which a new analyzer was acquired and a new station built. The new station at North Meadow Lake (Figure 2) was located on a raised former beach ridge at an elevation of 9 m above mean sea level. The observation program continued at Barrow until September 1967.

2.3 Regional Climatology

Barrow, Alaska is the most northerly point in the United States (71.3°N, 156.7°W). The climate is arctic maritime and the terrain is generally flat with a ground cover consisting of grasses, sedges, and mosses (Wiggins, 1951). The climate is characterized by low temperatures with a mean annual range of -12.4°C (U.S. National Weather Service Records). The month of February is the coldest and July is the warmest. The minimum temperature drops below freezing (0°C) on nearly 99% of the days while the minimum temperature is below -18°C on 50% of the days (Maykut and Church, 1973). The region is in close proximity to the Arctic Ocean, and is under the moderating influence of polar maritime air which exhibits polar continental characteristics in winter, due to the presence of an almost continuous cover of sea ice. During the summer when the ice pack retreats from the coast, the average air temperature differential between wind directions off the tundra and ocean, is higher than the small differential during the winter. The Barrow coastal area experiences a nearly constant average wind speed (approximately 5.4 meters per second), and wind direction (90°), which comes primarily from the open sea or pack ice.

The Barrow coastal area is dominated by fog and cloud cover reaching a maximum from May through November, and a minimum from December to April.

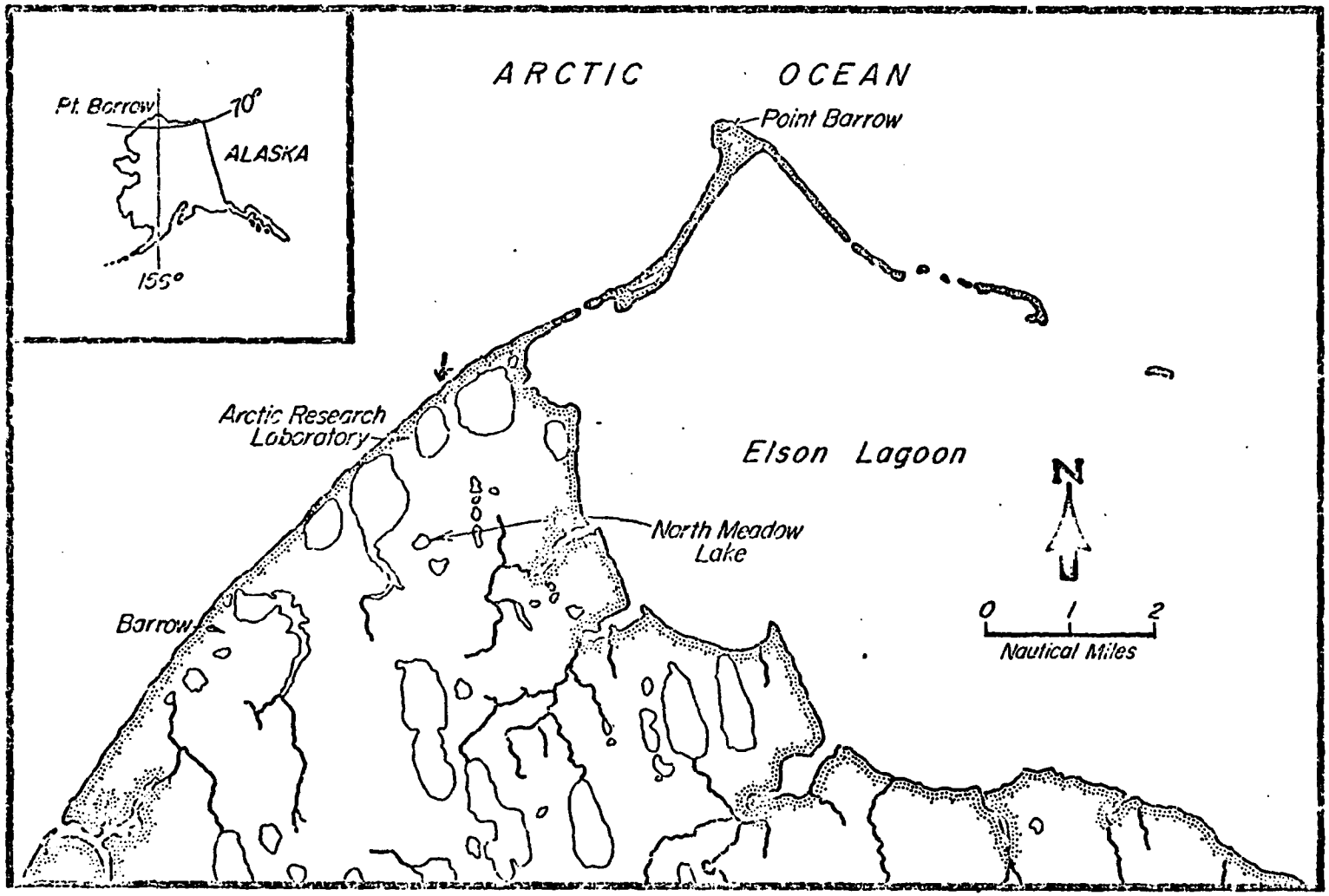

Figure 2. Location of the atmospheric carbon dioxide observation sites near Point Barrow, Alaska.

Annual precipitation is at a maximum July through August, and a minimum from February to March. Snow may occur at any time during the year. However, the summer precipitation is mainly in the form of light rain. Snow cover exhibits a maximum by mid-April. Thawing of the snow on the tundra is generally complete by late June, with refreezing occurring in early September. The radiation climatology and physical processes that occur in the near surface tundra layer and atmosphere, are discussed in detail by Maykut and Church, 1973, Kelley and Weaver, 1969, Weller *et al.*, 1972.

2.4 Experimental Procedures

2.4.1 The Gas Analyzers

Continuous measurements of atmospheric CO_2 relative to dry air were made with non-dispersive infrared analyzers. During the course of these observations, two analyzers of different manufacture (Analytical Systems [Series 700], Pasadena, Calif., 1961-1963; Hartmann and Braun AG [URAS-1], Frankfurt/Main, Germany, 1965-1967) were used. These analyzers were specifically designed for monitoring flowing air.

Both analyzers are similarly designed. They analyze CO_2 in air by measuring the amount of radiation absorbed by CO_2. Carbon dioxide concentration is related to the amount of radiation absorbed.

If an infrared ray with a wave length λ and an intensity I_o of a band at λ and whose molecular concentration is C, passes through the gas over a distance D, the infrared ray will emerge from the gas with the intensity I. The quantitative interdependence of this process is expressed by the Lambert-Beer law,

$$I = I_o e^{-\varepsilon(\lambda)CD}$$

where $\varepsilon(\lambda)$ is a factor which depends on the wavelength of the radiation of the component to be measured and to a lesser extent of the other gases present. Any increase of the concentration C of the measuring component or any extension of the absorption path D increases the absorption. The analyzer distinguishes between the infrared radiation absorbed by

the carbon dioxide, and that absorbed by the air by selective sensitization of the radiation detectors, and by selective filtering of the wavelengths of radiation transmitted through the gas stream to the detectors.

Radiant energy from two matched sources is chopped into pulses by a slotted disc rotated by a synchronous motor (Series 700, 20 Hz, URAS-1, 6.25 Hz). Pulses of infrared energy pass simultaneously through two parallel cells to the detector.

The transducer section of (Series 700) detectors are essentially condenser microphones. The output signals of the two detectors are combined. The polarization of the two detectors is such that these output signals are of opposite sign and will tend to cancel each other. The remaining signal, which is the difference between the output signals of the two detectors, is amplified and rectified by a synchronous rectifier to a DC signal whose magnitude and sign is a measure of the difference in output of the detectors. The DC signal is amplified and used as a correction bias on the polarizing voltage of one of the detectors. The other detector has a constant polarizing voltage. This change in polarizing voltage, changes the magnitude of the output signal from the detector and the magnitude of the difference signal is fed to the amplifier. The phase of the demodulator is chosen so that the effect on the difference signal is to make it smaller. The AC signal fed to the analyzer is zero. The electronic portion of the analyzer is designed to maintain the electrical output signal from the two detectors always equal in magnitude. This is done by adjusting the polarizing voltage of one detector microphone, while the polarizing voltage of the other selector microphone is held constant.

When the air containing carbon dioxide, the infrared absorber, is passed through a cell in one path of radiation but not the other, a lesser amount of radiation reaches the detector in that path, and the output signal of the detector is reduced. The analyzer amplifier will now change the polarizing voltage of one detector, and the amount of the change is a function of the amount of infrared energy absorbed, and the amount of carbon dioxide in the air. The control circuit (see Figure 3) converts the change in polarizing voltage to a millivolt signal suitable to drive a

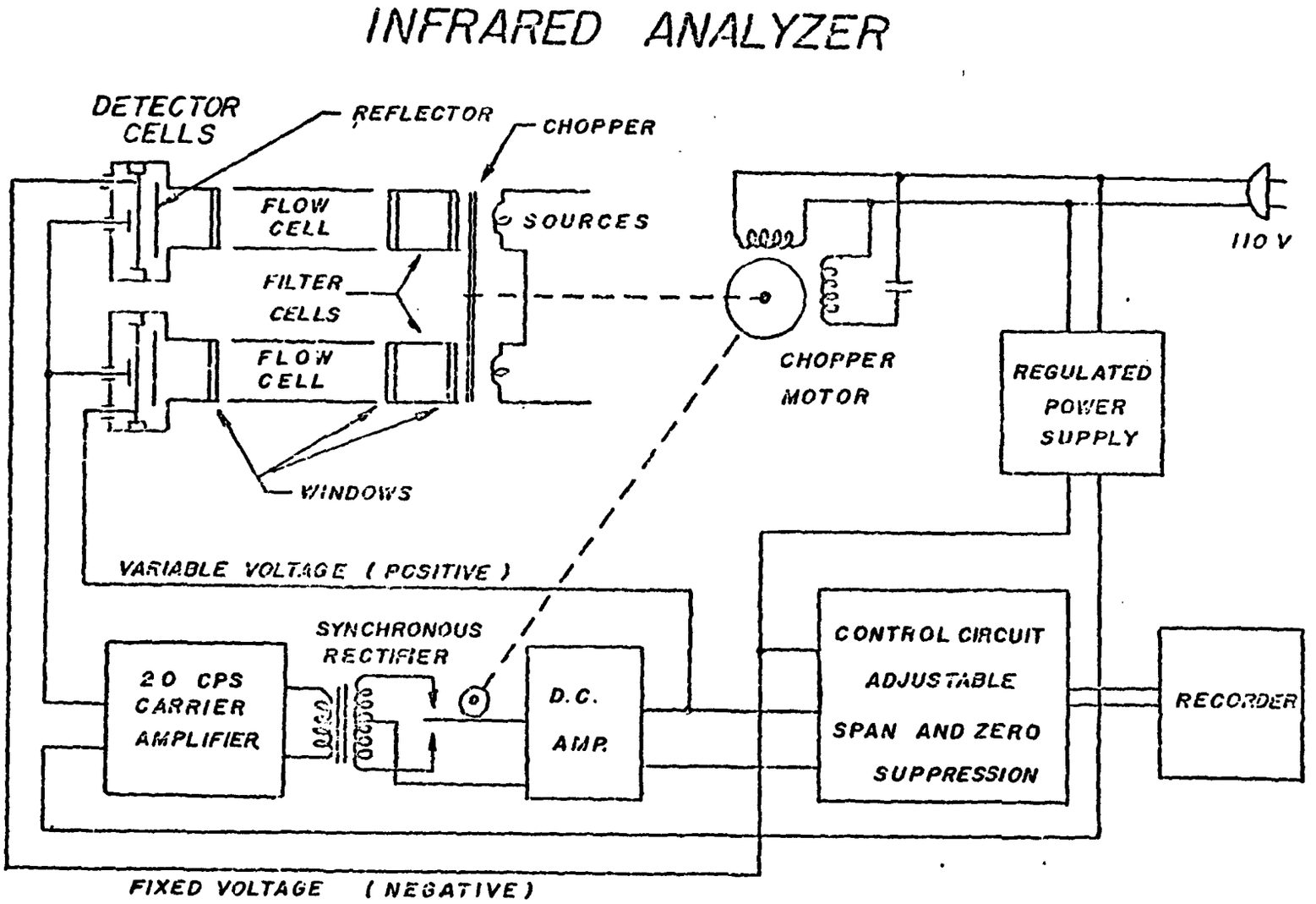

Figure 3. Schematic diagram of the Series 700 nondispersive infrared carbon dioxide analyzer.

potentiometric recorder. The voltage output then becomes a measure of the amount of infrared absorbing gas (CO_2) present in the sample. A block schematic diagram of the Series 700 Analyzer is shown in Figure 3.

Whereas the Series 700 analyzer utilized two detectors, the URAS-1 analyzer had a single detector consisting of two chambers of equal volume separated by a metal diaphragm. Both chambers were filled with a mixture consisting of the measuring component of the gas. For the purpose of static pressure equalization the two chambers are connected by a capillary. The radiated energy absorbed, caused periodic temperature and pressure fluctuations in the two chambers — whose difference produces vibrations in the diaphragm as is done separately in the Series 700. Opposite the diaphragm is a fixed electrode. The diaphragm and electrode together form the diaphragm capacitor which is connected to a DC voltage through a resistance of 10^9 ohms. For both analyzers, the fluctuations of capacitance induced by the vibration of the diaphragm, produce a periodic current which generated an AC voltage through the high resistance and further circuitry, to produce an output signal to a meter or recorder.

2.4.2 The Air System

A Block diagram (Figure 4) shows the air sampling scheme for infrared analysis at Point Barrow. Air is drawn through ports at four levels on an 8 m mast by the edge of the sea and conducted to the analyzer through aluminum tubing (1961-1963) or stainless steel tubing to a 16 m mast (1965-1967). The air then passes through a manifold which can either manually or automatically sample the reference gas or air. The air flow is checked and adjusted by a flow meter and needle valve, to give a flow rate of 0.5 liters per minute at atmospheric pressure. Because water vapor absorbs infrared radiation, it is necessary to remove it from the system or greatly reduce its effects by passing both the air and reference gas through a freezer cell held at -55°F. The regulated flow of reference gas and air, after passing through the freezer cell, goes to the analyzer.

Analysis of the air is accomplished by comparing air with reference gas standards. These standards were purchased from the Scripps Institution of Oceanography, and are similar to those used in their atmospheric carbon dioxide program at the South Pole and at Mauna Loa, Hawaii.

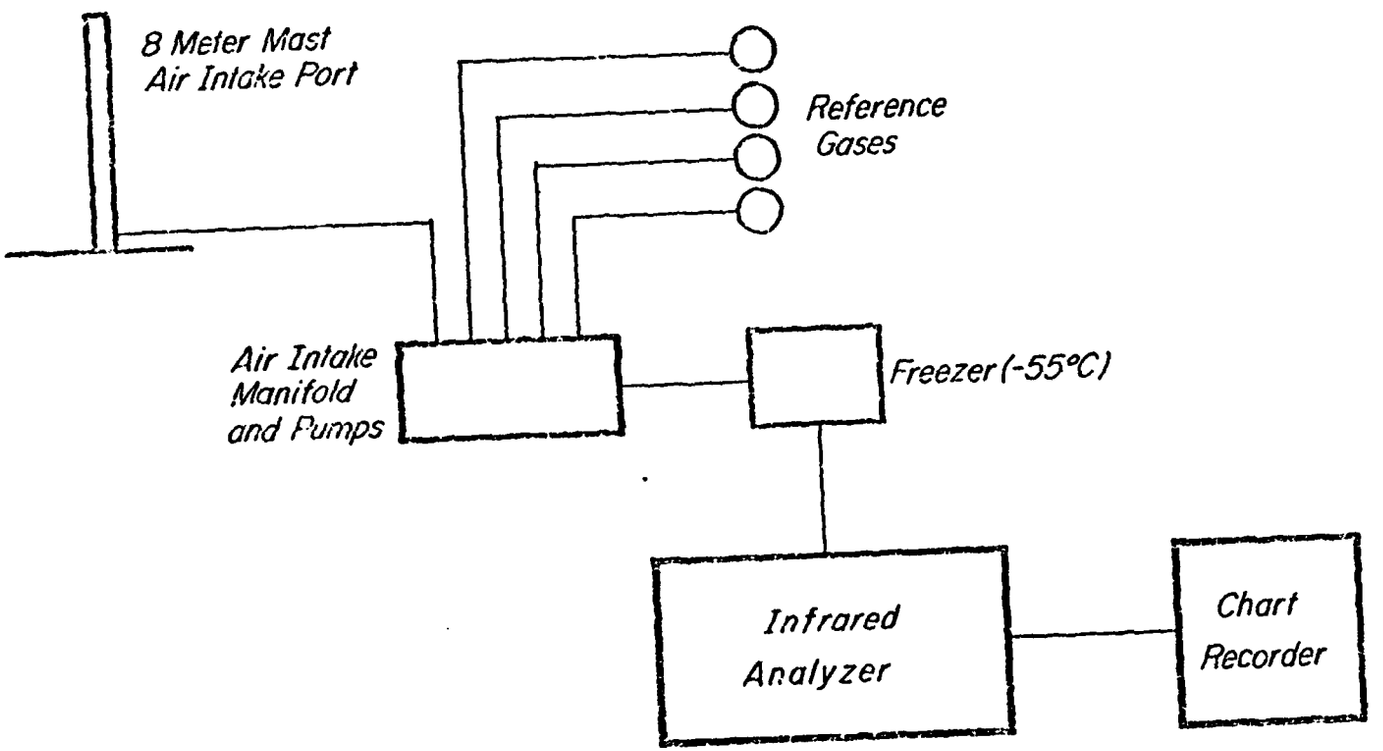

Figure 4. The air sampling system for the analysis of carbon dioxide in air.

2.4.3 Reference Gases

Important to the evaluation of secular and seasonal trends in carbon dioxide, was the method of calibration. All carbon dioxide observations at Barrow were referenced to common standards prepared by C. D. Keeling at the Scripps Institution of Oceanography. Carbon dioxide reference gases (CO_2 diluted in pure dry nitrogen) were provided in high pressure cylinders. A cylinder holds approximately 6000 liters of gas and is filled at an initial pressure of 150 atmospheres. During the course of analysis in the field a typical cycle included 25 minutes for the recording of CO_2 in air and 5 minutes for the recording of a reference gas. Periodically, several replicates of two reference gases of different concentration were run (single set). Three reference gases were used (mutual comparison method) three times during the lifetime of a reference gas cylinder. Under normal operating conditions ten comparisons were made by alternately passing one gas of a pair, and then the other, through the infrared analyzer for five minutes at the same flow rate employed in the air measurements (normally 0.5 liters per minute). As soon as one series of measurements was run, one or both of the cylinders were replaced and another pair of cylinders were compared. The recorder scale difference between two successive traces was read and recorded. The calibrations described, served to establish the recorder sensitivity of the infrared gas analyzer. From these comparisons a recorder scale factor was obtained (RSF). The recorder scale factor and a secondary reference were used to determine the index values of reference gases known as "working references" used in conjunction with air measurements. A schematic diagram of the standardization procedure is shown in Figure 5.

The recorder scale factor, RSF, is defined as the index difference between two reference gases divided by the number of scale divisions between the recorder chart traces for each reference gas with dimensions of ppm by volume per arbitrary scale division. The index of a reference gas is defined as a provisional CO_2 concentration, or volume mixing ratio, in ppm based on the initial analysis of the gas. Index units are used here, in the event that a calibration program is chosen where the reference gases will be analyzed by the supplier initially, and again when the

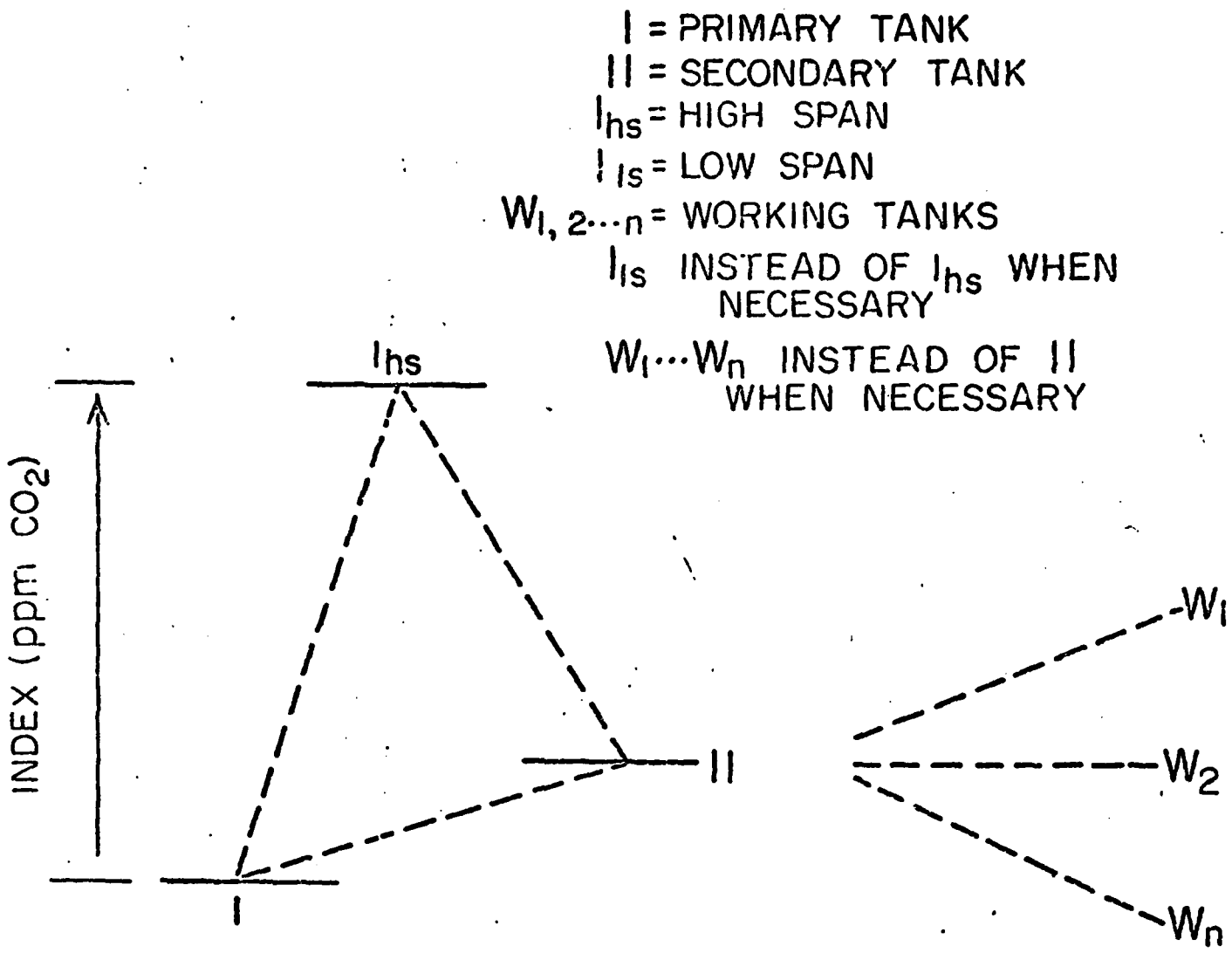

Figure 5. Mutual comparison method for tank standardization.

cylinder is "retired" from service. In this event a final value for the gas based on the average of the initial and final value is used for ultimate correction of all data. In the case where a set of standards are obtained, where only an initial value will be used, the initial value must be assumed to be equal to the final value. It must be emphasized though that all data will reflect small changes that may occur as tank pressures in the calibration standards decrease, and so be specified. It is further emphasized again that careful tank preparation be rigidly controlled.

The following scheme for calculating recorder scale factors was used, and is based on the method used on the S.I.O. program (Keeling and Pales, 1965).

Let A and B = Primary reference gas concentrations

Let X = The secondary reference standard concentration

Differences between A, B, and X will be noted in chart or arbitrary scale divisions. The reference gas, X, will be used to evaluate the concentration of the working reference gases, W ... Wn, and is designated the rank of a secondary standard. A format for calculating recorder scale factors may be established as follows (Table 1):

Table 1. Format for calculating recorder scale factors (RSF).

Standard Cylinder Number	Compared Cylinder Number	Observed Scale Difference	Number of Comparisons
A	X	[X]-[A]	a
B	X	[X]-[B]	b
A	B	[Y]*	(a or b)*

then:

[Y]-([X]-[A]) - ([X] - ([B] - [A]).

The asterisk on [Y] indicates the calculated value, and the brackets indicate index values. The number of comparisons assigned to [Y] is "a" or "b", whichever is smaller. Observed scale differences are taken from averages of individual chart scale differences, normally ten comparisons for each pair of references.

A table may be set up for the computation of recorder scale factors as given in the following example using simulated values (Table 2):

Table 2. Reference gases listed in order of rank.

Symbol	Cylinder Number	Concentration (PPM)
A	11589	314.59
B	10071	339.00
X	11111	309.55

Table 3. Calculation of RSF from data in Table 2.

1	2	3	4	5	6	7	8
Std Cyl. No.	Comp. Cyl. No.	Obs. Scale Diff.	No. of Compar.	Conc. Diff.	Single Set	RSF Wtd Ave.	Date of Anal.
11589	10071	5.02	10	24.41	4.86_3		1 Jan 1972
11589	11111	-0.89	10	-	-		-
10071	11111	-5.95	10	-	-		-
11589	10071	5.06	10*	24.41	4.82_4	4.84_4	-

The sign (plus or minus) of the values listed in column 3 designates the position of the trace compared to the reference numbers upscale (+) or downscale (-) of the standard reference gas cylinder. The calculated observed scale factor (*) is determined according to the formula where

$$[Y] = [-0.89) - [-5.95] = 5.06.$$

Working reference gases are used in the comparison of all expermintal data. Periodically, during the course of analysis the working reference gas is allowed to flow through the analyzer. Since the index or concentration of the reference gas is less well known than the standards used in the mutual comparison calibration, it is necessary to compute the values of the working reference gas each time the recorder scale factor is determined. This is accomplished by running a series of comparisons between the secondary

and working reference. Again, ten replicates are normally made. If ten replicates are desired, it is usual to run twelve or thirteen, discarding the first two or three in order to ascertain equilibrium between the two gases. Failure to achieve equilibrium initially may result for a variety of reasons, primarily due to mixing in dissicant cells and tubing. Average observed scale differences are determined. The computed working reference gas index is computed:

Computed Index = (Average Observed Scale Difference) (Weighted Average RSF).

A table may be kept to document these reference gas comparisons. For example:

Table 4. Documentation of changes which may occur in the concentration of the working reference gas, W.

1	2	3	4	5	6	7	8	9
Std. Cyl. No.	Comp. Cyl. No. W	Obs. Scale Diff.	No. of Compar.	Weighted R.S.F. Diff.	Comp. Conc.	Comp. Conc.	Supplier Conc.	Date
11111	10076	-1.72	10	4.84	-8.32	301.23	300.41	1/1/72

The sign of the value given in columns 3 and 6 denotes whether the concentration of the working reference gas (W), listed in column 2, is higher or lower than the concentration of the secondary standard. The concentrations listed in column 7 may be checked with the suppliers concentrations and followed during the life of the working reference until it is to be retired from use. When recorder scale factors are applied to the reduction of daily field observations they should be adjusted to a standard barometric pressure. For the Barrow program all recorder scale factors were adjusted to an average atmospheric pressure of 1015.9 mb:

$$\text{Adjusted Recorder Scale Factor} = \frac{\text{(Weighted Average RSF) (Observed Barometric Pressure)}}{1015.9 \text{ mb}}$$

It is possible, if not probable, because of various conditions prevailing under field conditions, that the RSF will vary appreciably between

periods when such determinations are made. It has been found useful to anticipate this in running short comparisons between the secondary and working reference daily. If variations occur, then the trend may be documented and a curve fitted to approximate the trend, or an average taken for the period. Figure 6 shows what may happen to the recorder scale factor when instrumental problems (respanning or realignment of analyzer) are encountered. Average recorder scale factors were determined for various periods of analysis. Where significant departures occurred, as in periods 5, 7, and 9, "sliding" RSF's were determined by scaling a daily RSF from the straight lines connected to adjacent periods. Again, daily comparisons between two gases will make it possible to determine whether a straight line can be drawn for period 5, 7, or 9. Complete documentation of all calibration data for the Barrow program, 1961 to 1967, has been published by Kelley (1969).

The scheme that has been described allows the investigator to maintain continuous control of the reference gas system based on a single set of standards. The ability to accurately document small changes in carbon dioxide over a long period of time will depend on the accuracy of these standards.

At the conclusion of the Barrow program the results of all working reference (W) gas calibrations were compared with the values obtained after reanalysis at S.I.O. Since the inception of observations in the Arctic, it had been the practice to not only monitor the working reference gas concentrations versus the Barrow standards, but to have each reference anaylzed at S.I.O. before and after use. Long term drift in the concentration of the reference or problems with the IR analyzer could be followed and corrected if necessary. Throughout the entire period of observations it is shown (Figures 7, 8) that very small differences were detected in the reference gas comparisons between S.I.O. and Barrow, so that comparison of data recorded at Barrow could be reliably compared with the observations from the S.I.O. program in the Antarctic and Hawaii. The trend toward more negative values observed in Figure 8 may indicate the effect of nonlinear response of the URAS-1 analyzer over the Series 700 employed during the period 1961-1963.

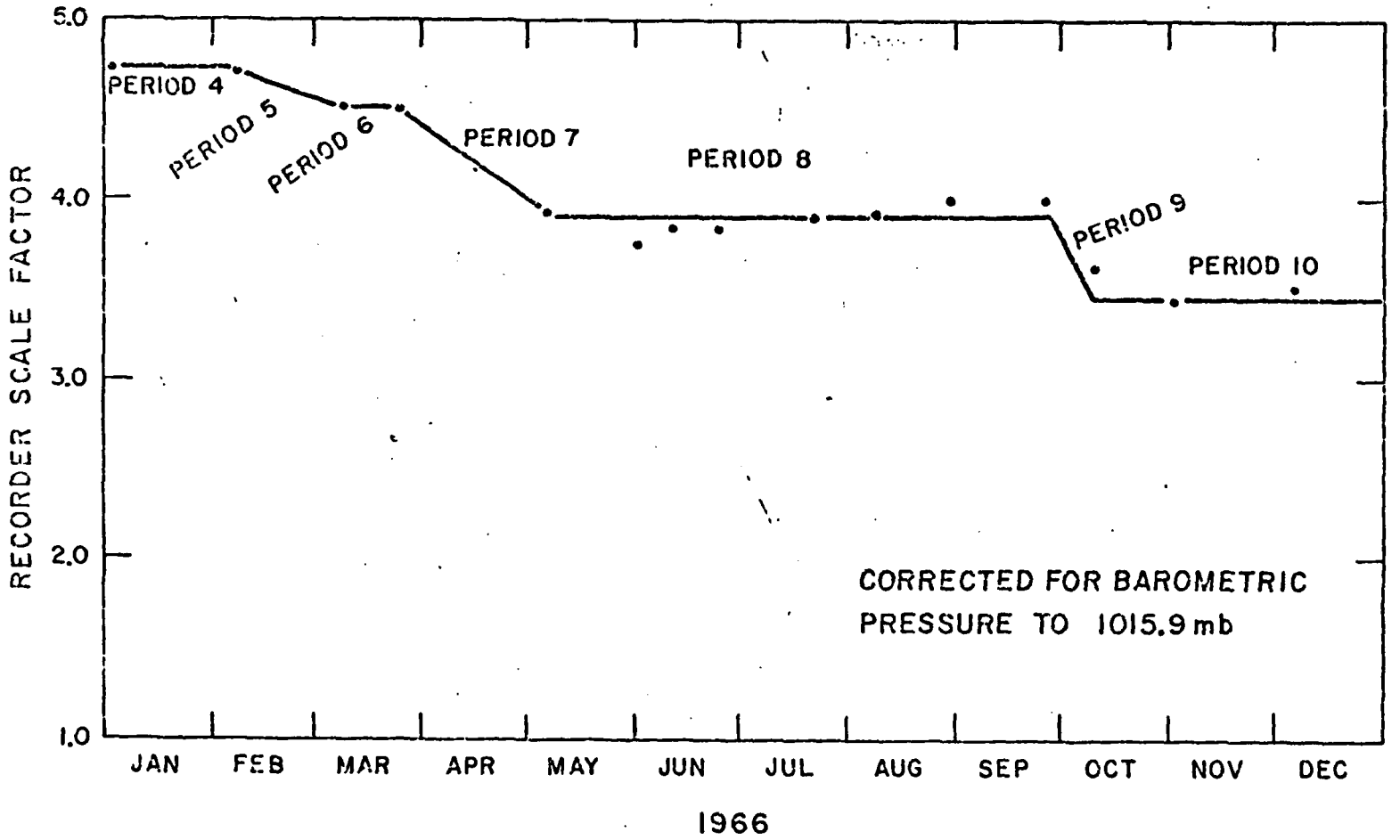

Figure 6. Recorder scale factors adjusted to standard barometric pressure versus calendar date.

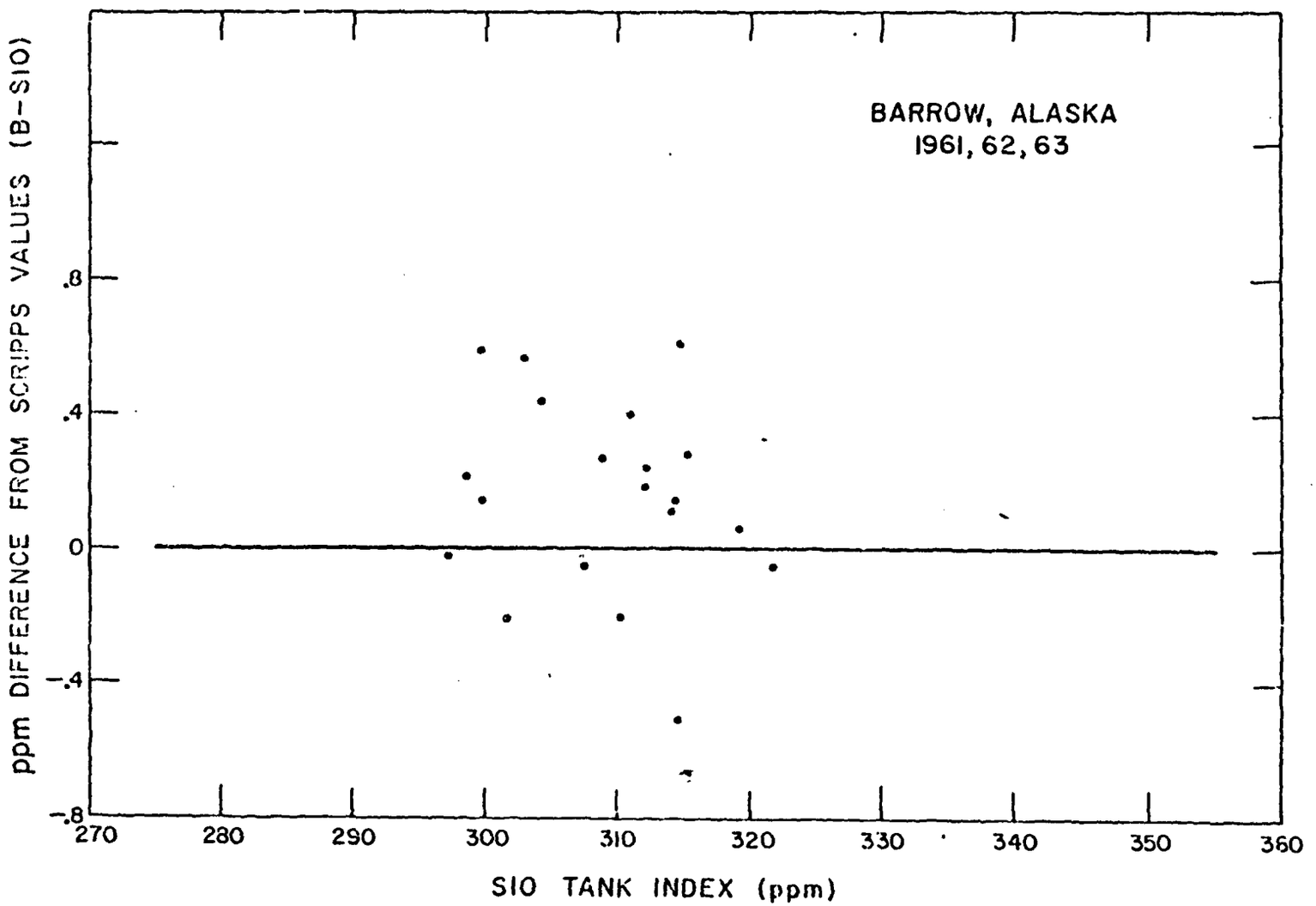

Figure 7. Differences between index values (ppm) obtained from measurements at Barrow and S.I.O., 1961-1963.

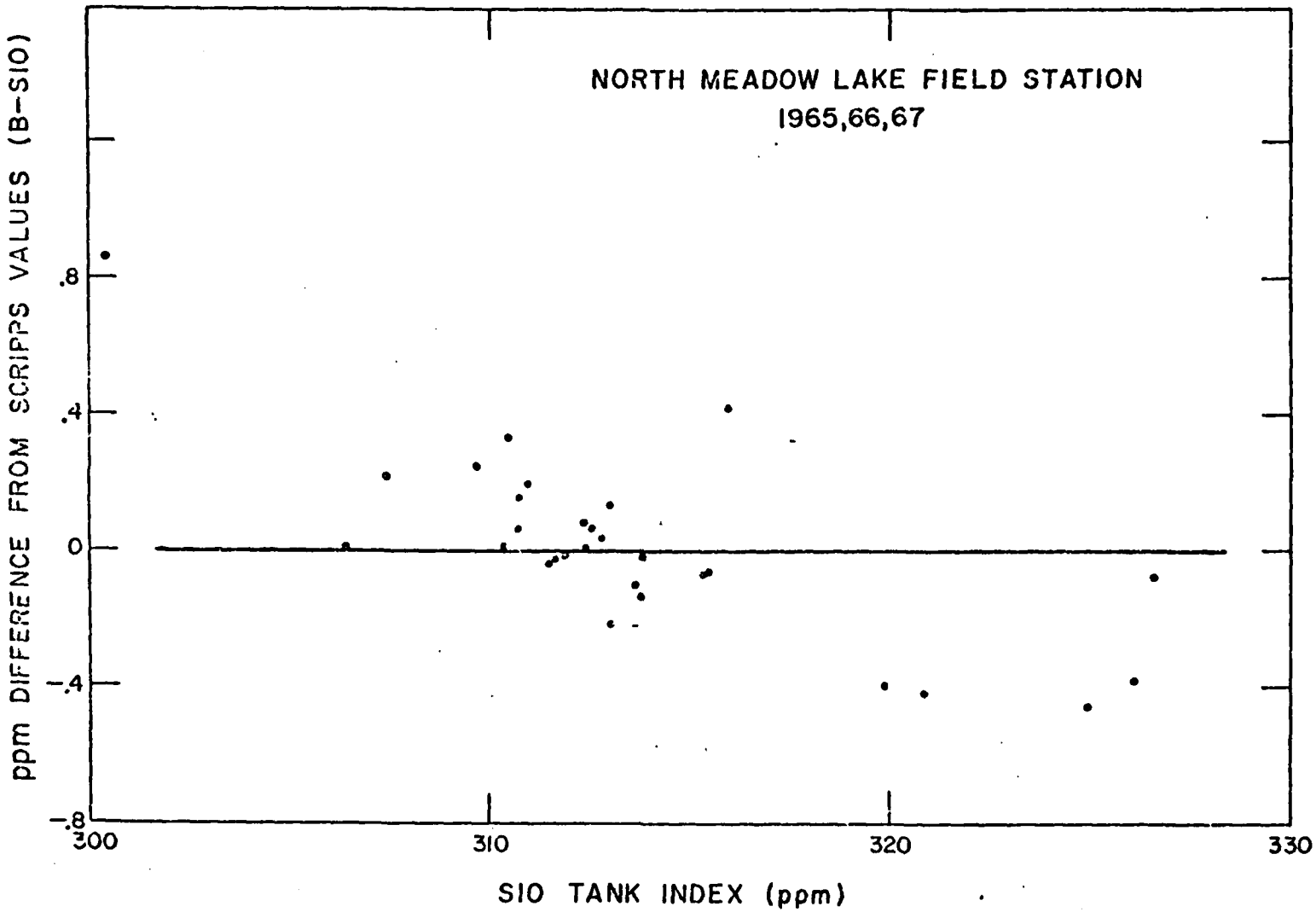

Figure 8. Differences between index values (ppm) obtained from measurements at North Meadow Lake and S.I.O., 1965-1967.

Reference gases are commonly used to standardize infrared gas analyzers. Experience has shown that reference gases of the same nominal concentration, supplied either by the same manufacturer or by different manufacturers, are subject to variations which result in gas mixtures unacceptable for IR analyzer calibrations. Evidence has been given by Kelley and Coyne (1973) for the necessity of providing accurate reference gases for investigations concerned with photosynthesis, mass transfer as well as CO_2 in the atmosphere.

Bate *et al.* (1969) showed that suppliers's specifications for gas components of less than 1% of the total mixture, were usually ± 5% when referenced against N.B.S. standards, with a tolerance of 1% at the 99% confidence level (N.B.S., 1970). Table 5 illustrates some examples of departures in CO_2 concentration between the supplier's analysis and that of Bate *et al.*, 1969, which were based on N.B.S. standards.

Table 5. Analyses of CO_2-air mixtures (ppm) from commercial suppliers (after Bate *et al.*, 1969).

Stated Conc.	Supplier Analysis (A)	Bate *et al.* Analyses (B)	B-A
250	255	259	4
50-55	55	62	7
95-100	98	113	15
100	110	114	4
350	348	362	14
250-260	255	273	18
360	355	369	14
340	345	360	15
290	285	293	8
340	340	349	9

2.4.4 Data Analysis

A normal cycle for the continuous analyses of air consisted of 5 minutes of reference gas followed by 25 minutes of air. Occasionally two reference gases were analyzed for 5 minutes each, followed by 20 minutes, as a check on analyzer drift and particularly after major electronic or mechanical servicing.

All measurements were recorded on a strip chart and the difference in chart ordinates between two successive traces was read and recorded.

The concentration of carbon dioxide in air was computed at the end of each month and recorded as a provisional concentration referred to as an index with dimensions in parts per million by volume (mixing ratio). Final values of the concentration were obtained only after all of the reference gases had received final analysis at S.I.O. — a delay of up to 2 years.

The observed scale difference taken from the chart record was adjusted to a standard barometric pressure of 1015.9 mb:

$$\text{Adjusted Scale Difference} = \text{Observed Scale Difference} \times \frac{1015.9 \text{ mb}}{\text{Average pressure for the day}}$$

The computed index difference (provisional ppm) was obtained by:

Computed Index Difference = RSF x Adjusted Scale Difference.

It was established provisionally at S.I.O. in 1959 that the true concentration in parts per million related to the index scale by:

Manometric Concentration = (C-311.51) 1.2186 + 311.51

where C is the index value. In 1959 a constant volume manometer with a precision capability of ± 1 part in 3000 was used to determine the CO_2 concentration of selected reference gases having CO_2 concentrations close to air. The CO_2 was first frozen out in liquid nitrogen by the method of Keeling (1958) and transferred to a 4 cc chamber where its pressure and temperature were determined. The manometrically calibrated gases were in turn compared repeatedly with a set of primary standards which have remained in use to the present time. Recent evidence based on gravimetric analysis standardization (Keeling, *et al.*, 1972) suggests a new provisional scale of concentration (Keeling, *et al.*, 1972):

$$q_g = 89.287 + 0.42353\ q_m + 0.00091838\ q_m^2$$

where q_g and q_m are the gravimetric and the former (1959) manometric scale concentrations. In the range of 300 to 350 ppm it is believed that this new quadratic expression is correct to within 1 ppm absolute accuracy. Until the S.I.O. manometric work is complete the 1959 calibration will be used. All of the data for the observations at Barrow were referenced to the 1959 manometric correction and are presented in detail in a report by Kelley (1969).

The amount of carbon dioxide in air is usually quoted in ppm (parts of CO_2 per million parts of air, by volume understood), v.p.m. (volume per million) or µl/l (microliters per liter), all three being numerically equal. Sometimes the term "mixing ratio" is used. Although this term is commonly used with water vapor measurements, it is nevertheless apropos to use it when discussing CO_2 measurements. Since most infrared measurements of CO_2 in air necessitate the removal of water vapor, the understanding is implied that the amount of CO_2 is ppm by volume of dry air. Most of the referenced data report dry air values. The relation between concentration ϕ (g m^{-3}) and volume fraction C (v.p.m.) is

$$\phi = \rho_c \cdot 10^{-6}$$

where ρ_c is the density of CO_2 in g m^{-3} at 20°C. Further discussion of the units used in reporting carbon dioxide values is given in Monteith (1973). All of the data reported for carbon dioxide in the atmosphere is given in parts per million by volume dry air.

2.4.5 Results and Discussion

The Barrow data for most of the year show little or no daily variation with the exception of July and August (Figure 9). The data for September through May resemble the daily trend observed in the Antarctic (Brown and Keeling, 1965). During the autumn the water and land surfaces freeze and become snow covered, beginning about September for the tundra and late September for the numerous lakes which cover over 50% of the tundra surface. Snow melt does not usually occur until late May or early June. Thawing of the lakes begins 2-3 weeks later. There is no vegetation to deplete the atmosphere near the ground of CO_2, and with tundra surface temperatures

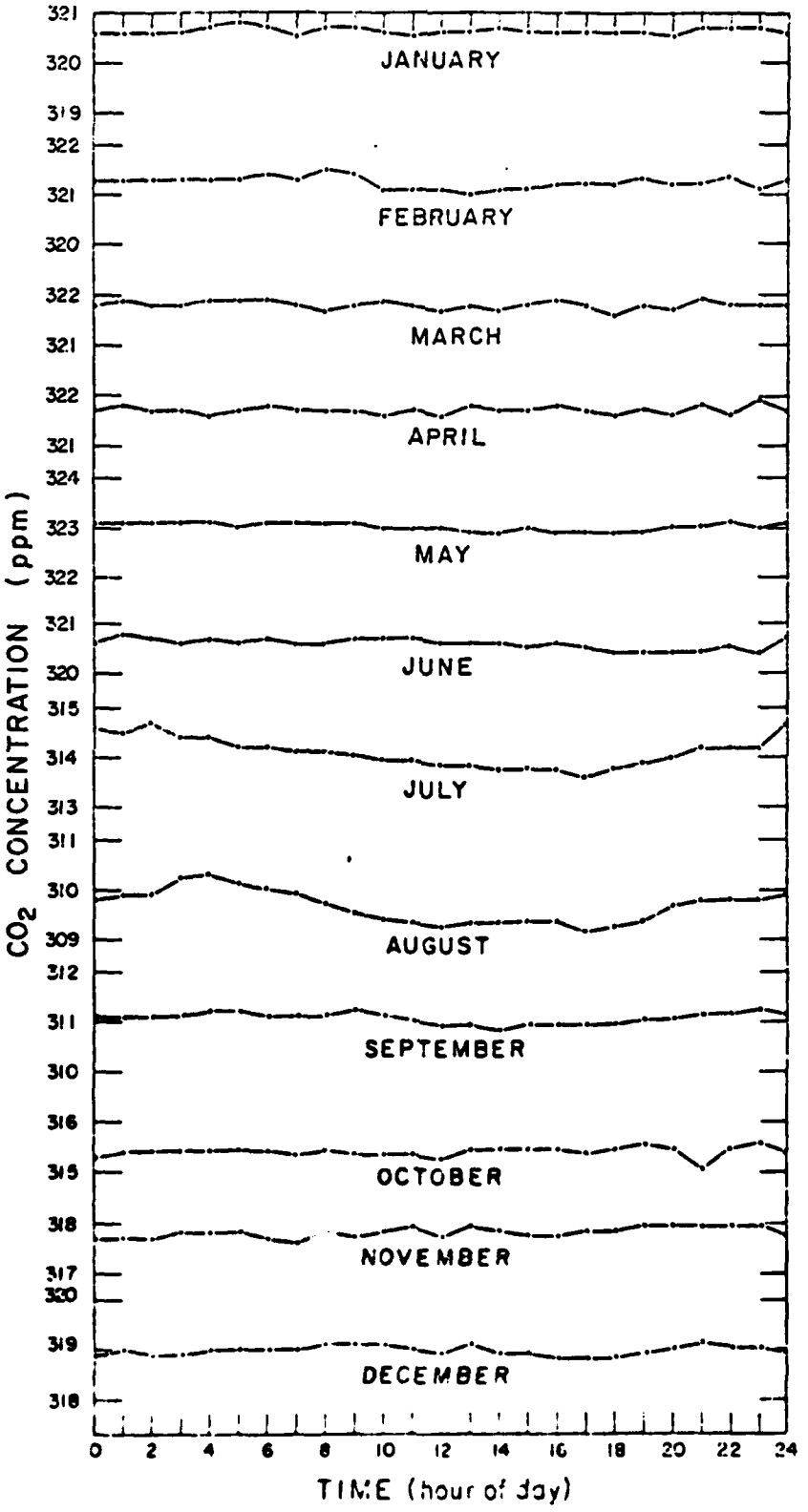

Figure 9. Average diurnal variation of CO_2 near Barrow, Alaska, 1961-1967.

below -10°C (Kelley and Weaver, 1969) for most of this period, soil respiration is negligible. By June, when the tundra snow cover is thawing, the surface temperatures are near the freezing point. A slight daily variation in CO_2 is noted in the average monthly variation of CO_2 at the 8 m level above the surface. For individual days the variation may be greater and is dependent on fluctuations of the wind speed, and air temperature. At this time, early stages of photosynthesis and soil respiration occur. July and August are the warmest periods of the year and a time of maximum plant productivity. Open water (sea and lake) affords exchange of CO_2 across the air water boundary. Average daily variations of CO_2 are greatest during this period, over 1 ppm, with maximum concentrations occurring in the early morning and minimum by mid-afternoon (Kelley, 1968; Kelley and Weaver, 1966). This period resembles, in general, the daily variations of CO_2 observed at the Mauna Loa Observatory, Hawaii (Pales and Keeling, 1965).

The daily variation in CO_2 diminishes greatly by September. The daily variation for individual days fluctuates much more for the month of September due to the alternate freeze-thaw conditions on the tundra at this time of the year. Air intake ports placed close to the tundra surface showed that the soil was still a source of CO_2 (Kelley *et al.*, 1968).

Carbon dioxide variations, averaged daily (Figures 10, 11), are shown for each year of observation (1961-1967) at Barrow (Kelley, 1969). The averages were computed for all periods when the recorder trace was steady (i.e., for no local pollution, and for wind directions that were not from the direction of the village).

A seasonal oscillation is clearly evident and probably produced principally by land plants. A detailed study of the amplitudes and phases at different latitudes (Bolin and Keeling, 1963), suggests the hypothesis that the summer decrease in CO_2 is produced principally by land plants, especially forests of North America and Asia which remove CO_2 from the atmosphere during the summer and release CO_2 to the atmosphere during the autumn, winter and spring.

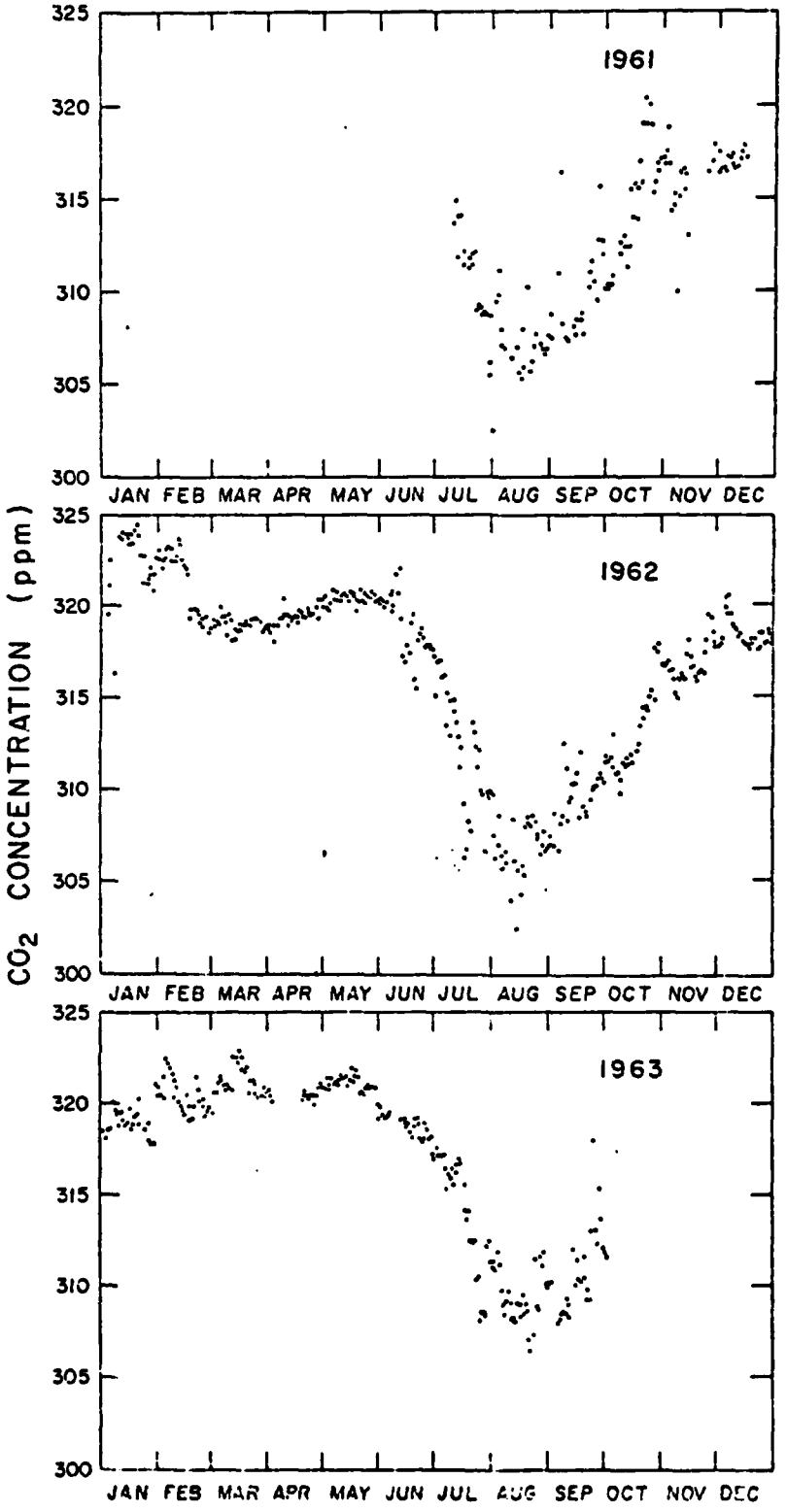

Figure 10. Daily average concentration of CO_2, 1961-1963.

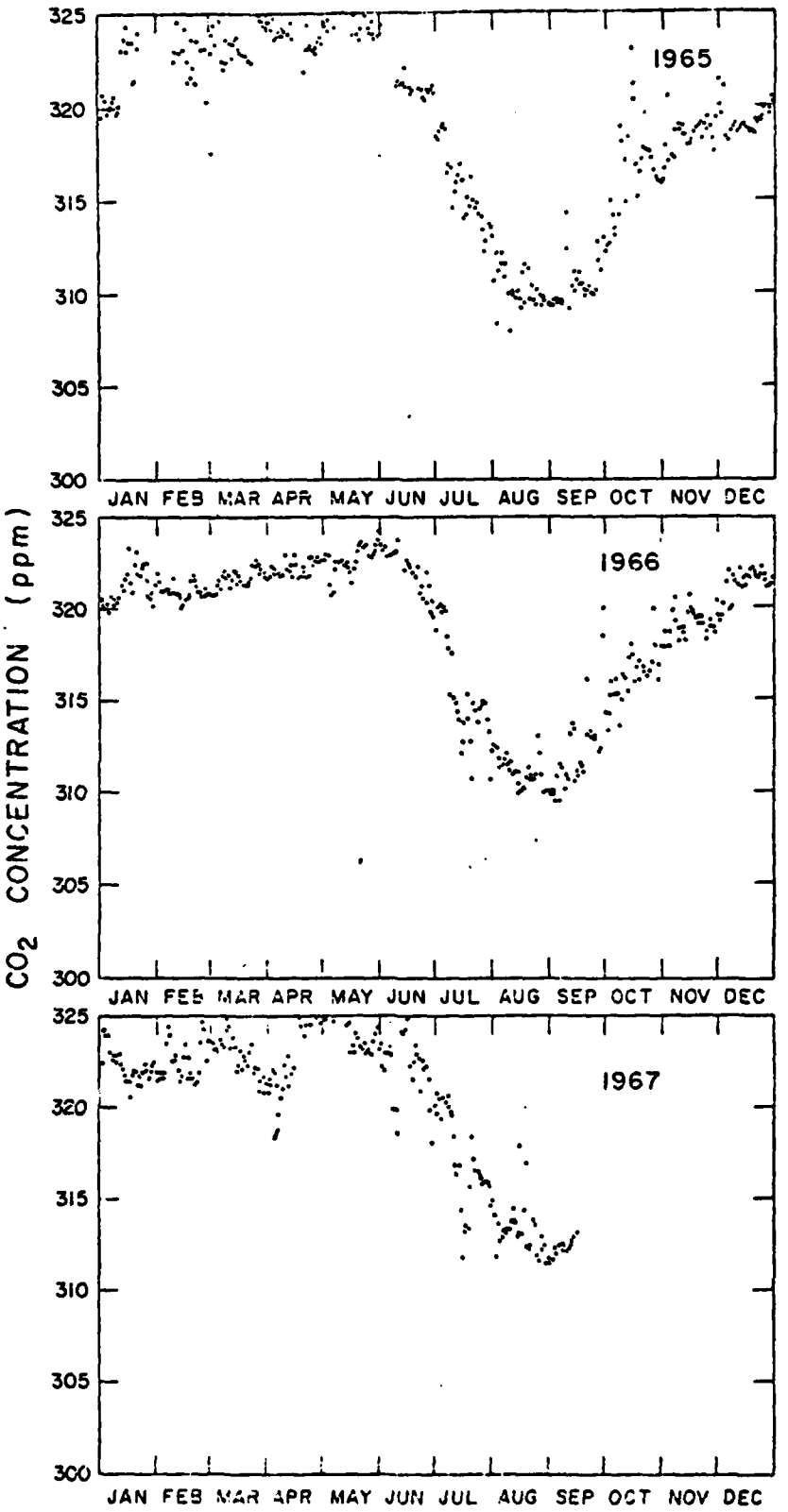

Figure 11. Daily average concentration of CO_2, 1965-1967.

Short term trends superimposed on the seasonal trend suggest a response of CO_2 to regional and local weather patterns and vertical mixing. Similar observations were made for daily ozone variations, which were monitored concurrently. Surface ozone showed maximum variability in the winter and spring. Storm passages in the Barrow area were generally associated with rapid increases in surface ozone (Kelley, 1973a). The interpretations of these data suggests that the ozone content near the surface is increased by downward transport from aloft at times of strong turbulence. Although there is strong evidence in support of ozone fluctuation and downward mixing since ozone is produced at high altitudes, the evidence is not strong for such an explanation for carbon dioxide in the absence of supporting data well above the surface during winter.

Carbon dioxide concentrations rise steadily to a maximum in May, and then rapidly decrease to a minimum in August just after the maximum in plant productivity is attained (Johnson and Kelley, 1970). In contrast, minimum values in CO_2 concentrations at Mauna Loa, Hawaii are reached in late September and early October (Pales and Keeling, 1965; Keeling *et al.*, 1972).

From August to December CO_2 in the air increases steadily with wide variations. Variable conditions of freezing and thawing and variable snow cover tend to diminish the effect of CO_2 sources from the soil and land plants. Monthly average concentrations of carbon dioxide in air are given in Table 6 and displayed in Figure 12. A significant rise in CO_2 concentration is evident from inspection of the data. By late May more radiation is gained by the tundra surface layers than is given out (Kelley and Weaver, 1969). Thawing occurs and carbon dioxide builds up under the snow pack reaching high concentrations by June (Kelley *et al.*, 1968). The CO_2 enters the atmosphere by diffusion and convection to add to the late spring rise in CO_2 in the atmosphere.

During the course of observations at Barrow, air was collected at flasks twice a month for analysis at S.I.O. This procedure was done as a further check on the Barrow infrared analyzer and to offer another means of comparison with the S.I.O. Program data. Evacuated flasks in

Table 6. Monthly average concentration of atmospheric carbon dioxide at Barrow, Alaska.

Month	No. of Days	Conc. ppm	No. of Days	Conc. ppm	No. of Days	Conc. ppm	No. of Days	Conc. ppm	No. of Days	Conc. ppm	No. of Days	Conc. ppm
	1961		1962		1963		1965		1966		1967	
January			26	322.45	27	319.10	24	322.14	31	321.24	31	322.14
February			28	321.21	28	320.48	18	323.04	28	231.01	28	322.56
March			29	318.97	30	321.22	28	323.49	31	321.71	31	322.69
April			30	319.42	15	320.54	25	323.64	30	322.25	30	323.41
May			31	320.39	31	321.06	29	324.83	31	322.71	31	324.25
June			30	318.74	26	318.81	19	321.22	25	321.98	29	322.11
July	21	310.70	31	311.97	31	314.08	31	315.61	31	315.47	31	316.93
August	24	307.14	29	306.78	31	309.47	31	310.16	31	311.15	31	313.02
September	23	310.07	28	309.43	27	310.73	30	310.58	30	312.27	15	312.40
October	28	314.92	30	313.07			31	316.79	30	316.34		
November	18	315.79	30	316.85			30	318.54	29	319.28		

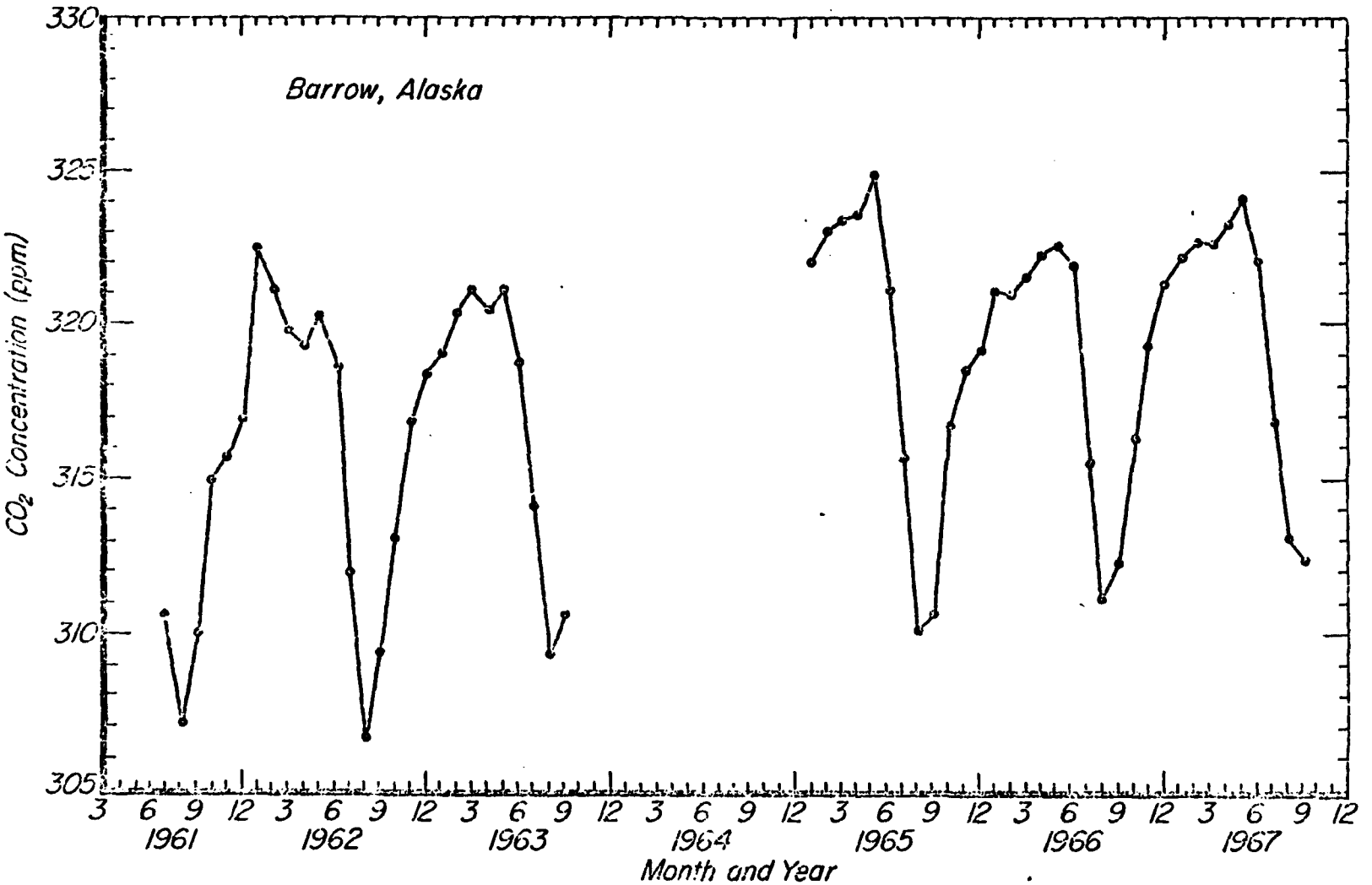

Figure 12. Monthly average concentration of carbon dioxide, 1961-1967.

pairs were used to carefully sample the air near the sampling site. At the same time the infrared analyzer chart record was marked for later comparison with the flask sample analysis. No samples were taken with wind speeds less than 2.5 meters per second. Air was also sampled by means of flasks twice a month on Ice Station ARLIS-2 from 1962 to 1964. This drifting station moved about the central Arctic basin at distances of 300 to more than 800 miles from the Barrow coast.

All of the data for carbon dioxide from flask samples at Barrow and ARLIS-2 are summarized in Table 7. These data are reduced to a datum of 1960 by adjusting the values on the basis that CO_2 increased at a constant rate of increase of 0.06 ppm per month.

Comparison between the analyses of air sampled by the flasks and by infrared analysis is very good. The concentration of CO_2 at Barrow closely follows the values for CO_2 at ARLIS-2 (Figure 13). The infrequent sampling at ARLIS-2 and the fact that the ice station was frequently in a new geographic location does not allow for reliable interpretation of the differences in concentration from those observed at Barrow.

During 1962 it was possible to sample air at several areas in northern Alaska (near Anaktuvuk Pass, 68°11'N, 153°25'W; Umiat, 69°20'N, 152°W; Bettles, 66°55'N, 153°15'W). Umiat is located on the treeless north slope of Alaska near the foothills of the Brooks mountain range. Anaktuvuk Pass is located within the Brooks mountain range and Bettles is located near the foothills south of the Brooks Range. Although these data are of much less reliability in following the seasonal trend of CO_2 than the Barrow or Ice Station data they do point out some interesting features.

During April all of the CO_2 values are nearly the same, with Bettles being a little over 1 ppm higher than the concentration at Barrow (Table 8). During early July the inland stations, with the exception of Umiat, are significantly lower than Barrow. At this time the snow has long cleared the region of Bettles and Anaktuvuk Pass while this does not happen at Barrow until late June. These low inland CO_2 values may reflect greater uptake of CO_2 by plants at this time. No explanation is readily apparent for the high CO_2 concentration at Umiat. By August minimum CO_2 concentrations are experienced at Barrow with carbon dioxide even lower at the

Table 7. Concentration of atmospheric CO_2 at ARLIS-2 at Barrow, Alaska, referred to a constant datum (January 1960).

Month	Barrow (IR) CO_2 (ppm)	Barrow Flasks No. of Flasks	Barrow Flasks CO_2 (ppm)	ARLIS-2 No. of Flasks	ARLIS-2 CO_2 (ppm)
Jan	318.10	12	317.11	14	319.62
Feb	318.29	16	318.33	14	319.79
Mar	318.18	20	318.90	24	318.57
Apr	318.36	16	318.78	20	318.90
May	319.10	20	320.09	20	319.74
Jun	316.96	16	318.55	16	319.85
Jul	310.89	15	313.84	22	315.84
Aug	306.32	16	308.06	20	309.71
Sep	307.55	18	307.80	22	307.18
Oct	312.22	20	312.33	12	311.02
Nov	314.50	12	314.91	12	314.70
Dec	315.84	20	316.83	20	316.81
Annual Mean	314.69		315.46		3.5.92

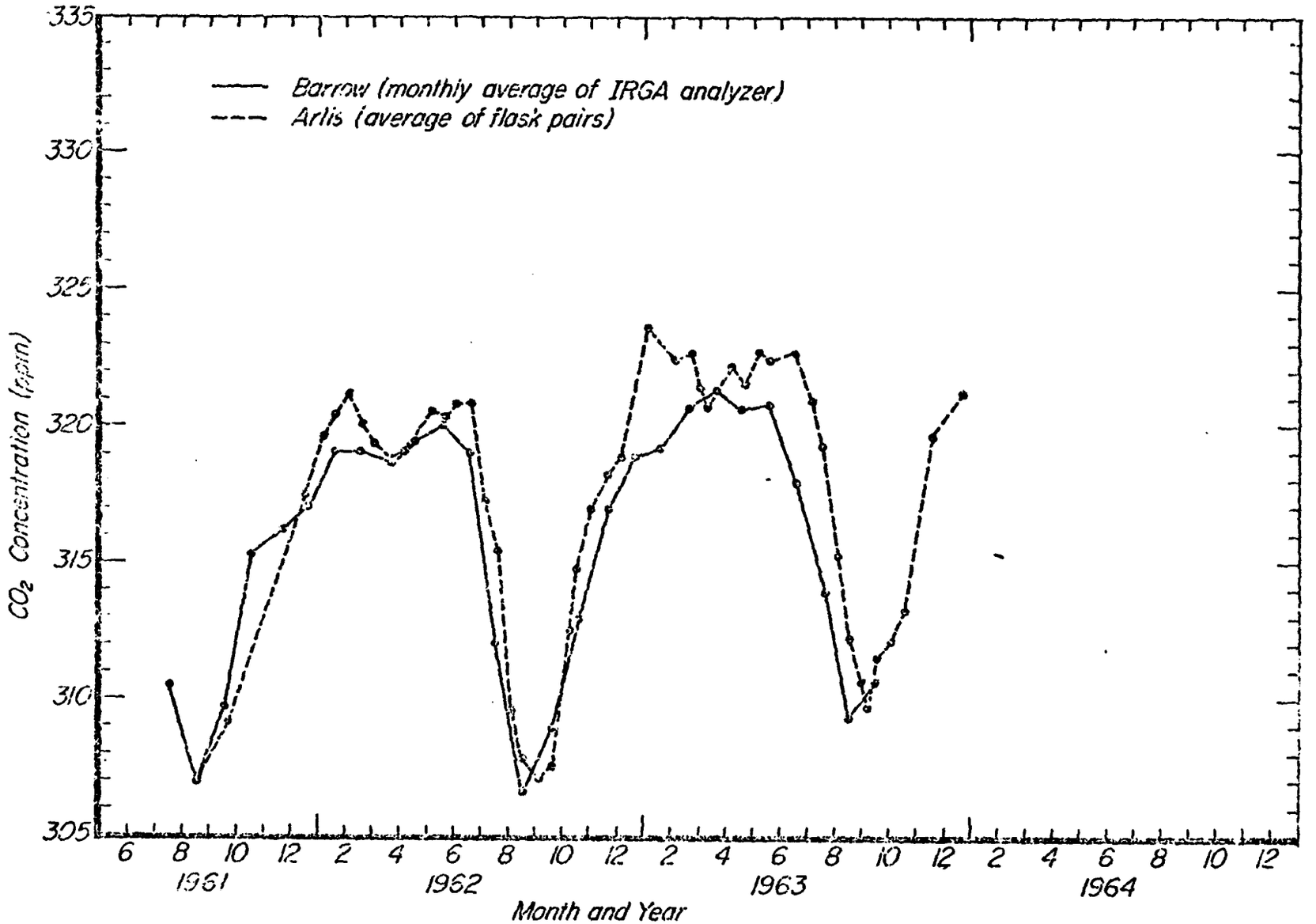

Figure 13. The seasonal variation of CO_2 at Barrow and Ice Station ARLIS-2.

Table 8. Concentration of atmospheric carbon dioxide at various Alaskan locations in samples collected in glass flasks (average of flask pairs in ppm)

Date	Barrow	Range (ppm)	Umiat	Range (ppm)	Anaktuvik Pass	Range (ppm)	Bettles	Range (ppm)
1962								
Apr 15	319.46	0.00	319.13*	-	319.69*	-	320.81	-
Jul 1	315.19	0.13	318.08	0.06	311.94	0.00	311.23	0.57
Aug 1	310.10	0.00	302.69	0.31	296.75	0.31	315.39**	0.46
Aug 15	306.56	0.00	-	-	-	-	308.44	1.24
Sep 1	307.63	0.14	307.95	-	307.68	0.51	305.70	0.00
Sep 15	308.45	0.24	312.74	0.21	314.68***	0.31	-	-
Oct 16	312.80	0.23	318.49	0.00	-	-	-	-
Dec 31	319.42	0.13	316.27*	-	316.71	0.41	317.52	0.00

* Lowest of two values accepted
** Forest fires in vicinity
***Forest fires south of the Brooks Range

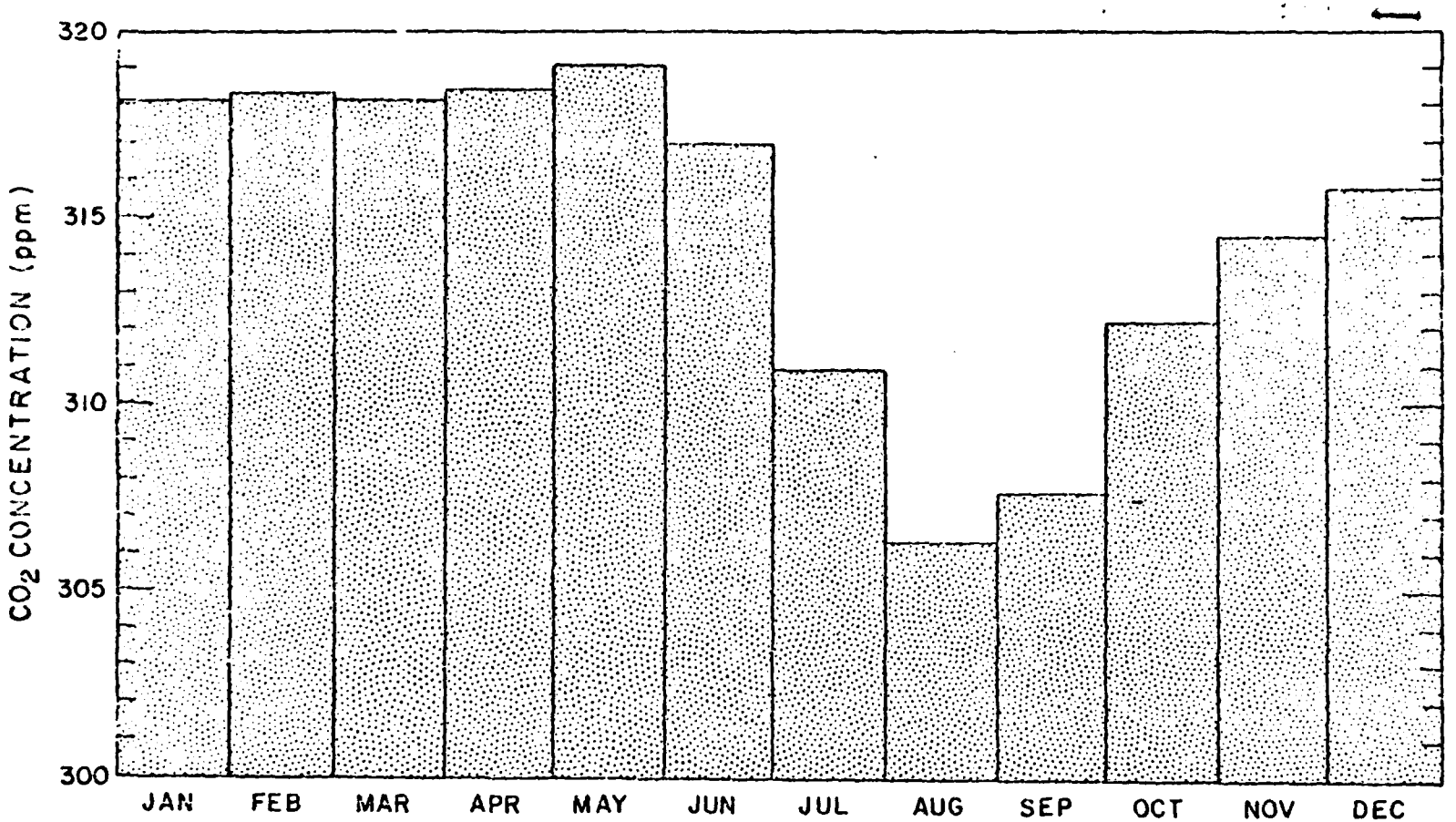

Figure 14. Monthly average concentration of CO_2 near Barrow, Alaska, referred to a constant datum (January 1960).

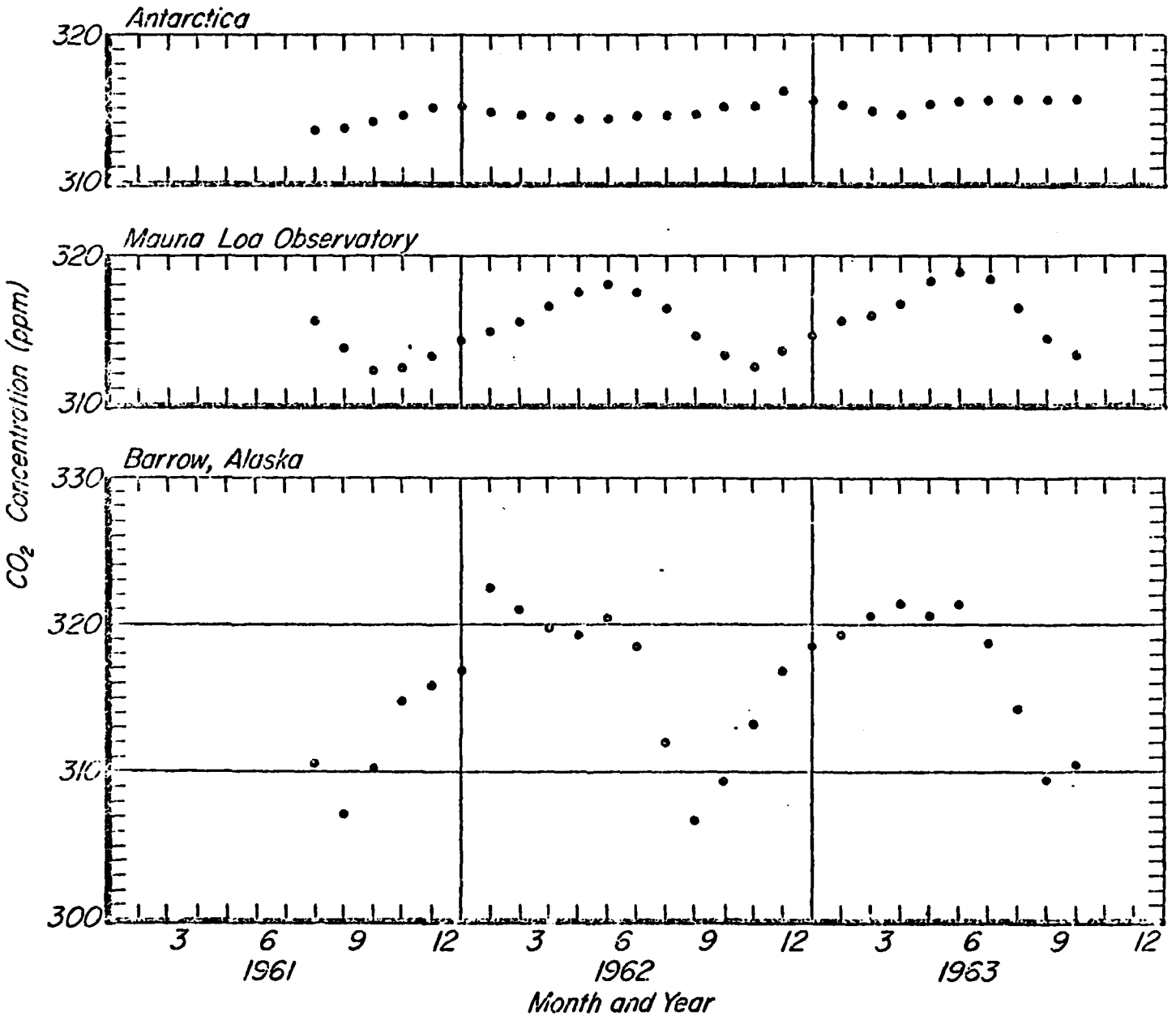

Figure 15. Comparison of average monthly CO_2 concentrations with Mauna Loa, Hawaii and Antarctica.

of Stockholm (Bolin and Bischof, 1970) have shown that the seasonal variation in CO_2 is about 6.5 ppm at 2 km and diminishes to 3.5 ppm in the upper part of the troposphere. The phase shift of the seasonal variation between these two levels is 25-30 days. On the basis of these data vertical eddy diffusivity, $K=2(10^5)cm^2sec^{-1}$ was derived. The amplitude of the seasonal variation in the lower stratosphere, 11-12 km, was less than 1 ppm and the phase was delayed at least 1.5 months as compared to the upper troposphere.

Primary emphasis on all of the measurements at Barrow, Hawaii and Antarctica was to establish the long term trend in atmospheric CO_2 in response to effects from anthropogenic sources and alteration of the natural environment. A secular trend at all stations was observed and is similar in magnitude. The trend is approximately 0.8 ppm per year from 1958 to 1972 at Hawaii (Keeling *et al.*, 1972), and Antarctica (1957-1971) (Keeling *et al.*, 1972a).

The record at Barrow, although not as long as at Hawaii or Antarctica was sufficient to establish the trend there. Table 9 summarizes the results of analyses used to show the course of the seasonal trend at Barrow (Figure 16).

Complete data are given in Kelley (1969). A long term trend of atmospheric CO_2 near sea level at Barrow was approximately 0.6 ppm prior to 1963 and 1.0 ppm per year after 1965. Elswhere, six years of data for atmospheric carbon dioxide in the troposphere and lower stratosphere reveal an annual increase of the CO_2 content of 0.7 ppm per year (Bolin and Bischof, 1970).

The CO_2 output over the last decade has increased by more than 50% (Bolin and Bischof, 1970; Keeling *et al.*, 1972a) as compared with the 1950's (6.8% and 4.4% respectively) while the annual increase in the atmosphere has remained about the same. A smaller percentage now seems to stay in the atmosphere than was the case in the later 1950's. There is always the question that the reference gases may have drifted as the data are highly dependent on calibration integrity. A change of 1.0 to 1.5 ppm would invalidate the data. Intercalibration of all reference gases will reveal any systematic drift in the primary reference gases. Frequent control and periodic checks fail to indicate any systematic drift.

Table 9. Yearly average concentration of carbon dioxide at Barrow, Alaska, from 1961 to 1967.

Period	No. of days	Concentration -ppm	Gradient ppm/yr
1961-1962	322	316.42	
			0.56
1962-1963	337	316.98	
			0.57
1965-1966	360	318.70	
			1.01
1966-1967	347	319.71	

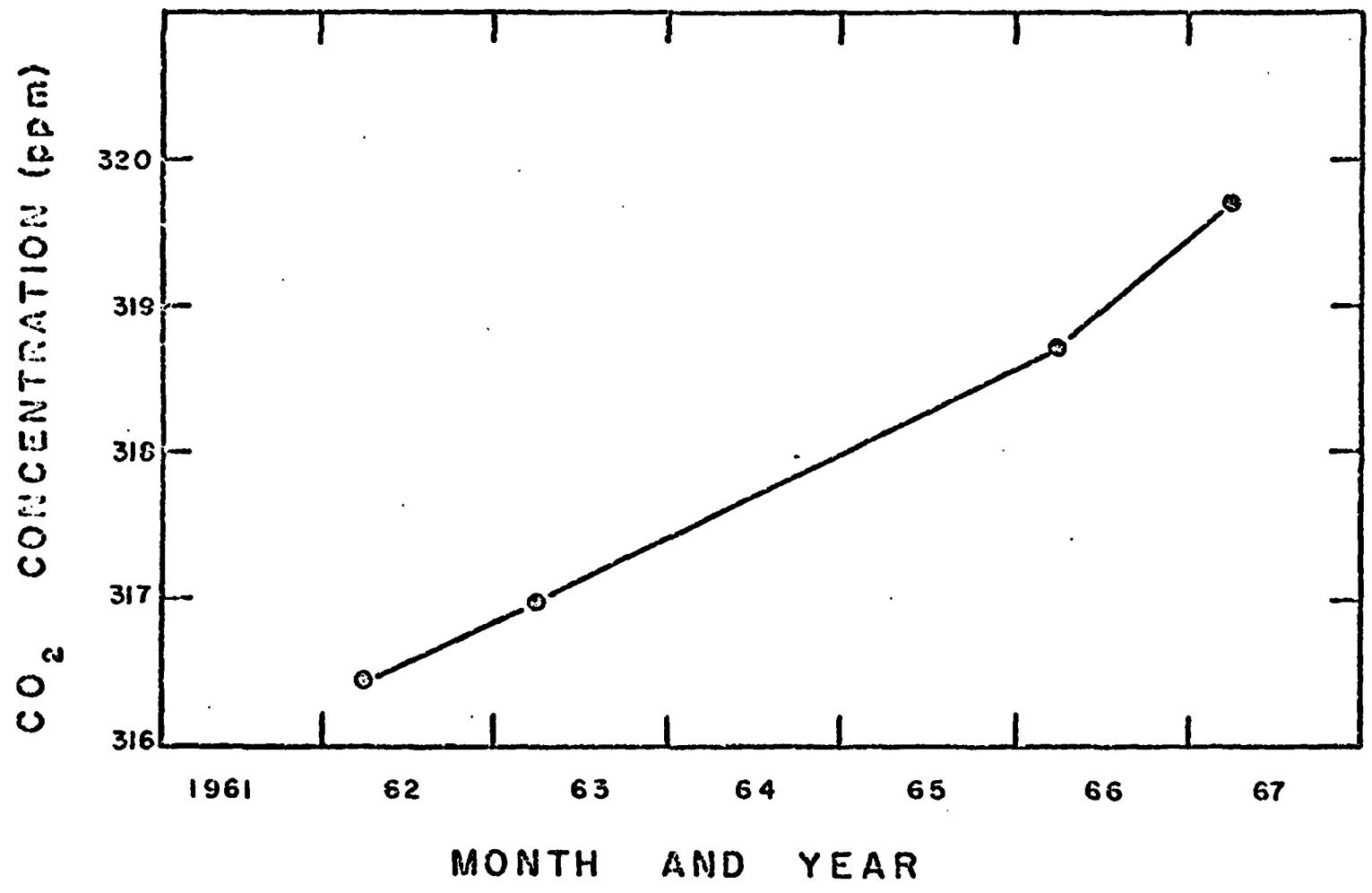

Figure 16. Long term trend of CO_2 concentrations at Barrow, Alaska.

Bolin and Bischof (1970) conclude that 35% of the CO_2 output stays in the atmosphere. The decline in the rate of CO_2 increase in the 1960's during a period of rising industrial CO_2 production, if real, may be the result of increased uptake either by the oceans or land plants (Keeling *et al.*, 1972a). Bainbridge (1971) suggested cooling of the surface ocean water may lead to increased CO_2 uptake from the overlying air. Namais (1970) demonstrated that a cooling trend began in 1963. The water north of 35°N cooled remarkably and remained cold for a few years. The cooling trend was associated with major changes in the atmospheric pressure gradient north of 40°N. These low pressures were also associated with abnormal cyclonic activity particularly in the eastern north Pacific Ocean as well as considerable wind and cloudiness. These factors are of prime importance in producing low sea surface temperatures, through water stirring, reduced insolation and increased sensible and latent heat losses from the water. Carbon dioxide exchange between the sea and air may be enhanced during this period. Keeling *et al.* (1972a), however, state that the period of cooler water is too short to account for the CO_2 trend.

CHAPTER 3

CARBON DIOXIDE UNDER THE SNOW

3.1 Introduction

From observations of the gradient of CO_2, ground surface to 16 m, it was observed that CO_2 concentrations close to the tundra surface show large deviations from ambient values for CO_2 (Kelley and Weaver, 1966; Figure 17). It was thought that the deviations possibly corresponded to changing tundra surface features, its biological constitution, and associated meteorological parameters.

To investigate the variations of CO_2 at the surface level of the tundra a procedure was used whereby CO_2 was monitored at the ground level and 16 m above the tundra together with other microclimatological observations: wind speed, temperature, net radiation, snow depth and density. Subnivean CO_2 concentration were observed for an entire period of snow cover from "freeze-up" to thaw during 1965-1966. Prior to the thaw in June anomalously high levels of CO_2 under the snow were noted. These became of special interest and the subject of future intensive investigation (Coyne and Kelley, 1973).

3.2 Methods, Results and Discussion

The initial experiment (Kelley *et al.*, 1968) to observe subnivean CO_2 variations was located near the atmospheric CO_2 monitoring station on a beach ridge at North Meadow Lake (Chapter 2).

The air intake port for sampling CO_2 at the ground surface consisted of an aluminum box open on one side, which was in contact with 400 cm^2 of tundra surface (Figure 18). Air was continuously pumped out of the aluminum box and conducted through stainless steel tubing to a freeze trap to remove water vapor and then to the infrared analyzer. The intake port was initially placed on the snow-free tundra. Alternate periods of snow and freezing rain during October and November resulted in a layer of loosely packed, coarse grained snow approximately 7 cm deep and overlain by a thin layer of clear ice. Above the ice layer, a continuous cover of

CHAPTER 3

CARBON DIOXIDE UNDER THE SNOW

3.1 Introduction

From observations of the gradient of CO_2, ground surface to 16 m, it was observed that CO_2 concentrations close to the tundra surface show large deviations from ambient values for CO_2 (Kelley and Weaver, 1966; Figure 17). It was thought that the deviations possibly corresponded to changing tundra surface features, its biological constitution, and associated meteorological parameters.

To investigate the variations of CO_2 at the surface level of the tundra a procedure was used whereby CO_2 was monitored at the ground level and 16 m above the tundra together with other microclimatological observations: wind speed, temperature, net radiation, snow depth and density. Subnivean CO_2 concentration were observed for an entire period of snow cover from "freeze-up" to thaw during 1965-1966. Prior to the thaw in June anomalously high levels of CO_2 under the snow were noted. These became of special interest and the subject of future intensive investigation (Coyne and Kelley, 1973).

3.2 Methods, Results and Discussion

The initial experiment (Kelley *et al.*, 1968) to observe subnivean CO_2 variations was located near the atmospheric CO_2 monitoring station on a beach ridge at North Meadow Lake (Chapter 2).

The air intake port for sampling CO_2 at the ground surface consisted of an aluminum box open on one side, which was in contact with 400 cm^2 of tundra surface (Figure 18). Air was continuously pumped out of the aluminum box and conducted through stainless steel tubing to a freeze trap to remove water vapor and then to the infrared analyzer. The intake port was initially placed on the snow-free tundra. Alternate periods of snow and freezing rain during October and November resulted in a layer of loosely packed, coarse grained snow approximately 7 cm deep and overlain by a thin layer of clear ice. Above the ice layer, a continuous cover of

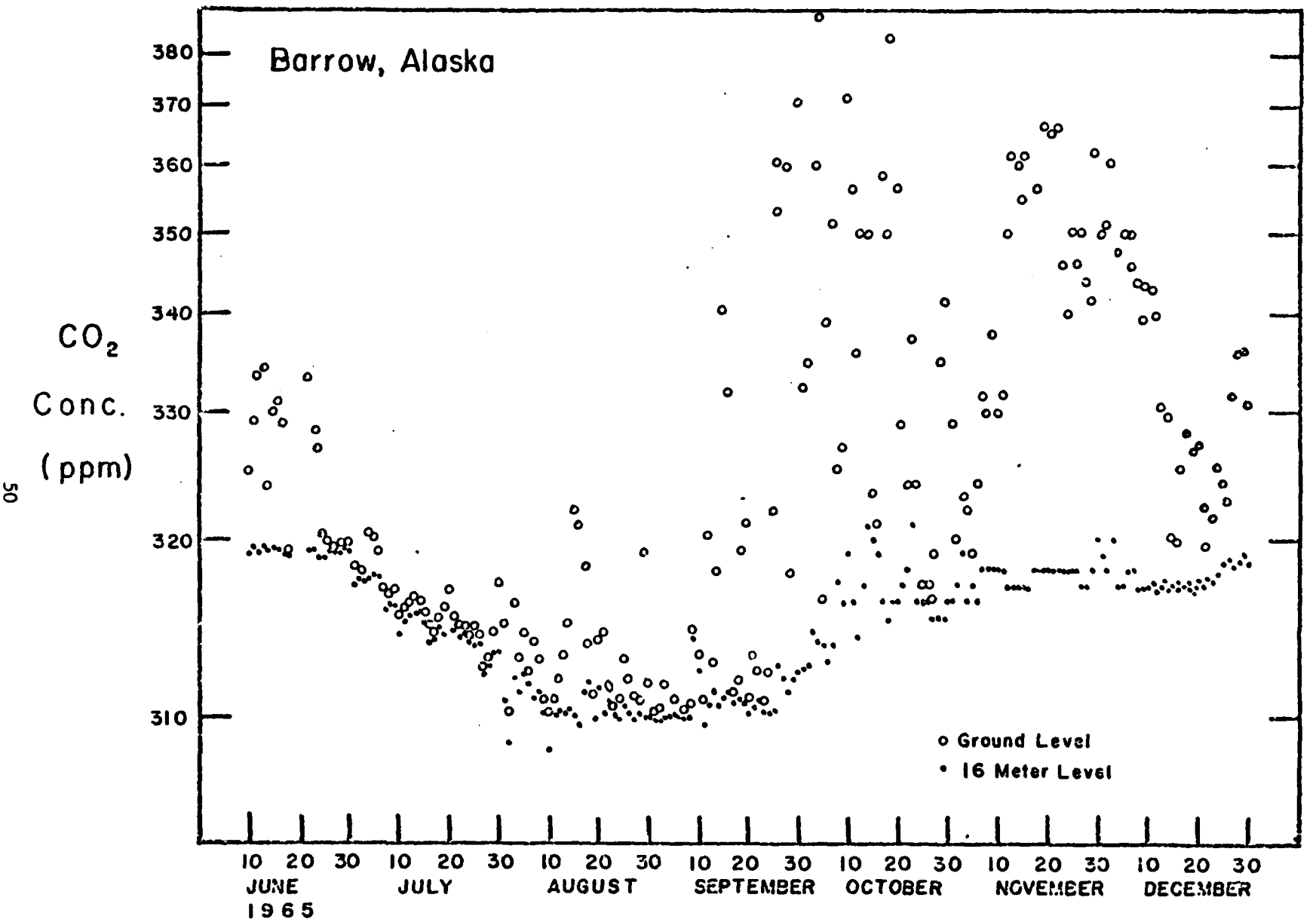

Figure 17. CO_2 concentrations at two levels in the atmosphere near Barrow, Alaska (North Meadow Lake).

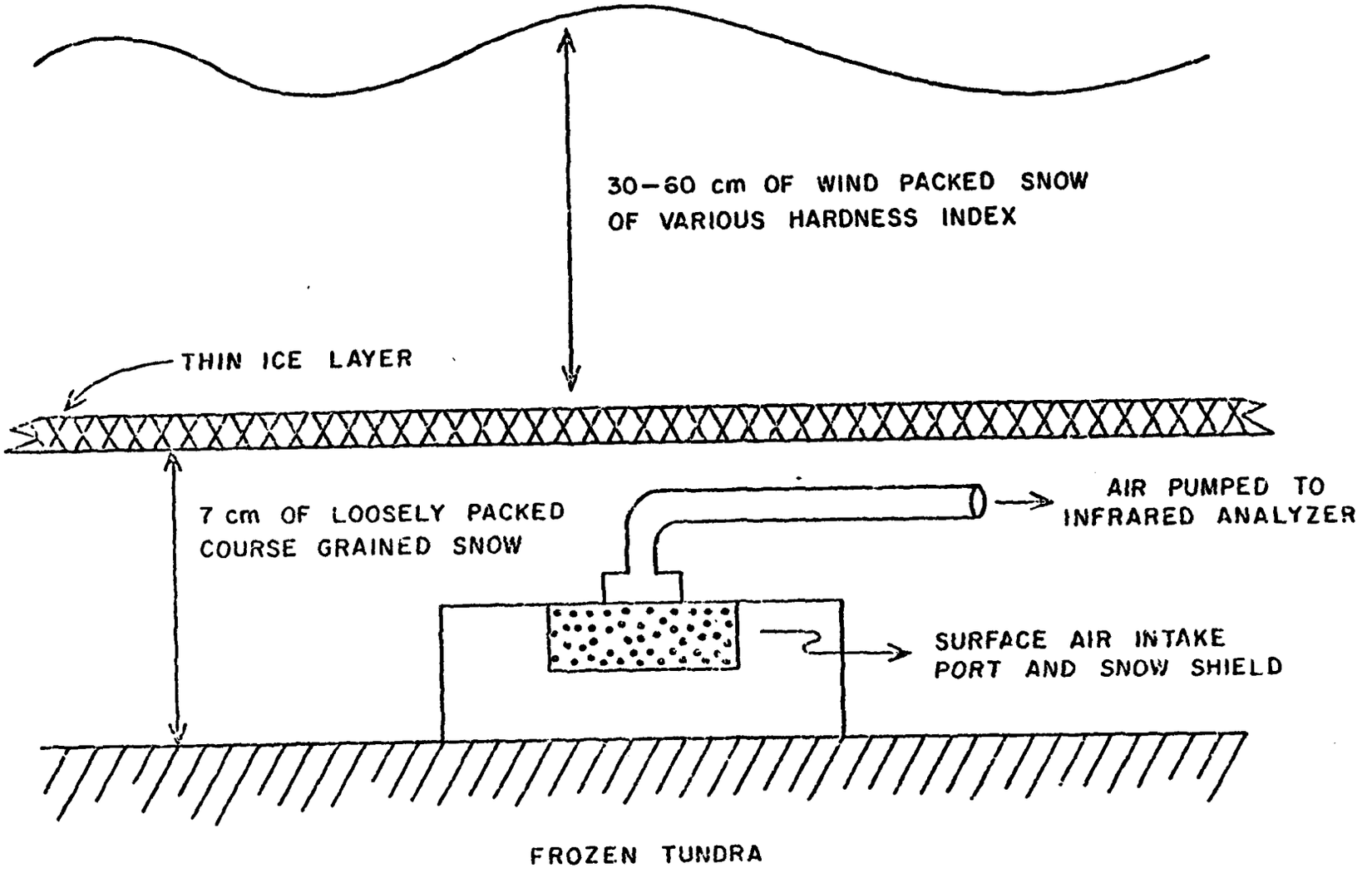

Figure 18. Location of ground air sampling port and vertical cross section of snow.

wind packed snow accumulated, reaching a maximum depth of 30 to 60 cm in April and May. The ground remained snow covered until the end of June.

A comparison of the monthly average CO_2 concentrations at the ground level and at 16 m, from September 1965 to June 1966, indicates that maximum concentrations of CO_2 at ground level occurred during the early winter months of November and December, 1965, and again in June 1966. The monthly average values of CO_2 as computed from daily means, show in all cases that the ground level concentrations of CO_2 were higher than those of the ambient air (Figure 19). Observations of average daily wind speed, ground level CO_2 concentration, net total radiation, and tundra surface temperature are given in Figure 20. The CO_2 concentration increased rapidly after the first snow cover in September. The temperature of the uppermost 8 cm of soil remained above freezing for most of September. By October the tundra was frozen at all depths.

It should be indicated here that the unfrozen surface layers refreeze bidirectionally and enter into the dynamics of CO_2 transfer during the fall of the year.

The seasonal freeze-and-thaw zone is called the active zone (Muller, 1947; Sterns, 1966). Environmental factors such as vegetation, soil moisture, exposure, temperature, and snow cover, affect the depths of seasonal freeze and thaw. Below the active zone lies the perennially frozen ground (permafrost) in the Barrow area; it is reported to be 314 m deep (McCarthy, 1952). The temperature of the tundra surface about 15 September 1965, and 20 September 1966, was within a few tenths of 0°C. At about the same time the temperature at the 16-cm level in the tundra remained relatively constant at about 0°C until all of the water in the soil above was frozen (Kelley and Weaver, 1969).

This phenomenon is called the zero curtain (Muller, 1947) with its depth and duration controlled by the available moisture, thermal properties of the soil, and weather conditions. The zero curtain effect lasts for a longer time as the moisture increases (Cook, 1955). The zero curtain occurs when the air temperature falls below 0°C followed by a rapid drop in soil temperature which holds at the freezing point because of compensation by the latent heat of fusion given off by the ground water until it has turned to

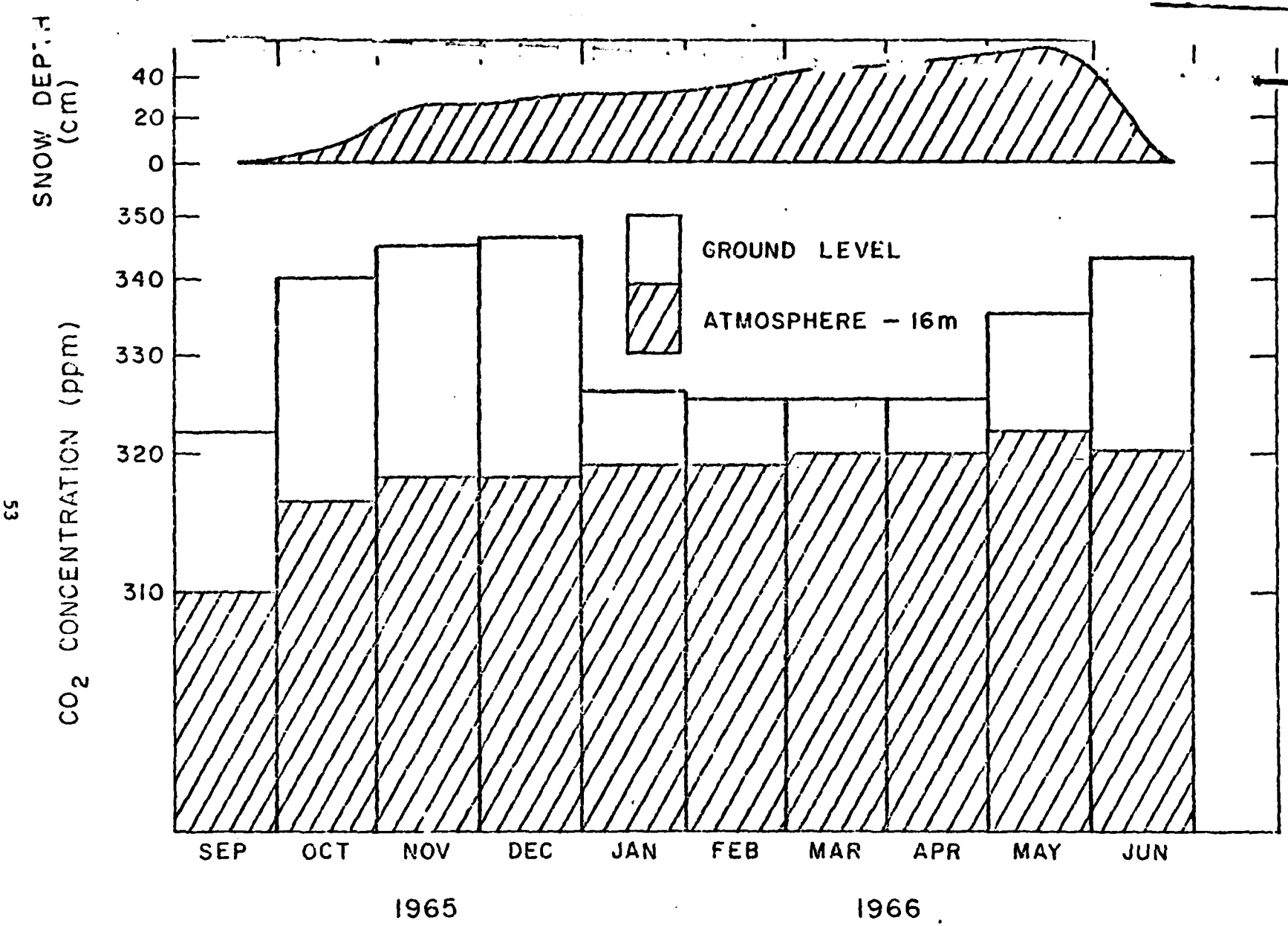

Figure 19. Average monthly concentration of carbon dioxide in the atmosphere and at the tundra surface (near Barrow, Alaska).

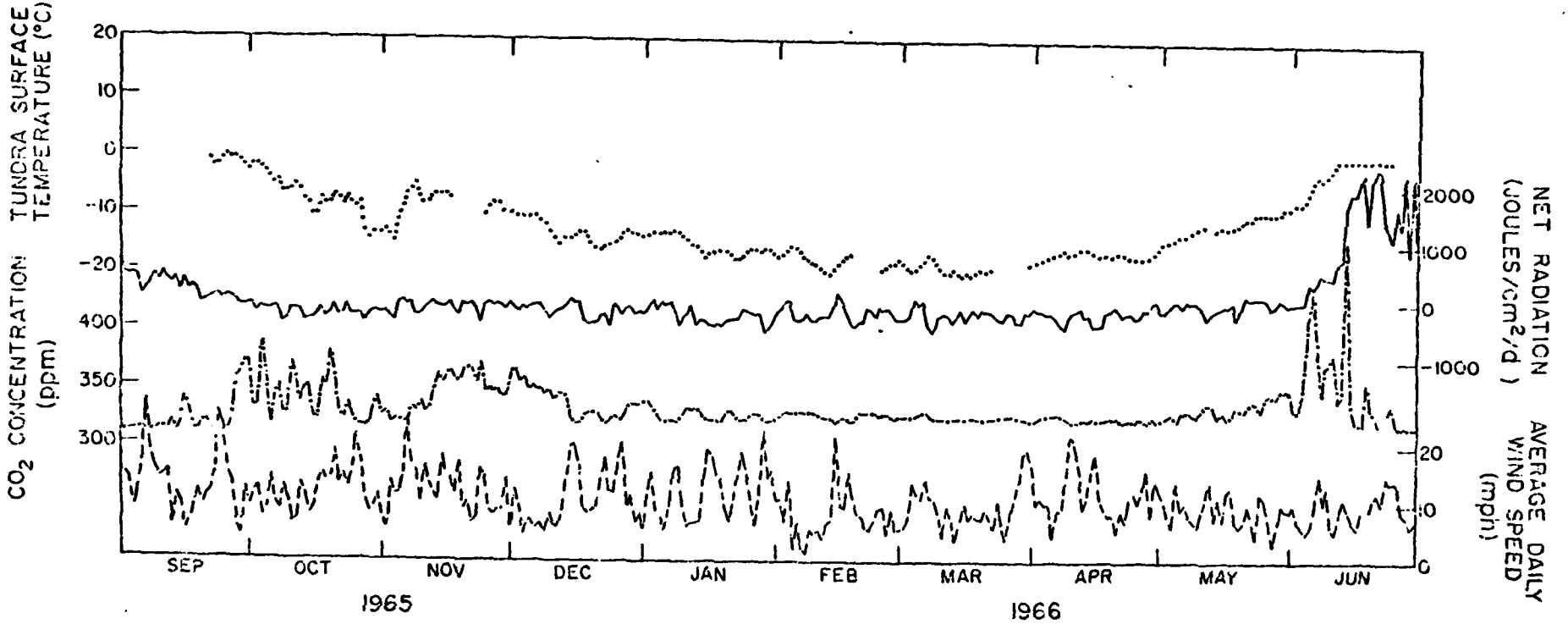

Figure 20. Average daily concentrations of atmospheric ground level CO_2 (dot-dashed), ground level temperatures (dotted), net solar radiation (solid), and average wind speed (dashed) at North Meadow Lake.

ice. This process lasted about two weeks in September 1965 and more than a month in 1966.

As soon as the tundra surface was frozen, the temperatures of the near-surface layers began to rise, reaching a maximum on 16 September 1965, and 26 August 1966. Within three days after the rise, the temperatures of the underlying layers fell again, and remained near 0°C for about two weeks in 1965 and nearly a month in 1966.

The CO_2 concentration at the surface showed only minor interdiurnal variations until the first snow cover. After the snow cover became permanent, there were wide variations fo CO_2 concentration from day to day (September through December). For example, from October 3 to 5, 1965, the ground level CO_2 concentrations decreased by 75 ppm by volume compared with a 1 ppm decrease in the air above. Ground level CO_2 concentrations varied indirectly with wind speed 63% of the time which suggests that the accumulated CO_2 within the snow canopy is more rapidly released under conditions of high wind speed.

By late December, ground level CO_2 concentrations decreased rapidly and showed less variation until late spring. Rapid changes in subnivean CO_2 began to occur in early May. Through late May and June, subnivean CO_2 concentrations showed marked daily variations as did net radiation and tundra surface temperatures. During this period the snow ablation rate was high, due to a rapid increase in net total radiation. Eventually the snow cover became so thin and perforated by the erosion of percolating water that the CO_2 concentrations at ground level approached that of the atmosphere at 16 m. A significant feature of this period was the large variable increases noted in June (Figure 20).

3.2.1 Release of CO_2 From Freezing Tundra Soil.

An investigation was undertaken by Coyne and Kelley (1971) to explain the source of subnivean CO_2 observed (1965-1966) at Barrow (Kelley *et al.*, 1968).

Soil cores, 2.5 cm in diameter, were collected from five sites in northern Alaska during 17-20 September 1970. The cores included organic and mineral material extending from the tundra surface to the level of

permanently frozen ground. Core length averaged 24 cm ranging from 17 to 31 cm. The cores were sealed, weighed, and stored at 4°-10°C until subjected to laboratory analysis.

The cores were weighed at the time of analysis to verify that water loss during storage was less than 1%. The experimental array for analyzing CO_2 changes under freezing conditions in shown in Figure 21.

The cores were then cooled to freezing temperatures during which CO_2 was monitored by infrared gas analysis. This was accomplished by placing the cores in a 2.5 cm diameter cylindrical "Pyrex" chamber with ball and socket joints to accommodate air intake and outlet, and a thermocouple to monitor core temperature during analysis. An ascarite cell in the intake line provided CO_2 free air to the core. CO_2 detected by the analyser in the outflowing air stream was concluded to be of core origin.

A series of accurately controlled CO_2 reference gases were used to calibrate the analyser. CO_2 from the cores and temperature were recorded simultaneously on a two-channel strip chart recorder. Total water content and pH were determined for each core subsequent to freezing.

The section of the CO_2 curve of particular interest in this investigation (Figure 22) corresponds to the period of phase change of the soil moisture. An important assumption was made that the evolved CO_2, represented by the area under the curve in Figure 22, above the dashed line, must be due to freezing of the core. A biological source is ruled out or diminished in importance in that biochemical reaction rates normally vary directly with temperature. Since core temperatures were held constant at 0°C during phase change, CO_2 production from biological sources would be expected to remain constant or perhaps be inhibited by solidification of the soil water.

The results of the analyses are shown in Table 10.

Assuming the lowest CO_2 quantity (0.1 µl/g) observed reflects the natural system and is constant over the tundra surface, approximately 500 l/Ha would be released from the surface 30 cm by the freezing process. A corresponding release for the highest observed value (2.0 µl/g) would be 90,000 l/Ha. The CO_2 thus released from solution apparently escapes to the

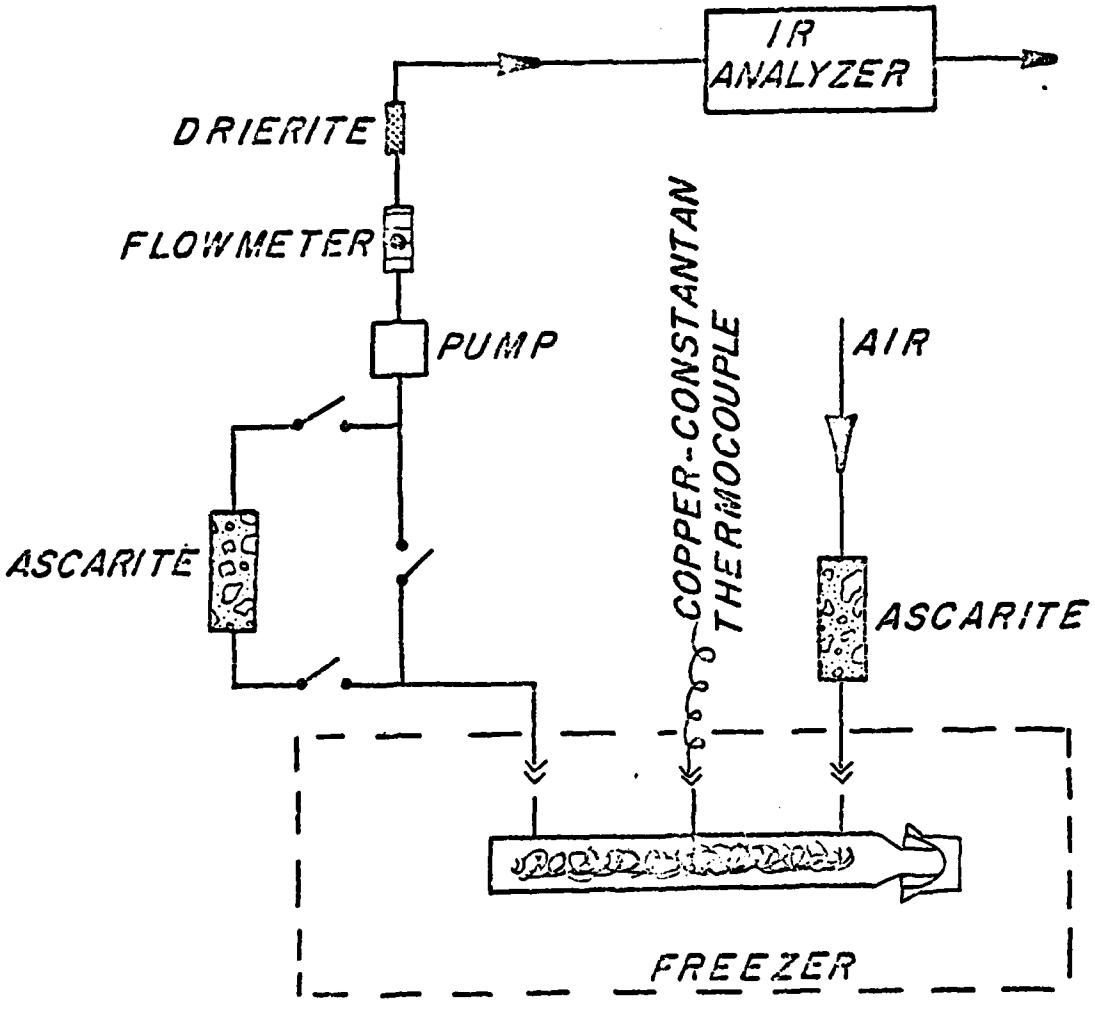

Figure 21. Experimental array for the determination of CO_2 release from freezing tundra soil cores.

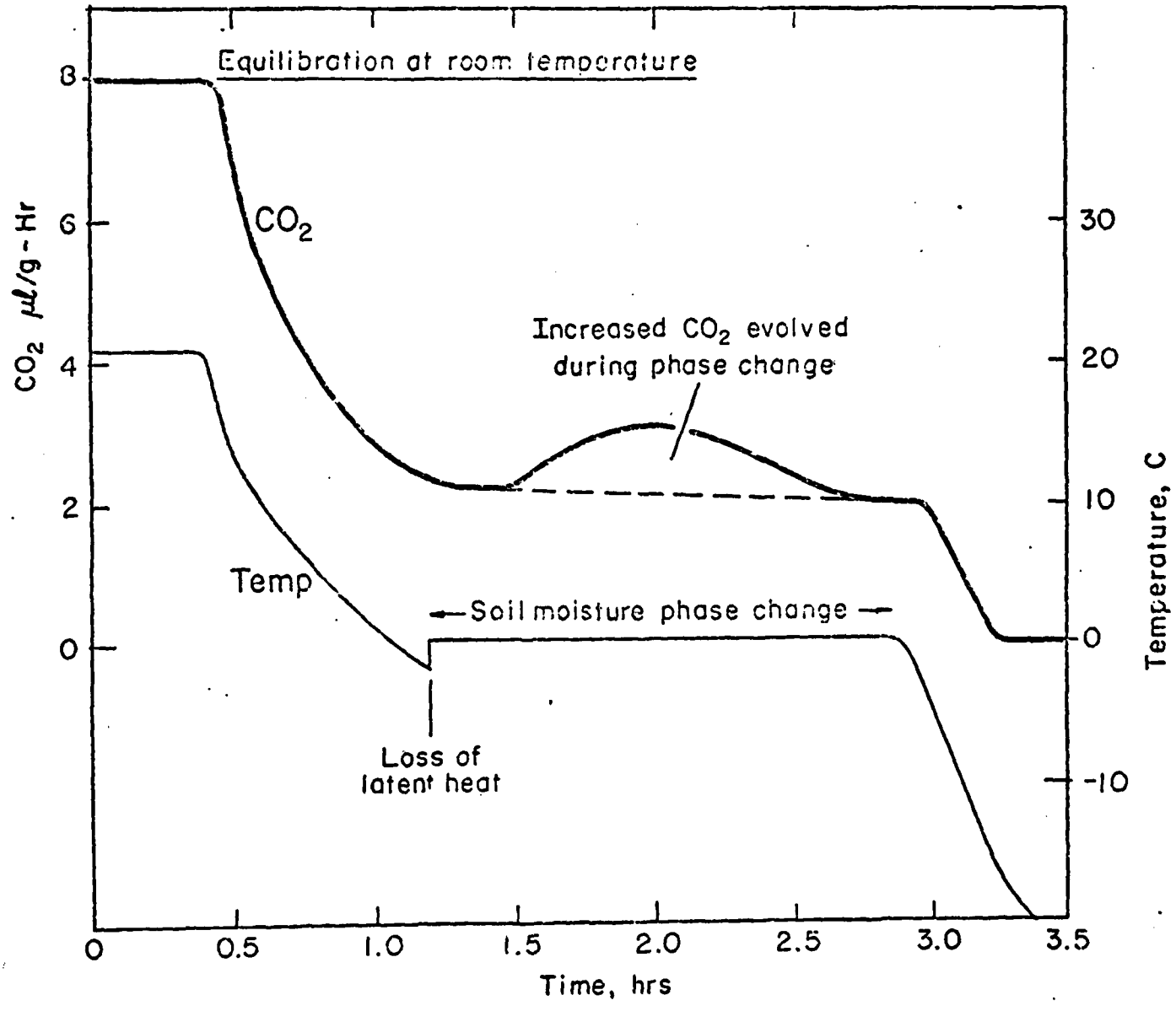

Figure 22. Evolution of CO_2 relative to temperature from a freezing tundra core (after Coyne and Kelley, 1971).

Table 10. Carbon dioxide concentration evolved from freezing tundra soil cores (after Coyne and Kelley, 1971).

Habitat	CO_2 µl/g dry soil	pH	Moisture content % wt
Umiat - Colville River floodplain	1.5	4.4	97.4
	1.0	4.9	77.9
	0.8	4.5	89.1
	0.5	4.7	92.9
	0.9	4.6	116.0
	1.2	4.9	83.3
	0.7	4.7	62.7
	0.9	4.9	66.5
	2.0	5.1	67.4
Barrow - wet sedge meadow	0.4	3.7	57.5
	0.3	3.7	76.4
	0.1	3.8	46.8
	0.1	3.7	54.9
	0.7	3.9	109.1
	0.6	4.1	63.8
Barrow - marsh	0.1	4.5	44.3
	0.2	5.1	40.9
	0.2	5.1	46.1
	0.1	5.1	44.8
	0.1	4.8	53.3
Barrow - raised beach ridge	0.1	4.3	30.1
	0.1	4.3	36.6
	0.7*	5.2	51.6
Barrow - raised beach ridge	0.1	5.2	33.8
	0.8	5.2	34.5
	0.2	5.0	38.9

*Data for this core are graphed in Figure 22.

atmosphere at varying rates throughout the period when soils are frozen. Greatest rates of escape occur in the autumn and spring.

During the summer, decomposition within the active layer of tundra results in a soil saturated with CO_2 (Johnson and Kelley, 1970). As the soil freezes, CO_2 should be evolved. Unlike the trapped gas that appears in the center of an ice cube when a volume of water is frozen, a soil core represents a different situation. The presence of plant roots, organic matter, and soil particles, allows many routes for entrained gas to escape.

The "ice cube" effect was apparently observed when autoclaved bentonite saturated with CO_2 enriched water was rolled into cores and subjected to the same freezing treatment as the soil cores. No increase in evolution of CO_2 occurred on freezing. The possibility that a high proportion of the CO_2 remained dissolved in unfrozen, interfacial water in the clay core, cannot be discounted.

Cores that provided the highest evolution of CO_2 were characterized by coarse texture and high moisture content. Cores collected from a sandy bluff along the Meade River, 100 km south of Barrow, were relatively dry and showed no increase in CO_2 evolution on freezing (not included in Table 10). Cores from a beach ridge near Barrow which contained much gravel mixed with silt and clay size particles and with 5 to 15% higher moisture content than the Meade River cores, had detectable CO_2 evolution.

The cores in this investigation were frozen from the surface to the center. Since the tundra freezes bidirectionally, sub-freezing temperatures at the soil surface and at the upper surface of the permanently frozen ground give rise to two freezing fronts. As these two fronts approach each other in the autumn, CO_2 is evolved into the unfrozen layer. Some of the CO_2 may escape to the tundra surface in proportion to texture, cracking, and other avenues of escape producing a highly variable autumn rise in CO_2 concentration as observed by Kelley *et al.* (1968). Some CO_2 may become trapped within the freezing active layer and may slowly escape, causing a soil surface CO_2 level slightly higher than ambient air during the winter months.

Associated with the increase in tundra surface temperatures in the spring is an increase in the subnivean and ambient concentrations of CO_2. Further release of trapped gas as a result of differential warming of the

soil may be the source of the spring rise reported by Kelley *et al.* (1968). Amplification of this spring rise by biological systems cannot be ruled out once minimal conditions for growth and assimilation are met.

3.2.2 CO_2 Variations Across the Snow-Air Boundary During Late Spring.

Based on the results of Coyne and Kelley (1971; Section 3.2.1). As the soil begins to warm differentially from the surface in spring, but while temperatures are still below -10°C, pockets of trapped gas may be released quite suddenly at the snow soil interface.

In order to further investigate the phenomenon of the high concentrations in subnivean CO_2 during late spring (Coyne and Kelley, 1973) air sampling ports were positioned in an area of drifted snow on the tundra during the spring of 1971.

The study area was located on the U.S. IBP Tundra Biome intensive site (Site II, 71°17'42"N, 156°41'10"W), approximately 2.5 km south of the arctic coast and 5 km northeast of the village of Barrow. This area was selected in order to have sufficient snow depth to allow a vertical array of sensors and because two distinct layers were present. The lower port was at ground level, the second and third were in the snow at 25 and 50 cm above the soil surface respectively, and the fourth was at a height of 100 cm and sampled ambient air. Air was pumped through approximately 20 m of 1 cm diameter polyethylene tubing to an automatic switching manifold. The CO_2 concentration of the air streams was measured sequentially by shunting each stream to an infrared gas analyzer (MSA LIRA 200). A reference gas of known CO_2 concentration was also part of the sequence. During sampling, flow rate was maintained at 0.5 ℓ/min and water vapor was removed prior to analysis by a dry dessicant. Between sampling, the air lines were continually flushed at 2 ℓ/min. Five minutes were programmed for sampling each level and the cycle was completed every half hour on a near-continuous basis from 1 May to 9 June 1971.

A problem associated with continuous sampling of subnivean air at a specific datum level is concerned with the heterogeneous structure of the snow and horizontal and vertical diffusional resistance. Some of the air may have been aspirated from above or below the level at which the sampling

port was located, thus disturbing the gradient even though the sampling rate was kept low. Variations in CO_2 gradients within the snow pack would occur because of errors of this kind, but these errors would have little effect on the interpretation of the variations of CO_2 observed between subnivean levels and atmospheric CO_2 levels.

The gas analyzer was calibrated periodically with specially prepared mixtures of CO_2 in nitrogen using a mutual calibration scheme described in Chapter 1. Accuracy of CO_2 measurements, based on the manometrically controlled reference gases in the concentration range of air, was approximately 2 ppm. During the sampling period, CO_2 concentrations ranged from 325 to 2000 ppm. Accuracy of the measurements decreased in proportion to the increase in concentration range and was possibly no better than ± 5% at the upper end of the range. A calibration curve for the gas analyzer was determined over the range 0 to 2200 ppm. This method has been described by Kelley and Coyne (1973). Using zero gas as 300 ppm, departure from the linear was evident at about 700 ppm, and beyond this value data were adjusted upward to correct for the non-linear response of the gas analyzer. A linear interpolation was used to normalize sequential data from each sensor to a common time base, the hour and half hour. Interpolations were not used when sample points were separated by more than 30 minutes.

The physical characteristics of the snow cover in the study area have been described by Benson (1969) and Weller and Benson (1971). The snow in the vicinity of the sensors fit the two-layer type, characterized by a hard, fine-trained, high density (0.35 to 0.40 g/cm^3), windpacked layer or often a wind slab underlain by a soft, coarse-grained, low density (about 0.20 g/cm^3) layer which is almost entirely depth hoar. Depth hoar develops at the base of the snow cover by recrystallization directly from water vapor when a temperature gradient exists in the snow.

The lowermost sampling port was at the base of the depth hoar while the second port was approximately 5 cm above the depth hoar-wind slab interface. The third port was initially near the top of wind slab but was closer to the middle of the slab layer, by the end of the sampling period. On the night of 13 May, approximately 25 cm of fresh snow were deposited. This layer gradually increased in density and hardened into a slab by wind

action. Snow depth in the vicinity of the sensors ranged from 67 cm at the start of the study, to a maximum of 95 cm on 14 May, to 45 cm by the end of the sampling on 9 June. Average depth for the 40-day period was 72 cm. Snow depths on the open tundra isolated from drift traps ranged from 10 to 40 cm (Weller and Benson, 1971).

Thermocouples positioned at the air intake ports were monitored continuously from 17 May to 2 June. Soil surface temperatures at 3-hour intervals were made available for the entire period from areas of similar snow cover adjacent to the study area by U.S. Army CRREL (USIBP, Tundra Biome Project 3741). Continuous air temperature and wind speed were obtained from the National Weather Service at Barrow.

The CO_2 differential for the first 13 days of May (Figure 23) was relatively constant with air in the snow being approximately 20 ppm more concentrated than the air above the snow. An increase in the CO_2 differential across the pack was detected on 14 May which corresponded to an increase in snow depth of approximately 25 cm in the area of the sensors and thus an increased diffusive resistance to the subnivean CO_2. A rather large injection of CO_2 was observed during 19-20 May. Points on the curve included only 10 half hours from 0000 to 1330 hours for 18 May and 16 half hours from 1600 to 2330 on 19 May. Sampling during several days on either side of the mid-May peak was nearly continuous throughout the 24-hour period. Therefore, the peak for 19 May may be somewhat inflated. However, 24 consecutive half-hourly sample points from 1600 on 19 May to 0330 on 20 May had a mean CO_2 differential of 484 ppm showing that the occurrence of the peak was real.

The soil surface had begun to warm noticeably on about 10 May, but the active layer temperature was still well below -10°C at the time of the 19 May peak (Figure 23). The injection may have been the release of a trapped volume of gas possibly resulting from expansion of the soil matrix as heat was absorbed at the surface. Soil temperatures rule out soil biological activity as the CO_2 source for the injection in light of the results of Benoit *et al.* (1972) and Flanagan and Scarborough (1972).

One subnivean biological CO_2 source, the brown lemming (*Lemmus trimucronatus*) cannot be completely eliminated as the case of this peak.

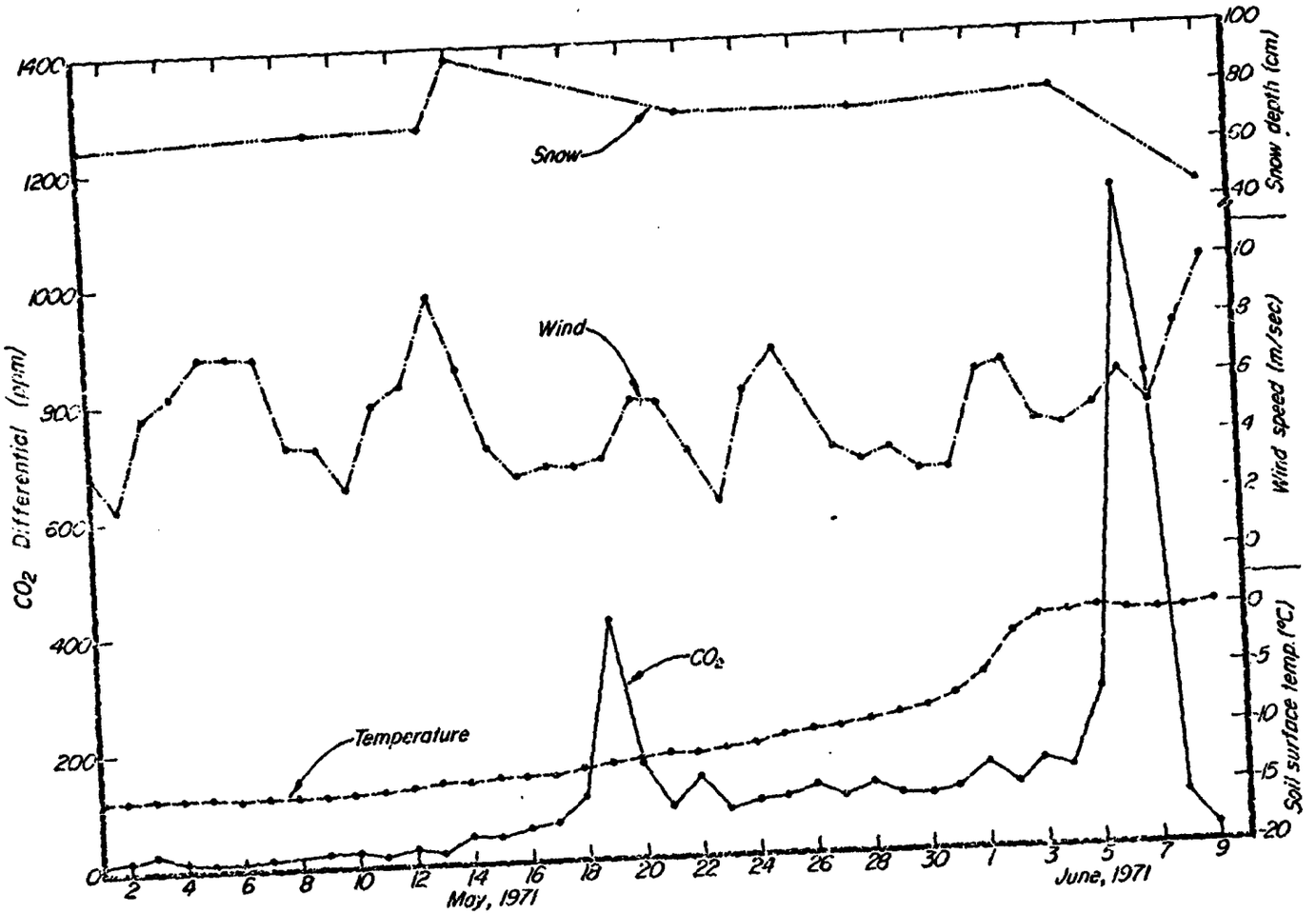

Figure 23. Snow depth and daily mean wind speed, soil temperature, and CO_2 differential (between the snow at 25 cm above the soil surface and ambient air at 100 cm). The CO_2 concentration differential across the entire snowpack equals approximately 1.4 times the CO_2 differential shown.

Studies of brown lemmings in summer indicate they are not gregarious animals (H. R. Melchior, personal communication). Except for females with young, adult lemmings usually occur singly or in pairs. Lemmings rarely remain in one location for more than 4 or 5 hours yet high subnivean CO_2 ground surface concentrations remained stable for as long as 12 hours. Summer observations further indicate that it would be highly unlikely for more than two lemmings to occupy the same burrow system unless there was a female with young. This latter situation can be ruled out on the basis of time, since the young could be expected to remain in the nest for up to 14 days while the peak injection period began and ended in less than two days.

Wind speed during a several day interval preceding the mid-May peak was low compared to the entire sampling period (Figure 23). Yen (1965) reported that increased air flow over snow reduced resistance to the simultaneous transfer of heat and mass. If low wind stress were the cause of the observed CO_2 increase, similar responses would be expected at other times when wind stress was low.

A simple correlation coefficient between the CO_2 differential and wind speed for all data was zero. Kelley *et al.* (1968; Section 3.2) also found no statistical association between subnivean CO_2 and wind speed on a seasonal basis but graphically determined that ground level CO_2 concentrations varied indirectly with wind speed 63% of the time. Perhaps, the variable time lag between changes in wind conditions and CO_2 response obviates attempts to show a statistical cause and effect relationship.

Plots of the data on a diurnal basis indicated that the CO_2 differentials varied indirectly with wind speed during certain periods but varied directly with wind speed during other periods. Simple correlation coefficients between wind speed and CO_2, using all data points for a single date, ranged between ± 0.9 with a mean r of -0.1 and a standard deviation of 0.5. Mean daily wind speed for the period 16-19 May was relatively constant ranging between 3.2 and 3.7 m/sec. If the injection peak resulted from low wind speed, it should have occurred before the 19th. The rapid decline in the CO_2 differential on the 20th, may have been a reduction in CO_2 evolution from the soil and/or the result of wind aspiration, since the mean wind speed

for this day increased to about 6 m/sec. The simple correlation coefficient between CO_2 concentration and wind speed for 20 May data was -0.7.

Following a secondary peak in the CO_2 concentration on 22 May the CO_2 differential leveled off and increased only slightly until the end of May. CO_2 differentials between the injection peak of 18 and 19 May and the end of the month were about 80 ppm higher than those prior to the injection peak. The higher post-peak CO_2 differentials could have resulted from either an increased rate of CO_2 release at the soil surface and/or an increased diffusive resistance to CO_2. The latter is supported by an average snow depth approximately 5 cm greater after the peak than before. Soil temperatures between 22 and 31 May were probably still too low to support appreciable soil respiration. However, efflux of CO_2 from the soil in response to a gradual warming of the active layer may have increased the rate of CO_2 release to the subnivean environment. June 1 was the approximate date when soil surface temperatures reached -7°C and the CO_2 differential was extremely sudden, rising from less than 300 ppm at 1030 on 6 June to nearly 800 ppm at 1100 to over 1200 ppm at 1230. By 1400, the differential exceeded 1500 ppm. The predicted ground level concentration [(1.4 x 1500) + ambient air CO_2] at 1400 was nearly 2500 ppm. The CO_2 differential between the 25 cm sensor and the atmosphere, remained above 1000 ppm for nearly 24 consecutive hours with half of this period greater than 1200 ppm.

It is improbable, that decomposition processes at the soil surface, could respond this suddenly without temperature increasing at a corresponding rate. Allowing for higher temperatures than indicated, due to differences in the microenvironment, and assuming a Q_{10} of 3 where Q_{10} is the increase in reaction rate for a 10°C temperature change, it is doubtful that the peak was the result of respiratory products. The ground temperature sensors remained near 0°C throughout this period. Benoit *et al.* (1972) have observed a depression rather than an acceleration in soil respiration, as the soil solution undergoes a phase change near 0°C. On the other hand, respiratory products must contribute a portion of the total subnivean CO_2, a portion that is probably more commensurate with the pre-peak activity level considering the similarity of soil surface temperatures before and during the peak.

Extracellular enzyme systems are another possible source of CO_2 apart from biological respiration. Evidence for the existence of extracellular enzymes in an active state has been reviewed by Skujins (1967). Little is known, however, of the significance of these enzymes and their activities in relation to their environment because of the strong binding of proteins by soil colloids making isolation difficult. Thus information is lacking which might allow speculation on the CO_2 contribution of reactions catalyzed by extracellular enzymes. Certainly, the immediate products of most reactions tabulated by Skujins (1967) for which enzyme-like catalysis has been detected in soils do not include CO_2.

As with the mid-May peak, lemmings cannot be totally eliminated as the cause of the late spring CO_2 injection, as lemming activity was significant at this time. Brown lemming abundance fluctuates markedly with peak numbers occurring at 3 to 7 year intervals (Pitelka, 1972). The last peak was in 1965. Kelley *et al.* (1968; Section 3.2) observed similar subnivean injections of CO_2 during the spring of 1966, a year of very low lemming numbers, which is additional evidence against lemmings causing the two observed peaks in 1971. The quite rapid decline of the subnivean CO_2 after 7 June reflects the increase in ablation and snow porosity as melt water percolated through the pack and the corresponding increase in wind speed.

Observation of inundated areas during spring breakup offered a final bit of evidence to support the hypothesis that the observed injection peaks in this study and that of Kelley *et al.* (1968) resulted from release of trapped gas pockets by physical processes. Very frequently, large gas bubbles up to approximately 4 cm in diameter, were observed escaping from surface cracks at frequencies of 1-3 per second for periods of several hours or longer. This obviously was the release of trapped gas through soil fractures. The hypothesis purporting a slower leakage between peak injection periods is supported by the soil core experiment (Coyne and Kelley, 1971) and appears in part a function of temperature.

The effect of the temperature gradient across the snowpack on the magnitude of CO_2 differentials was not readily apparent from the data. The simple correlation coefficient between the CO_2 differential and soil surface temperature for all data during the sampling period was 0.5. The

correlation between CO_2 differential (25 to 100 cm) and temperature differential (25 to 100 cm) across the snowpack was approximately zero. Air temperatures fluctuated widely in relatively short time intervals compared to soil surface temperatures which had only slight diurnal variation. This would tend to reduce the calculated association of these two parameters. For the period 18 May to 2 June extensive snow temperature data were recorded. To eliminate the variability of air temperatures the intra-snow temperature difference between 0 and 50 cm was used for comparison to the CO_2 differential (25 to 100 cm). The temperature differential widened steadily from 3.4°C on 18 May to 7.9°C on 2 June, while the CO_2 differential remained relatively constant (Figure 1). The effect of an increase in temperature across the snowpack on CO_2 diffusion through the snow, apparently was confounded with the effects of an increasing temperature on soil CO_2 source intensity.

Mean CO_2 concentrations for the sampling period are presented in Table 11. For the same period in 1966, Kelley *et al.* (1968) reported a mean concentration between 0 and 16 m of about 17 ppm compared with approximately 150 ppm for the present study. The most important factor causing the much higher concentration difference in 1971 was probably the greater snow depth in the drifted study area and possibly a greater CO_2 source potential represented by the substratum.

Table 11. Mean CO_2 concentrations for the period 1 May to 9 June 1971.

Sensor Location	N	Mean	Standard Deviation	Half-width 95% CI
0 cm (soil surface)	-	507	300	-
25 cm (snow)	1474	456	229	117
50 cm (snow)	1444	401	145	8
100 cm (ambient air)	1480	330	2	0.1
Differential (25-100 cm)	1481	127	214	11
Differential (0-100 cm)	-	178	300	-
Ratio difference 0-100/25-100	496	1.4	0.2	0.02

CHAPTER 4

CARBON DIOXIDE IN THE SURFACE WATERS OF THE TUNDRA

4.1 Introduction

Surface water is a significant part of the landscape of the Arctic Coastal Plain of Alaska during the summer thaw period, comprising up to 50-80% of the land area (Brown and West, 1970) and conceivably influencing the atmospheric levels of CO_2. The sizes of these water bodies form a continuum from pools only a few meters in diameter to lakes 8-16 km or more in length (Britton, 1967). In order to understand the effect of these water bodies on the variation of CO_2 in the atmosphere, an investigation (Coyne and Kelley, 1973a) was initiated to determine the CO_2 exchange between arctic surface waters and the atmosphere.

The interaction between the atmosphere and surficial water, with respect to the direction of CO_2 transfer, can be evaluated in terms of the partial pressure gradient across the air-water interface. When the partial pressure of CO_2 in the atmosphere (pCO_2) differs from that in the water (PCO_2) there is a net flux of CO_2 from one phase to the other in the direction of the smaller partial pressure (Riley and Skirrow, 1965).

PCO_2 may be mathematically related to the concentration of CO_2 in air that is in equilibrium with the water:

$$PCO_2 \text{ (atm)} = [CO_2] \text{ ppm} \times P_T \text{ (atm)} \qquad (1)$$

At 1 atmosphere pressure, each ppm of CO_2 in air which has equilibrated with the water, is numerically equivalent to a PCO_2 of 1 microatmosphere. In this work, PCO_2 is expressed on a dry air basis and P_T in equation 1 is reduced by an amount equivalent to the water vapor pressure.

For the case in which the water is supersaturated with CO_2 with respect to ambient air, an estimate of the CO_2 evasion rate can be obtained by measuring the rate of CO_2 increase in a closed, known air volume. One essential condition during the measurement is that the PCO_2 should remain nearly constant. If the water is not turbulent, a free exchange rate can be calculated. The mass of CO_2 in the air phase, Q, at any time t in the

air volume of a closed system such as a cuvette can be calculated as follows:

$$Q_t = [CO_2] \text{ cuvette} \times PCO_2 \times V \times 10^{-6} \text{ (air phase)} \quad (2)$$

where Q is in mg, $[CO_2]$ is in ppm, PCO_2 is the density in mg/cm^3 and V is the volume in cm^3. The partial pressure difference, ΔP, between the cuvette air and the water controls the rate of CO_2 diffusion into the cuvette and is given by:

$$\Delta P = PCO_2 - pCO_2. \quad (3)$$

The rate of CO_2 transfer across the air-water interface has been defined in terms of the evasion coefficient α (Bohr, 1899) in the equation

$$\frac{dQ}{dt} = \alpha A \Delta P \times 10^{-6}, \quad (4)$$

where Dq/dt in mg/min is the change in cuvette CO_2 concentration, A is the area enclosed by the cuvette (cm^2), and ΔP is in atmospheres. The coefficient, α, has dimensions of mg CO_2 $cm^{-2}atm^{-1}min^{-1}$ and is negative for transfer from the gas to the liquid phase (invasion) and positive for transfer from the liquid to gas phase (evasion). The derivative, dQ/dt can be solved either graphically or numerically and regressed on ΔP. The slope of the regression line is αA.

4.2 Methods

Diurnal and seasonal fluctuations in the partial pressure of CO_2 (PCO_2) with respect to air were measured in a tundra pond (PBP Pond C; 71°18'N, 156°42'W, location 2 in Figure 24) and North Meadow Lake (71°18'N, 159°39'W, location 3 in Figure 24) near Barrow, Alaska, in 1971 and 1972 respectively. The sampling periods and some descriptive parameters are presented in Table 12.

PCO_2 was determined by measuring the CO_2 concentration of air in equilibrium with the water by infrared gas analysis. The analytical system is depicted schematically in Figure 25. The equilibrator consisted of a floating Plexiglas cuvette (similar to a design by Kelley

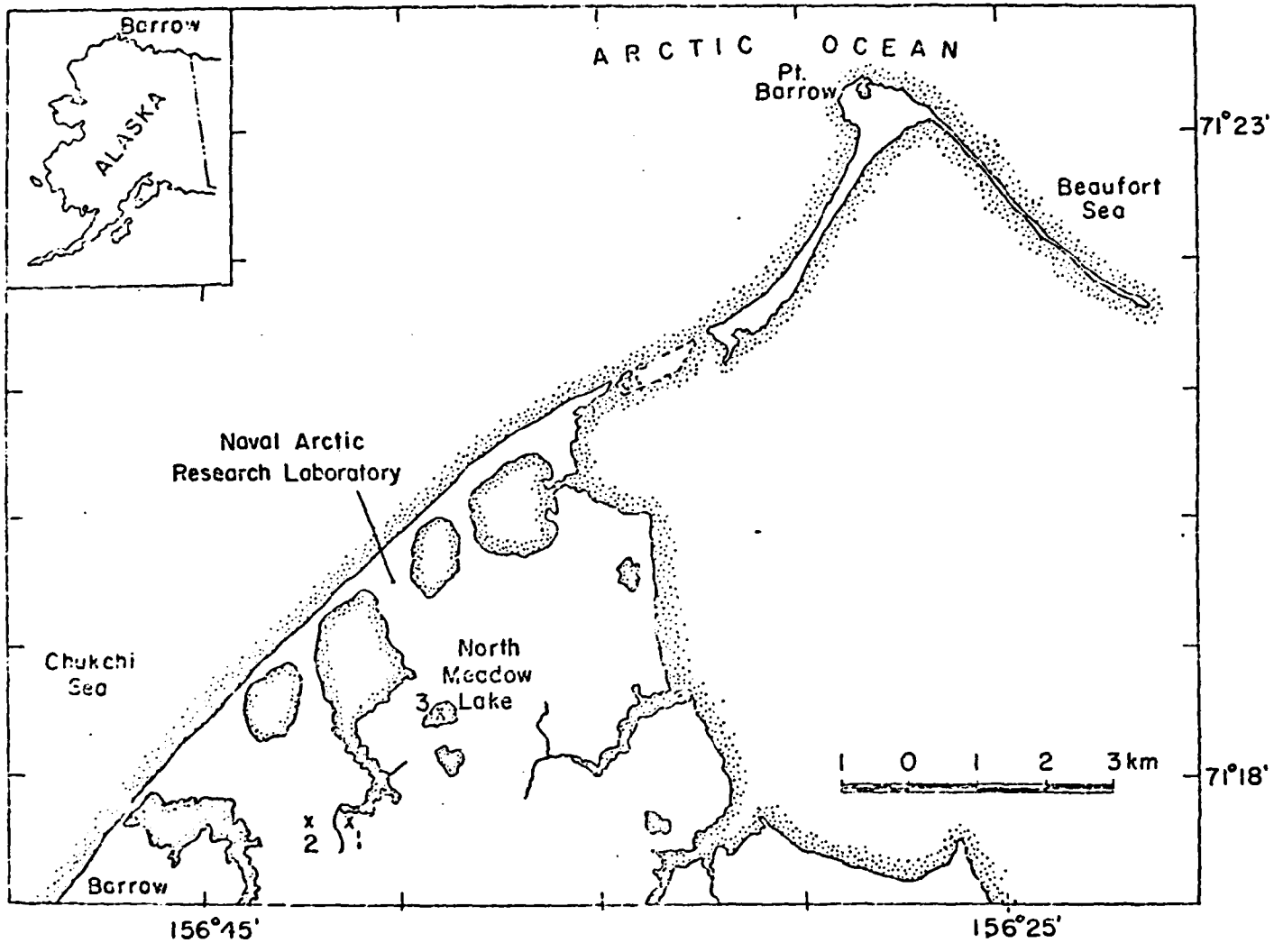

Figure 24. Location map of the study area. The pond and lake were location 2 and 3 respectively.

Table 12. Sampling dates and physical characteristics of Pond C and North Meadow Lake.

Parameter	Pond	Lake
Sampling period	9 July - 16 Aug 1971	25 June - 15 Sept 1972
Depth	40 cm	70 cm
Surface area[a]	765 m^2	116,000 m^2.
Thaw depth	30 cm	61 cm
Period of open water	Mid-June to mid-September	

[a]Measured by planimetering aerial photographs. Area includes peripheral aquatic emergent vegetation. Data from aerial photographs was provided by R. Lewellen (I.B.P. Tundra Biome Project).

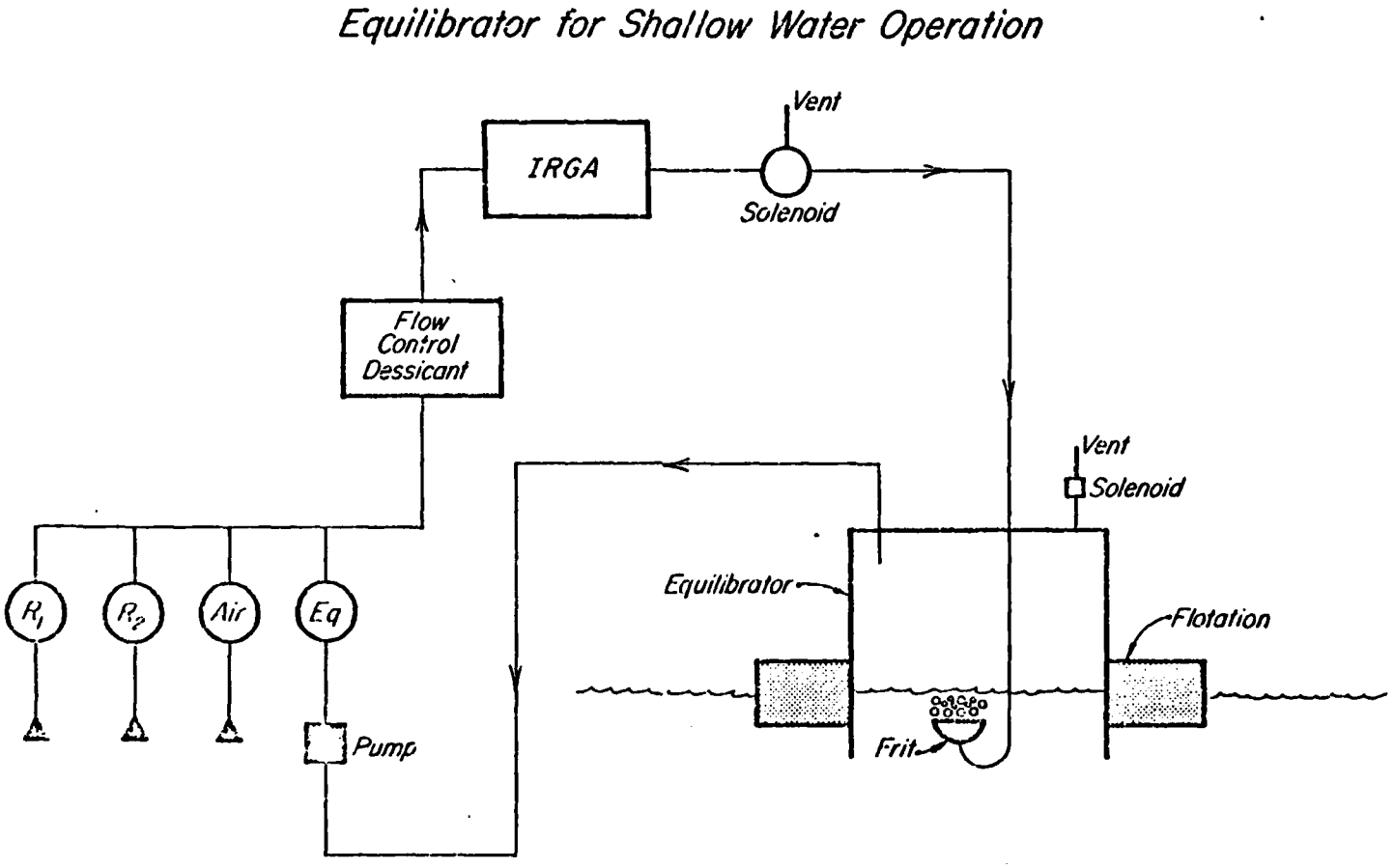

Figure 25. Schematic of system used to measure CO_2 partial pressure in the water and ambient air.

and Hood, 1971a) having dimensions 30 x 30 x 23 cm^3. An automatically switched solenoid manifold provided for sequential measurement of PCO_2, ambient air CO_2 (pCO_2) and reference gases of known CO_2 concentration. The infrared gas analyzers were calibrated by measuring the perpendicular distance between recorder traces of zero and span CO_2 reference gas standards.

Pond: Initially, the automatically switched manifold was timed for a half-hour cycle (PCO_2, 20 min; air, 5 min; reference gas, 5 min) which did not allow sufficient time for equilibration. During the period 9-26 July 1971, the system was operated manually with cycles of several hours duration. From 26 July to 16 August 1971, the system was in automatic mode with one-hour cycles (PCO_2 40 min; air, 10 min; reference gas, 10 min).

Air was pumped from the cuvette through approximately 30 m of 1.2 cm O.D. stainless steel tubing by a rubber diaphragm pump to the gas analyzer at about 1 ℓ/min (Figure 2). Short lengths of medium density polyethylene tubing (0.95 cm O.D.) were used as needed between the shore and the equilibrator for flexibility. Dry dessicant was used to remove water vapor from the air streams. Air returning to the cuvette was released through a fritted glass disc approximately 3 cm beneath the water surface. The air bubbles collected in the chamber headspace after breaking through the surface, thus hastening the equilibration process.

During a large portion of the pond sampling period, PCO_2 values were several hundred ppm higher than ambient air. To measure the high PCO_2 values, the gas analyzer had to be underspanned to remain on scale. Under these conditions, the relative error associated with ambient CO_2 measurements was unacceptable. In final analysis, ambient CO_2 data were taken from our concurrent atmospheric monitoring study (1.6 m level), located less than 1 km from the pond (Location 1, Figure 24). The CO_2 measuring system for this project was similar to the pond equipment.

Accuracy of CO_2 measurements in the concentration range of air was approximately 2 ppm. Pond PCO_2 values ranged from 450 to over 1500 ppm. Accuracy of the measurements decreased in proportion to the increase in concentration range and was possibly no better than ± 5% at the upper end of the range. A post-season calibration curve for the gas analyzer was

determined over the range 0 to 2200 ppm after procuring a higher span gas of 1088 ppm (Kelley and Coyne, 1973). Concentrations greater than 1088 ppm were achieved by pressurizing the gas at the analyzer sample cell which yielded a calibration curve for the range 0 to 2500 ppm (Figure 26).

Using 300 ppm as zero gas, departure from the linear was evident at about 700 ppm. Data greater than 700 ppm were adjusted upward to correct for the non-linear response of the gas analyzer.

Pond temperature data included ambient air and water temperatures for the entire sampling period and sediment temperatures after 17 July. Copper-constant thermocouples were referenced to an ice point instrument and the output was recorded. Accuracy was within 1°C at 0°C. The water temperature sensor was positioned approximately 2 cm beneath the water surface by attaching it to the lower side of a white styrofoam float. In this way it was shielded from direct solar radiation. The sediment temperature sensor was located about 3 cm below the sediment surface. Wind speed data (2 m level) were provided by the U.S. IBP Tundra Biome Micrometeorological project.

Lake: An automatically switched air sampling manifold was programmed for an hour long cycle allocating 40 minutes to PCO_2, 10 minutes to ambient air, and 5 minutes each to zero and span reference gas measurements. Generally the reference gas traces bracketed the sample traces. Calibration of the infrared gas analyzer was performed on a continuous basis as part of the automatic cycle. Water vapor was removed with a freeze trap maintained at -30°C. High density polyurethane tubing (Tygothane; 0.95 cm O.D.) was used between the cuvette and the analyzer, a distance of about 15 m. Ambient air samples were drawn through a 1.2 cm O.D. stainless steel mast with intake port at 4 m above the water. CO_2 and temperature instrumentation were situated inside a mobile laboratory aboard a raft anchored approximately 60 m off the north shore of the lake.

After the formation of a permanent ice layer on North Meadow Lake, a new system (Figures 27, 28) was devised to allow intermittent monitoring of PCO_2 beneath the ice. A Plexiglas container (15 x 15 x 15 cm^3) was designed for continuous water flow through the container. Water was pumped by means of a Peristaltic pump, from under the ice near the lake bottom to

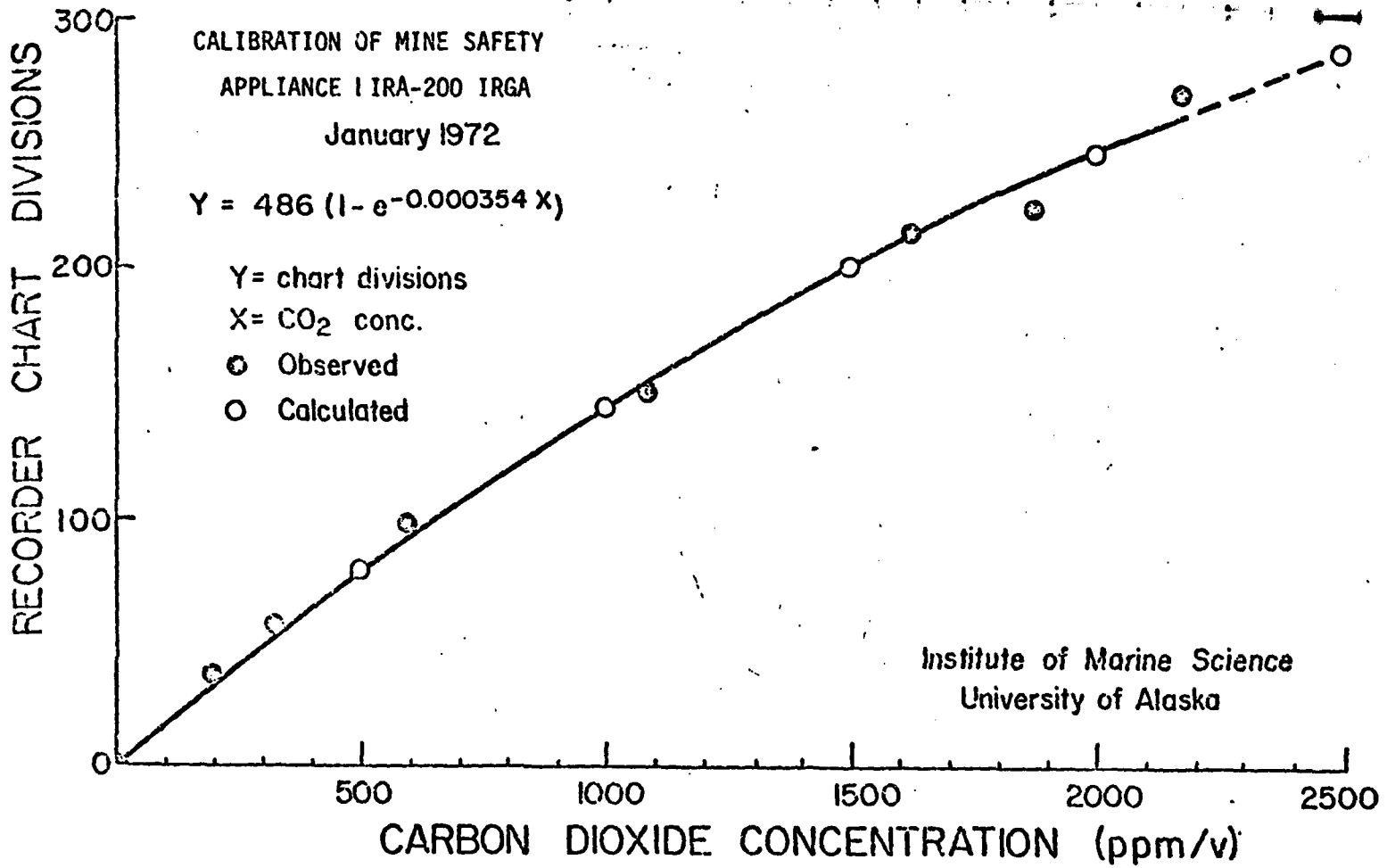

Figure 26. Calibration of infrared gas analyzer.

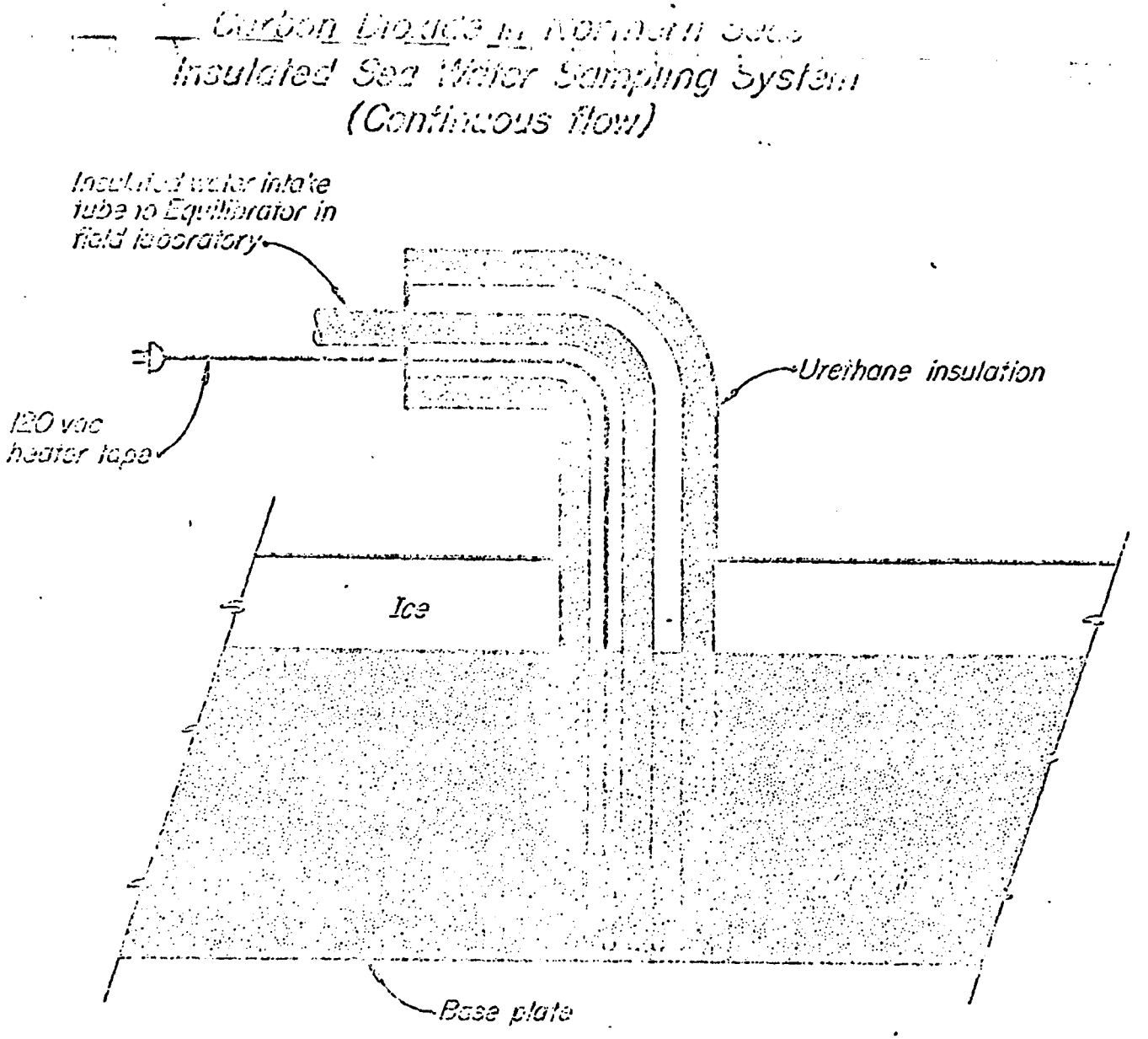

Figure 27. Array for sampling water under an ice cover.

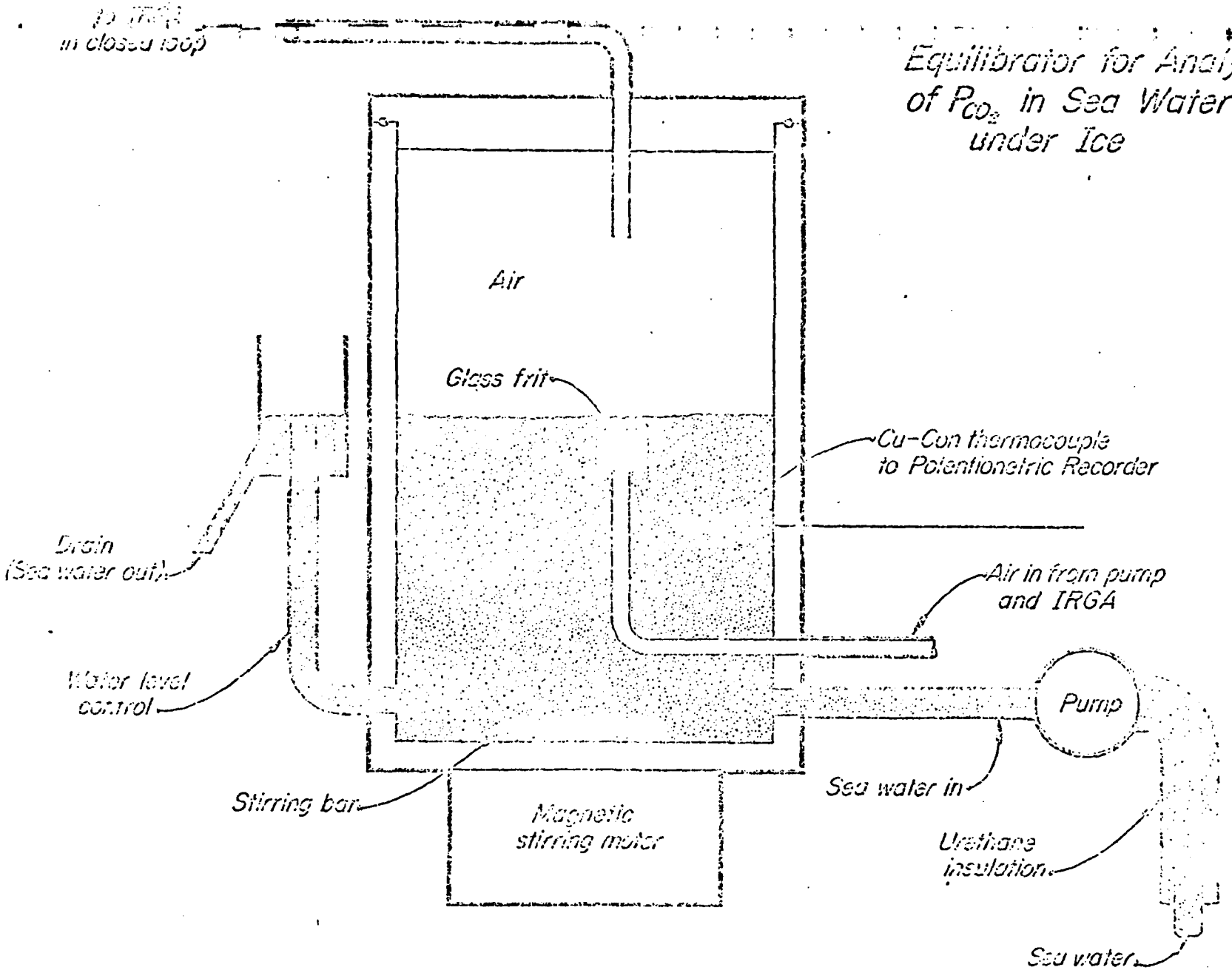

Figure 28. Small volume equilibrator for measuring PCO_2 in water under an ice cover.

the chamber inside the floating laboratory. PCO_2 was measured by determining the CO_2 concentration in air equilibrated with the water as described above. Water level in the chamber was maintained at a constant level of about 7 cm by a stand pipe. Water in the chamber was continually stirred by a magnetic stirrer to hasten equilibration, and water lines were wrapped with electric heating tape to prevent freezing. Temperatures in the cuvette were about 0.5°C higher than at the water intake below the ice.

Wind speed prior to 25 July 1972 were converted from National Weather Service (Barrow, Alaska Station). After 25 July, a propeller vane, anemometer was installed 2 m above the soil surface on a bluff adjacent to the north shore of the lake, and wind speed and direction were continuously recorded. Relief between the bluff and lake surface was about 1.5 m. The prevailing wind direction was ENE. Pond and lake data for each of the parameters were reduced from strip charts at either half-hourly or hourly intervals. All CO_2 concentrations were adjusted to standard pressure and reported in ppm (by volume) on a dry air basis.

More than 25 attempts were made to assess the CO_2 evasion rate at North Meadow Lake during the 1972 sampling period. The measurement technique included a second floating cuvette and infrared gas analyzer system similar to that used for PCO_2 measurement except that air returning to the cuvette (flowrate 0.5 ℓ/min) entered the cuvette above the water surface rather than by bubbling below the surface (Figure 25). The system is also similar to that reported by Siguira *et al.* (1963). An evasion rate experiment consisted of calibration of the analyser followed by establishment of a zero line which represented the ambient air CO_2 concentration, pCO_2. The cuvette was then placed in the water and the CO_2 in the cuvette was monitored continuously until the recorder trace leveled off. The cuvette was removed from the water and a second zero line was established to account for electronic and optical drift. The analyzer was again calibrated at the end of the experiment. Continuous observations of the equilibrium concentration of CO_2, PCO_2, in the surface water were made concurrently with the rate experiment.

An exponential decay equation of the following form was fit to the data points (t, Q_t), with Q_t being calculated as in equation 2:

$$Q_t = Q_e + (Q_o - Q_e)\ \mathrm{EXP}(-Rt) \qquad (5)$$

where Q_e is the asymptote, Q_o is the intercept, and R is the time sensitivity coefficient. Q_t is monotonically increasing if Q_o (Q_e at t=0) is less than Q_e, or monotonically decreasing if Q_o is greater than Q_e. The data conform to the former case. The derivative of equation 5 (dQ_t/dt), was solved at times t for which discrete data were available for ΔP (see equation 3). A simple linear regression analysis was used to determine the evasion rate. The dependent variable dQ_t/dt was regressed on ΔP with the regression line being forced through the origin. The slope of the regression line is the product of the evasion rate coefficient and the surface area of the water included by the exchange measurement (see equation 4).

4.3 Results and Discussion

The seasonal courses of daily means of temperature, wind speed, and CO_2 gradient ($PCO_2 - pCO_2$) for the pond and lake, are presented graphically in Figures 29 and 30. Missing wind speeds were derived from National Weather Service data (Barrow Station) by correlating wind data obtained at the site of the experiment, with Weather Service data before and after each period of missing data. Missing CO_2 gradient data in Figure 29 were predicted from a multiple regression equation which included independent variables of wind speed and air, water, and sediment temperatures. The regression explained only 58% of the variability in the CO_2 gradient, and the standard error of estimate was 143 ppm. Predicted values were not included in seasonal means discussed below. Pond water was supersaturated with CO_2 with respect to air throughout the period of sampling. A short interval of undersaturation (10-13 July 1972) was observed for the lake (Figure 30). The short period of undersaturation may have been caused by a photoplankton bloom. However, no pH, oxygen or nutrient data are available to support such speculation. Pond measurements included approximately the middle half of the period of open water, while lake measurements spanned

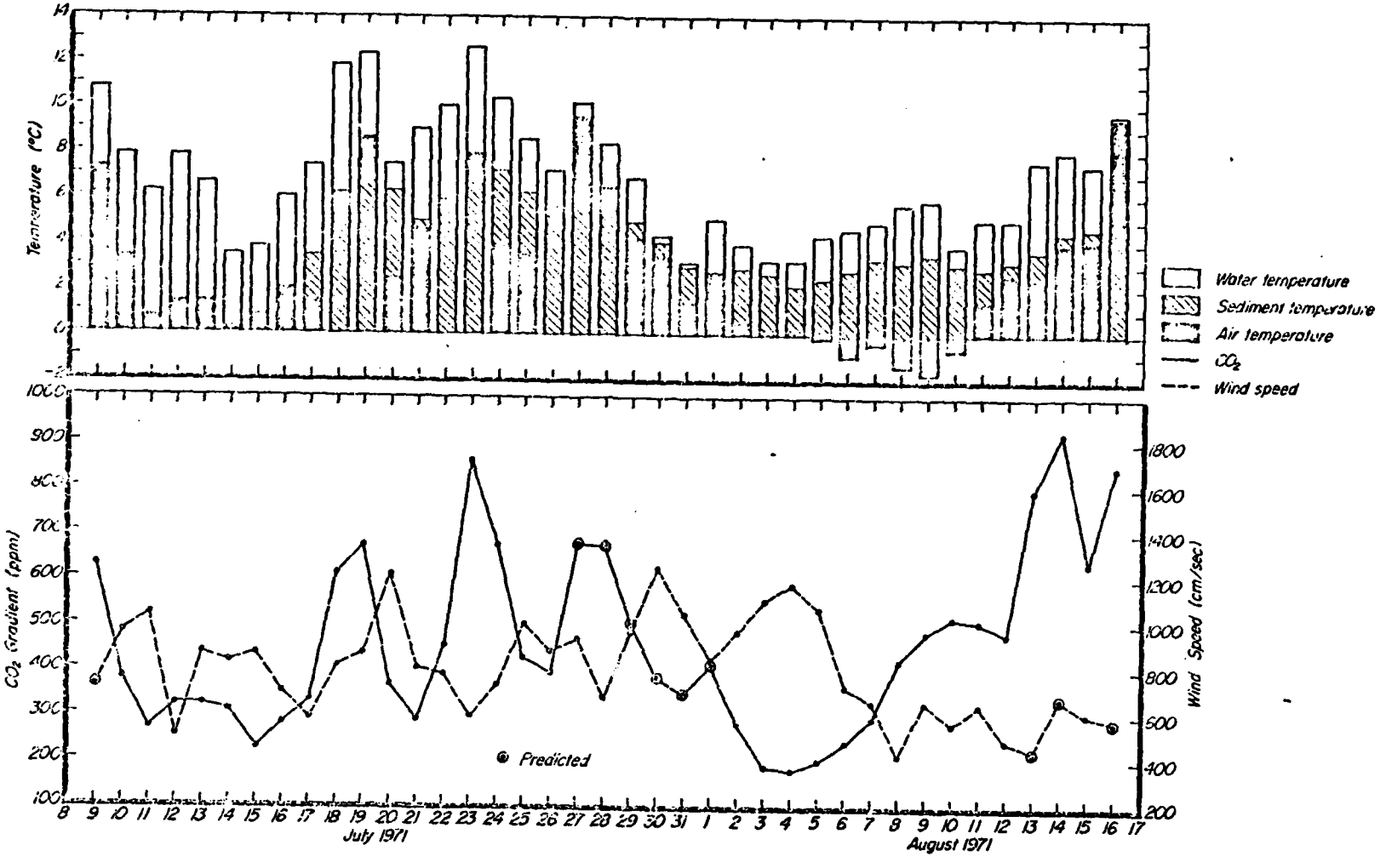

Figure 29. Mean daily temperatures (air, water, sediment) and CO_2 (PCO_2-pCO_2) for Pond C.

AD-A082 453 ALASKA UNIV FAIRBANKS INST OF MARINE SCIENCE F/G 4/1
DYNAMICS OF THE EXCHANGE OF CARBON DIOXIDE IN ARCTIC AND SUBARC--ETC(U)
1973 J J KELLEY N00014-67-A-0317-0001
UNCLASSIFIED NL

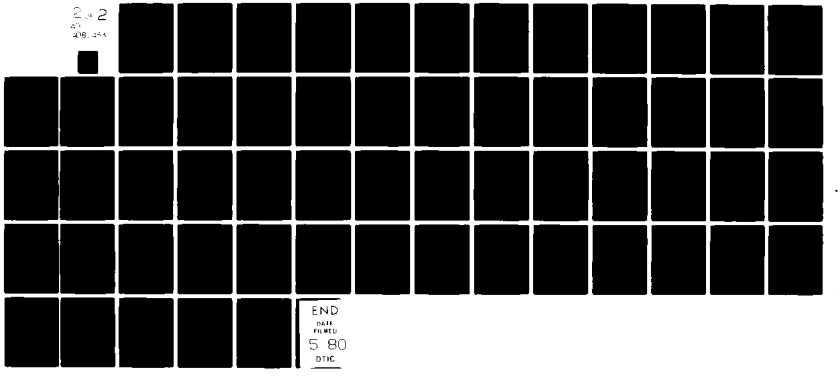

END
DATE FILMED
5 80
DTIC

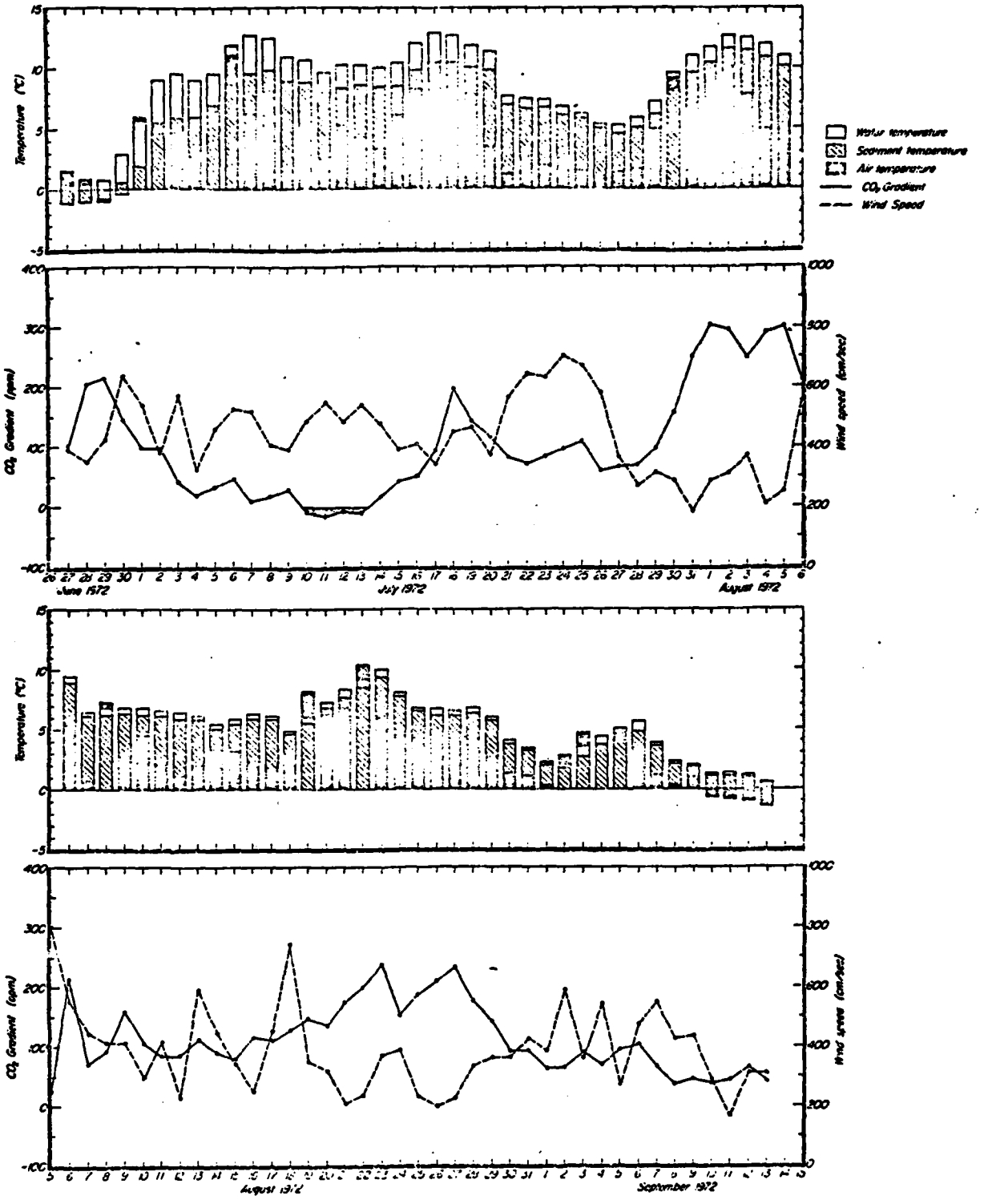

Figure 30. Mean daily temperatures (air, water, sediment) and CO_2 (PCO_2-pCO_2) for North Meadow Lake.

the entire thaw period including melt water on the bottom-fast ice in spring, and spot measurements under the ice in the fall. Air-pond CO_2 gradients were approximately three-fold greater than the air-lake gradients. Thus it is doubtful that the pond water was ever undersaturated in CO_2 with respect to air.

An attempt has been made to model carbon standing crops and transfers of carbon between compartments of a tundra pond ecosystem by U.S. Tundra Biome investigators based on data from a pond similar to the one in this study (Hobbie *et al.*, 1972). According to the model, the primary source of CO_2 to the water is benthic respiration, with plankton contributions being relatively minor in comparison (about 2% of benthic input). Assuming a common Q_{10} of 2 relationship between temperature and respiration, the effect of increasing sediment temperatures should be to increase benthic respiration, and therefore the magnitude of the CO_2 gradient. Conversely an increase in water temperature should act to diminish the CO_2 gradient because CO_2 solubility in water decreases as temperature increases. The rate of turbulent exchange of CO_2 across the water surface should increase with wind speed thereby decreasing the CO_2 gradient.

Kanwisher (1963) has discussed theoretical aspects on the exchange of gases between the atmosphere and sea. Seasonal water temperature variations force the movement of gas into or out of the water to adjust for the changing solubility. Further, the rate of exchange of gases between the oceans and the atmosphere depends largely on molecular diffusion through a thin laminar surface layer of water. The surface layer thickness is a function of surface water turbulence, which in turn depends on the shearing stress exerted by the wind on the water surface. Thus, the exchange rate is proportional to the wind speed.

A number of parameters for the pond and lake are compared in Table 13. Ambient pCO_2 was relatively constant during the study so that most of the variability in the ΔP gradient was attributable to PCO_2 fluctuations. Maximum instantaneous PCO_2 values emphasize the magnitude of CO_2 increases which can occur in these fresh water systems. Park *et al.* (1969) measured PCO_2 in the Willamette and Columbia rivers between Portland and Astoria, Oregon, in December of 1968. They found both rivers were supersaturated

Table 13. Comparison of Pond C and North Meadow Lake data. Range of values presented with the means is one standard deviation.

Parameter	Pond	Lake
Seasonal mean PCO_2	715 ± 184 ppm[a]	435 ± 82 ppm[b]
Seasonal mean pCO_2	318 ± 2.0 ppm[a]	320 ± 4.1 ppm[b]
Seasonal mean CO_2 gradient (PCO_2 - pCO_2)	397 ± 185 ppm[a]	115 ± 83 ppm[b]
Maximum mean daily CO_2 gradient	923 ± 208 ppm[a]	306 ± 47 ppm[b]
Maximum instantaneous CO_2 gradient	1217 ppm	404 ppm
Maximum instantaneous PCO_2	1530 ppm	722 ppm
Minimum instantaneous CO_2 gradient	136 ppm	-32 ppm
Seasonal mean temperature Air	2.5 ± 3.4°C	4.0 ± 3.5°C
Seasonal mean temperature Water	7.1 ± 3.5°C	7.0 ± 3.5°C
Seasonal mean temperature Sediment	4.5 ± 1.7°C	6.0 ± 3.1°C
Seasonal mean wind speed	399 ± 139 cm/sec	409 ± 174 cm/sec

[a]No. observations = 780

[b]No. observations = 1786

in CO_2 with values up to 340 ppm over ambient CO_2 concentrations for the Willamette and up to 325 ppm for the Columbia. Published data for fresh water PCO_2 are generally lacking. It does appear however that arctic fresh water lakes and ponds and temperate river estuaries are more supersaturated with CO_2 than are surface waters of oceans. The mean gradient for the lake, when computed over a period corresponding to the pond sampling period, except one year later, was 115 ppm, which coincidentally was the mean gradient for the entire sampling period in 1972 (Table 13). The lower CO_2 values for the lake are probably the result of dilution effects of the greater water volume of the lake. This conclusion is based on the fact that seasonal mean water temperatures and wind speeds were not significantly different (.05 probability level), while mean sediment temperature differences between the pond and the lake were highly significant (.01 probability level) which should have caused a greater CO_2 input rate in the lake. This explanation does not allow for differences in biological composition between the lake and pond which may be important. Seasonal air temperatures for 1972 were significantly higher (.01 probability level) on the average, than in 1971.

It is evident in the seasonal curves (Figures 29, 30) that large changes in PCO_2 can occur in a relatively short period of time. The arctic waters in this study generally start out quite low in alkalinity, and typically level off around 0.4 meq/ℓ as the season progresses (R. J. Barsdate, personal communication), whereas the world's ocean may average 2.3 meq/ℓ (Harvey, 1960). In seawater, near the equilibrium point metabolic addition or subtraction of dissolved CO_2 produces about 1/13 the change in PCO_2 that would occur in distilled water (Kanwisher, 1963). PCO_2 changes in seawater resulting from biological activity will persist and be detectable for weeks or months, thus providing a means of measuring the amount and distribution of biological activity (Teal and Kanwisher, 1966). The data suggest that spot measurements of PCO_2 in smaller fresh water systems, which are closer to distilled than to seawater, are indicative only of immediate conditions and do not represent an integral of earlier time periods. Therefore, attempts to follow biological activity with PCO_2 in lakes and ponds requires intensive monitoring of PCO_2.

Skim ice began forming on the lake by 11 September 1972, and the entire lake surface was ice covered by 15 September. However, a permanent ice layer did not form until 27 September. Ice thickness was about 30 cm by 26 October, and the lake was completely frozen by 4 January 1973. Intermittent monitoring of PCO_2 beneath the ice continued until 22 October. Although water and sediment temperatures were at or near 0°C, PCO_2 data indicated considerable biological activity was occurring below the surface ice layer. PCO_2 levels increased from over 800 ppm on 28 September to 2000 ppm by 12 October, to over 3,000 ppm by 22 October. These values are uncorrected for nonlinearity in gas analyzer response, and thus underestimate actual conditions. Because of the long optical path length in the IRGA it was not possible to measure further increases in CO_2 above 3000 ppm. On 16 October, PCO_2 was calculated from precise pH and alkalinity measurements of water samples taken from the lake. Values approaching 12,000 ppm were indicated (S. Kanamori, personal communication). Thus the season of benthic decomposition extends well into the arctic winter and probably continues until the lake is frozen to the bottom (4 January in 1973).

The assumptions of constant PCO_2 and nonturbulent conditions required for measurement of evasion coefficients and the assumed physical behavior of the exchange process (equation 5) were discussed. Under the rapidly fluctuating temperatures and the generally windy conditions common at Barrow, these assumptions could not be strictly valid, since periods up to 6 hours were often required to attain equilibrium CO_2 concentrations with the cuvette. PCO_2 generally increased somewhat during a run in response to increasing sediment temperature, and thus afforded greater CO_2 input from respiration. As a result, scatter plots of dQ_t/dt vs. Δp, which should be linear if the theoretical assumptions were valid, were often concave upward. This would be expected if PCO_2 increased during a rate determination. Several experiments were eliminated on the basis of these plots.

The data were further edited by observing plots of dQ_t/dt vs. t. The time at which the data began to depart from the predicted values was relatively abrupt. Data beyond this point were rejected and the computer program was rerun. The remaining data were then taken from periods of

relatively constant PCO_2. Generally PCO_2 remained constant for periods of 100 to over 300 minutes, long enough to obtain the general shape of the curve for a particular PCO_2 regime. When curvature was still evident in the data after the second run, an arbitrary decision was made to retain all experiments of the second run for which the data points fell within the 95% confidence belt of the linear regression line. A total of 17 experiments out of 25 were retained using this editing process.

The mean and standard deviation of evasion coefficients obtained from the 17 exchange experiments, which encompassed a variety of wind and temperature conditions between 19 July and 6 September 1972, was 0.34 mg $cm^{-2}atm^{-1}min^{-1}$ and 0.17 respectively. The average ΔP at North Meadow Lake from 26 June to 13 September 1973 was 115 ppm (Table 13). The calculated transfer of CO_2 for this period based on an average ΔP and evasion rate was 0.56 g $m^{-2}day^{-1}$. Assuming that the evasion rate for the pond was similar to the lake under similar gradient conditions, the average daily CO_2 transfer for the pond based on an average ΔP of 397 ppm (Table 13) for the sampling period was 1.95 g $m^{-2}day^{-1}$.

Published values for CO_2 evasion rates in fresh water are lacking. Those which have been published for seawater exhibit wide variability probably because (Riley and Skirrow, 1965) of the strong influence of turbulence which cannot be controlled in a reproducible manner. In this study, water was generally turbulent during the rate experiments. Although the cuvette prevented direct shearing stress on the water surface where the evasion rate was being measured, it did not attenuate the wave train significantly so that large scale turbulent effects were reflected in the data. Therefore, the measured evasion rates probably lie somewhere between those for diffusion and turbulent exchange rates.

It might be generalized that the smaller arctic fresh water ponds and lakes along Alaska's northern coast are probably supersaturated with CO_2 with respect to air throughout most if not all of the period of open water. PCO_2 continues to increase after the first permanent ice layer forms in the fall, until the lake sediments are completely frozen and become too cold to support biological oxidation. During the open water period, CO_2 continually is transferred from the water to the atmosphere.

CO_2 evasion rate measurements for the lake indicate that the flux of CO_2 per unit water area is probably less than 15% of the CO_2 flux per unit land area, resulting from ecosystem respiration in adjacent tundra areas. Terrestrial respiration estimates are based on the dark period flux of CO_2 to the atmosphere as measured by a bulk aerodynamic experiment (Coyne and Kelley, 1973b, in preparation), and from *in situ* respiration measurements of Billings *et al.* (1973).

The season of decomposition in aquatic habitats is apparently longer than that of terrestrial habitats so that total evolved CO_2 per unit area may be more comparable over the annual cycle. In addition, decomposition activity continues for a longer time than primary productivity, since light becomes limiting in the fall at arctic latitudes.

Definite conclusions regarding the equilibrium between productivity and decomposition in aquatic habitats cannot be made at this time, but it may be possible, based on PCO_2 data, that more carbon substrate is being respired than is being fixed *in situ* by autotrophic organisms. If this is true, the source of the excess carbon substrate could be derived from lateral transport of particulate and dissolved carbon compounds by surface run off or soil water percolation, or from organic matter fixed by terrestrial organisms but incorporated into the pond and lake sediments as part of the "thaw lake cycle" as described by Britton (1967). The behavior of ponds and lakes on the arctic coastal plain of Alaska, in light of their physical extent, suggest that they have a significant role in the functioning of the arctic CO_2 budget.

CHAPTER 5

CARBON DIOXIDE PARTIAL PRESSURES IN THE SURFACE WATERS OF NORTHERN SEAS

5.1 Introduction

A chart of the global distribution of CO_2 in the surface waters of the world's oceans had been prepared by Keeling (1968). Major features of the CO_2 distribution are summarized in Chapter 1. Notable among all of these data are a lack of information on the distribution of CO_2 in the surface waters of both polar seas. At the conclusion of observations on atmospheric CO_2 at Barrow, Alaska (1961-1967) further efforts were directed to investigations of CO_2 within the various arctic terrestrial and aquatic systems.

The objectives of research presented here was to examine the distribution of CO_2 in various surface waters of polar seas and its seasonal variations. Included in these objectives was an investigation of CO_2 in coastal waters particularly in regions that exhibited upwelling and river influx.

5.2 Measurement of PCO_2 in Seawater

The method for the calculation of PCO_2 in fresh water bodies from experimental measurements has been given in Chapter 4 and is similar for the sea.

All of the data for CO_2 concentrations are expressed as volume mixing ratios where,

$$\mu CO_2 = \frac{PCO_2}{P-\varepsilon}$$

PCO_2 is the equilibrium partial pressure of CO_2 in the seawater, P is the total atmospheric pressure and ε is the vapor pressure. If Dalton's law is obeyed,

$$PV = V(p_1 + p_2 + p_3 \ldots pm)$$

then this is identical to the volume fraction of CO_2 in the air. If the total pressure is 1 atmosphere then the mixing ratio is numerically equal

to the partial pressure in atmospheres (Chapter 2). The unit adopted here is the partial pressure of CO_2 in the air (pCO_2), or seawater (PCO_2) expressed in 10^{-6} atmospheres, or ppm-atm (Gordon, 1973), or simply ppm which is used throughout this discussion.

Occasionally during the discussion of the results, PCO_2 anomaly is used to delineate the departure of PCO_2 in the sea from the air. The PCO_2 anomaly, ΔPCO_2, is defined as

$$\Delta PCO_2 = PCO_2 - pCO_2$$

The PCO_2 anomaly indicates the degree of saturation, undersaturation, or whether CO_2 is in equilibrium with CO_2 in the atmosphere. The water is said to be saturated if: PCO_2 is greater than pCO_2; undersaturated if PCO_2 is less than pCO_2; and at equilibrium if PCO_2 is equal to pCO_2.

5.2.1 Temperature Effects

The sampling of seawater for PCO_2 usually involves pumping the water a considerable distance to the analytical system; thus warming it. This warming causes an increase in the measured PCO_2 and a correction must be applied to correct for this effect. Various authors have chosen various approaches to the solution of this problem, which is discussed in detail by Gordon (1973). Miyake and Sugimura (1969) maintained a tempera ture differential under 0.5°C which incurred a negligible error. Kelley *et al.* (1971) kept temperature differential less than 0.5°C and concluded that the error was less than 2°C, based on the data of Harvey (1960).

Kelling and Waterman (1968) established an increase in PCO_2 with increase in temperature nearly constant at 3% of the value of PCO_2/C. Li *et al.* (1969) established a 5% correction.

Kanwisher (1960) measured the effect of a rise in CO_2 with temperature for natural seawater of salinity 31.5°/$_{oo}$ and at various values of total carbon dioxide from 10°C to 24°C. He obtained a uniform 4.5%/C correction. He also pointed out that the increase of 1%, as given by Harvey (1960), is what the increase would be if the pH remained constant, which is unlikely in the sea. When water is heated pH decreases by approximately

0.01 pH unit/C. Takahashi (1961) reported a correction of 4% which was in close agreement with Kanwisher (1960).

Gordon and Jones (1973) derived a correction formula to evaluate the change in partial pressure of carbon dioxide in seawater upon heating over the range of values for PCO_2 from 0 to 1200 ppm. The constraints were constant salinity, total alkalinity, and total carbon dioxide concentration. The resultant equation is

$$\Delta PCO_2/\Delta t = 4.4 \times 10^{-2}\ PCO_2 - 4.6 \times 10^{-6}[PCO_2]^2.$$

The maximum error resulting from the use of this equation to $\Delta PCO_2/\Delta t$ for a 1°C increase in temperature of a seawater sample is 0.4% of PCO_2. The value of $\Delta PCO_2/\Delta t$ is almost constant at +4.4%/C. This is in agreement with Kanwisher's (1960) value of 4.5%/C.

5.3 The Equilibrators

Unlike the equilibrator (cuvette) used for the measurement of PCO_2 on lakes and shallow ponds (Chapter 4), sea water equilibrators are mounted within the research vessel's laboratory with the seawater pumped to it. It would be difficult to describe a single equilibrator which would represent all that are currently in use, for there are perhaps more different configurations than there are investigators using them. An equilibrator is essentially a system which allows air to come in constant contact with flowing water. Two types of equilibrators used in the measurement of PCO_2 in seawater discussed in this chapter will be described here.

5.3.1 Showerhead Type

The semi-open type equilibrator was initially used for measuring PCO_2 in the sea aboard the *Eastwind* (Kelley, 1970). Seawater was sampled by a brass submersible pump from a depth of from 1 to 5 m depending on the roll of the ship. The water was first drawn into a stainless steel sea chest located on the starboard deck and then withdrawn by a small electric screw type conveyor pump and sprayed into the equilibrator. A constant level of the water in the equilibrator was maintained by discharging the water

through a seawater manifold and standpipe (Figure 31). The water temperature in the equilibrator was monitored continuously by a platinum resistance immersion temperature sensor. The temperature difference between sea and equilibrator was small (less than 0.7°C).

The equilibrator was a stainless steel cylinder with a tight-fitting clear plastic top through which passed the air lines and temperature sensor. A safety switch connected to a float (not shown in Figure 31) was built into the equilibrator. If the water should suddenly rise in the equilibrator, the switch would activate a relay that would turn off the pump and close solenoid valves V8 and V9 to prevent seawater from being pumped into the infrared analyzer.

Equilibrated air was analyzed for CO_2 by continuously circulating it in a closed loop containing the equilibrator, solenoid valves, V4, V5, V6, V7, V8 and V9, diaphragm pump, pressure regulator, dryer, filter flow gauge, and infrared analyzer.

Air for analysis was drawn through an intake port near the bow of the ship 10 m above the sea. An alternate air sampling system aft of the ship's stack was used whenever a following wind caused stack gases to be blown forward. The air passed through Tygon tubing to the analytical system. To prevent solar radiation induced CO_2 evolution from the plastic tubing, the tubing was laid along covered portions of the deck to shield it from direct sunlight. An air flow of 1 ℓ/min was maintained by connecting each line to the suction side of a rubber diaphragm pump. Water vapor was removed from the air by passing the ambient air, reference gas, and air after equilibration with seawater through a Drierite moisture trap.

While the ambient atmosphere was being analyzed for CO_2, the equilibrator and reference gas sections were isolated from the infrared analyzer by solenoid valves V2, V3 and V5, shown in Figure 31. During the reference gas cycle, solenoid valves V2 and V3 were alternately open to the infrared analyzer and valve V1 shunted the ambient air to the room. The sequence of sampling was controlled from a console consisting of twin millivolt recorders, power supplies, and programming circuits. The sampling period consisted of 5 min for reference gases, 5 min for air, and 20 min for air after equilibration.

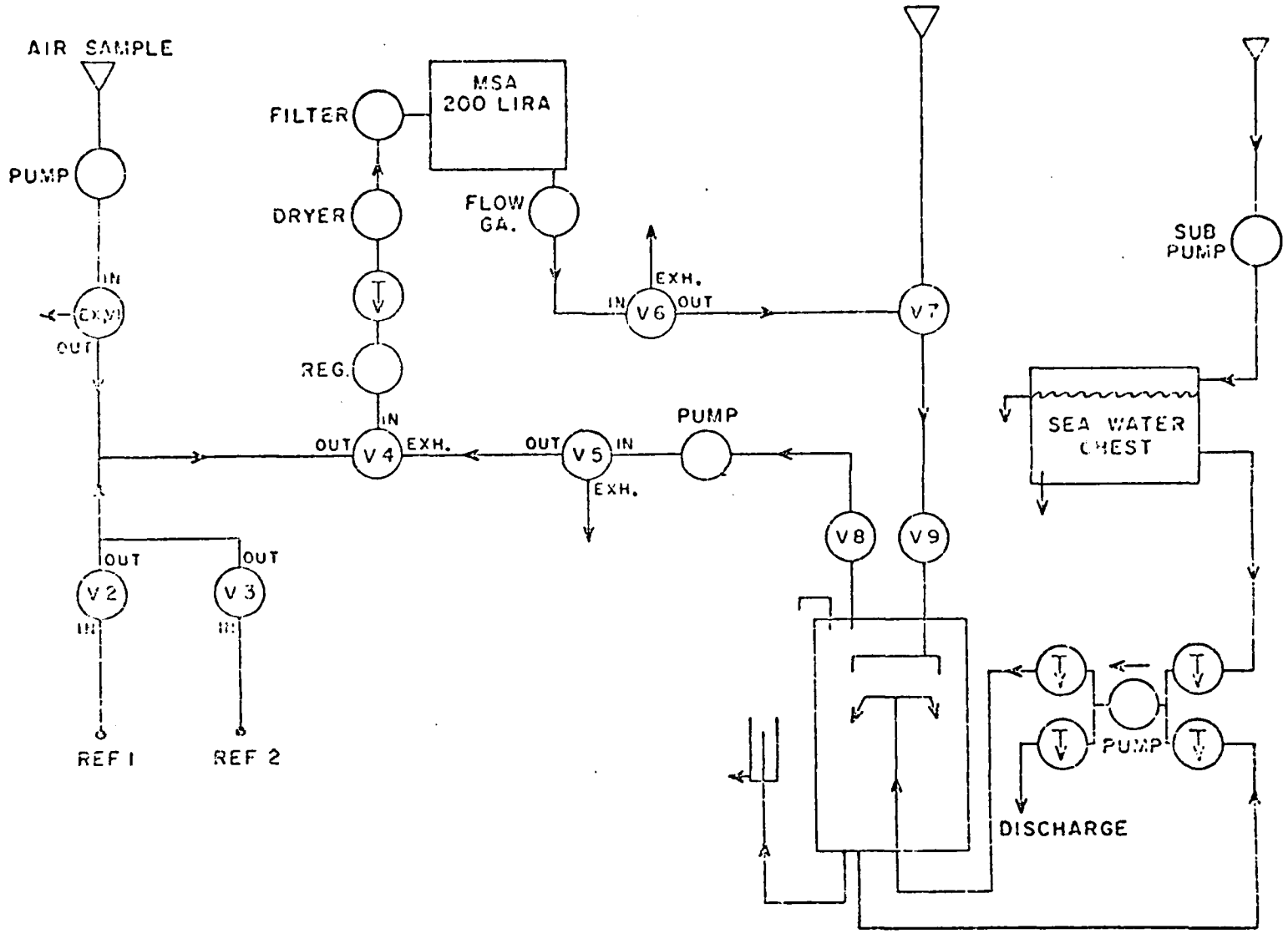

Figure 31. Flow diagram of the air, water, and semiopen equilibrator system. The shaded portion of the inset figures shows the amount of time each solenoid valve was actuated during each complete cycle.

When the equilibrator was not in operation, as between oceanographic stations, a complete cycle consisted of 5 min of a single reference gas, and 25 min of ambient air.

5.3.2 Aspirator Type

Measurements of CO_2 in surface seawater were accomplished with a six-stage water-aspirated equilibrator (Ibert and Hood, 1963). Figure 32 shows the design of the equilibrator. It consists of six individual-phase separation chambers into which six water-driven aspirators, in parallel arrangement, discharge a stream of gas that is fed in series from chamber to chamber, and finally through an infrared gas analyzer. By using the ship's internal seawater bow intake pumping system, water was kept flowing past the sampling point in excess of 20 ℓ/min to maintain temperature excursions to a minimum. Five ℓ/min of the water stream were passed through the equilibrator to ensure a sufficient volume of water to permit equilibration of the gas stream without distorting the CO_2 equilibrium of the water in the last stages of the equilibrator.

Hold-up time in the equilibrator was less than 1 min. The water stream from each aspirator was discharged into a phase-separation chamber which contained a loosely packed fiber mat. The water and gas phase were separated there. Very few bubbles were carried below the surface of the outflowing water, which eliminated pressure gradients due to hydrostatic phenomena or surface tension on submerged bubbles.

The equilibrator is based on the assumption that Henry's law applies. This six-celled equilibrator was tested for efficiency by Ibert and Hood (1963), who found that the gas stream reaches 99% of the equilibrium value after three stages and was reconfirmed for a modification of this equilibrator (Kelley and Hood, 1971) (Figure 33). The CO_2 values in the IR analyzer reach steady state in less than 6 min.

5.4 PCO_2 in the Surface Waters of the North Pacific Ocean, Barents and Kara Seas.

Carbon dioxide in the surface waters of the north Atlantic Ocean was evaluated by Buch (1939b) on two trans-atlantic cruises in 1935. The course

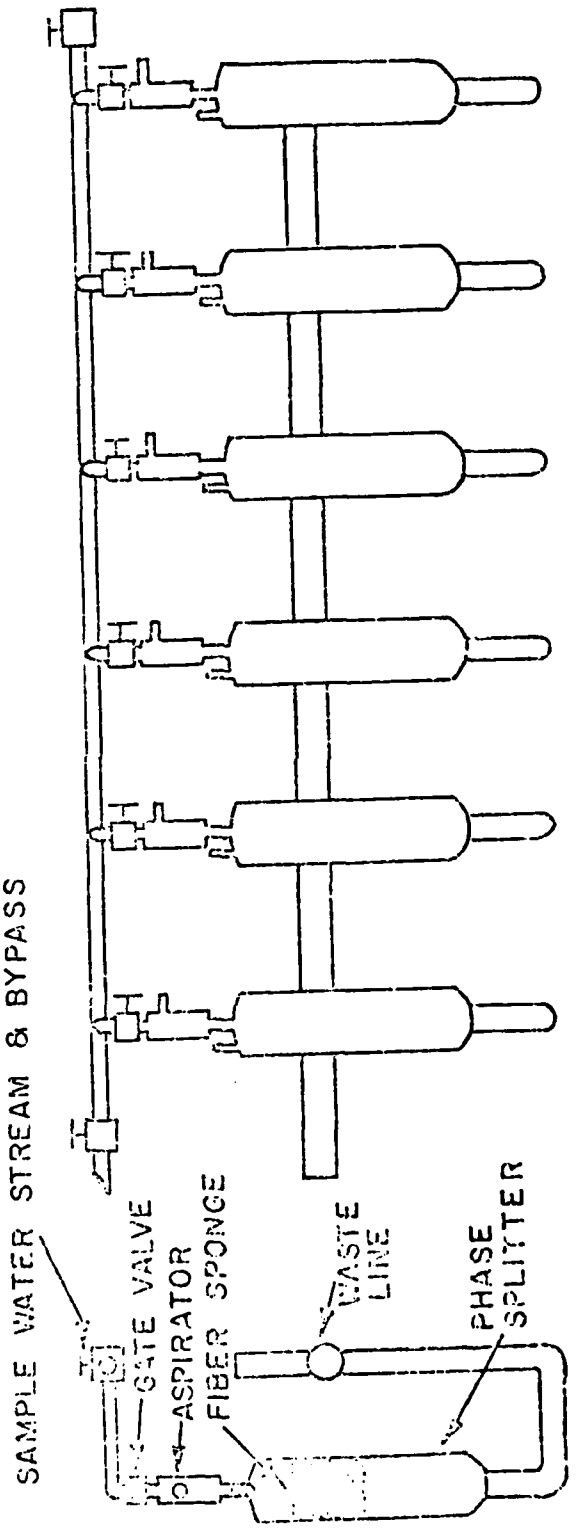

Figure 32. The aspirator type equilibrator.

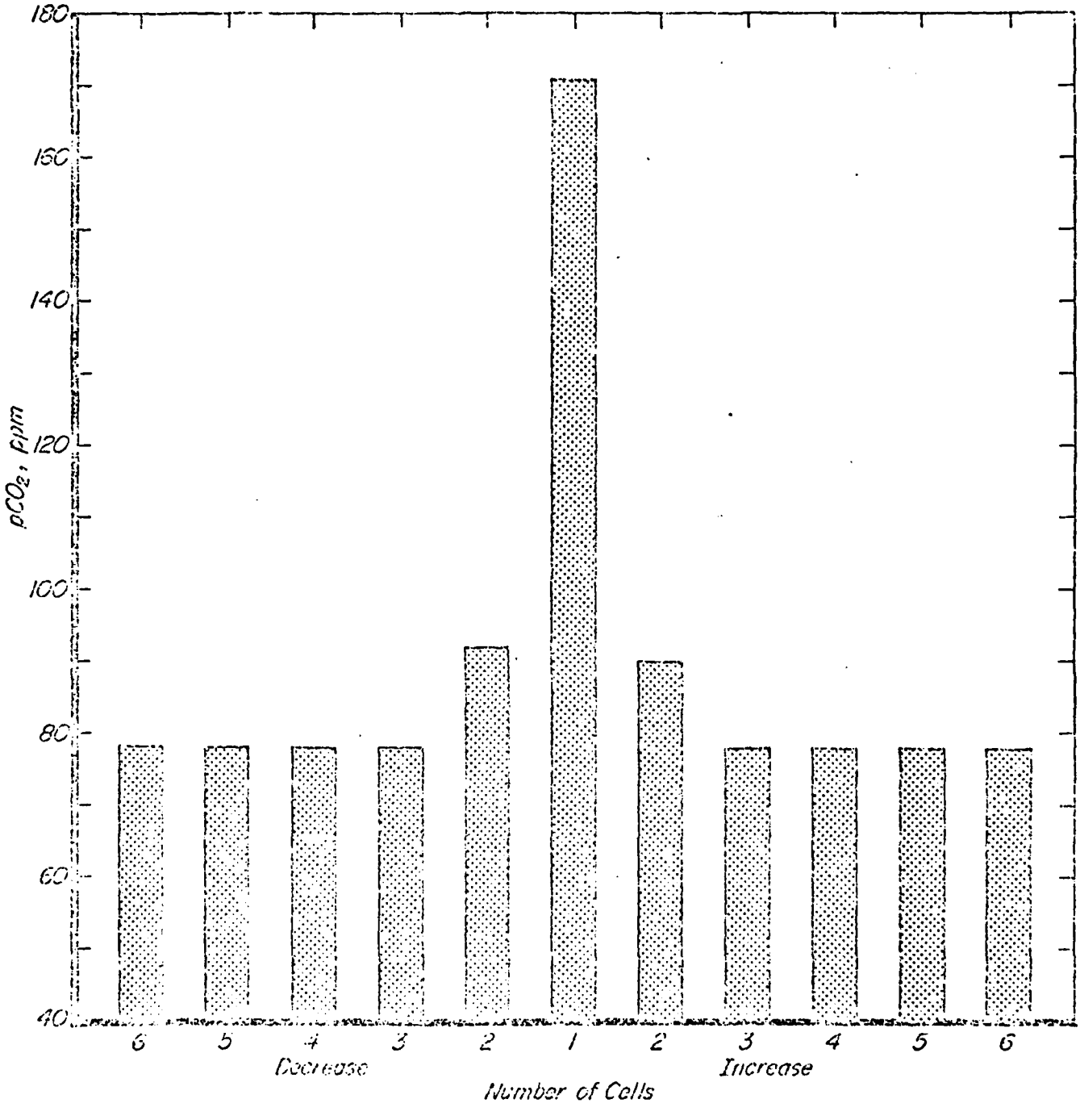

Figure 33. Equilibration of atmospheric air (340 ppm CO_2) with undersaturated seawater (78 ppm) using the 6-cell aspirated equilibrator.

of the *Eastwind* during the summer and fall of 1967 closely followed the routes taken by Buch. The data for CO_2 on the *Eastwind* cruise across the Atlantic Ocean were obtained underway. The results of the *Eastwind* data closely agree with the September results of Buch (1939b) as presented by Keeling (1968) (Figure 34).

The measurements of CO_2 that were taken at oceanographic stations in the Barents and Kara Seas are shown in Figure 35. Smooth curves were drawn to reflect significant surface features in the distribution of CO_2. A negative value indicates undersaturation with respect to air in the sea surface water. A solid line was used to connect points of equal concentration if the oceanographic stations were close enough to fit the curve to the observed data, with due regard to temperature and currents in these relatively shallow seas. A dashed line was used if the oceanographic stations were far apart. In this case the lines of equal concentration were drawn to conform to reported surface temperatures and currents.

Nansen (1915) represented the movement of water in the Barents Sea as one great cyclonic vortex. Cold polar water becomes stagnant over shallows and basins where eddies are formed in the central portion. Counterclockwise circulation prevails in the Barents Sea with the relatively warm Atlantic waters flowing in the North Cape and Murman currents in the south. Arctic waters of the Bear Island and East Spitzbergen currents flow in the northern part of the Barents Sea.

The Barents Sea is relatively shallow (average depth 229 m) and exchanges water only with the upper layers of adjacent seas (Zenkevitch, 1963). Warm Atlantic water flows from the region of the Norwegian Sea to the north, and cools from 8°C to -1 3°C. Arctic waters flowing in the East Spitzbergen and Bear Island currents are so different from water of Atlantic origin that they should not easily intermix. As a result, irregular fingers of the intrusions occur in the central regions of the Barents Sea, as seen in the record of the currents and CO_2 concentration (Figure 35).

The Kara Sea is bounded on the west by Novaya Zemlya, and in the east by the Taimyr Peninsula and Severnaya Zemlya. The average depth is 118 m and a trench of 200 m depth lies off the coast of Novaya Zemlya. The Ob and Yenisey Rivers flow into the southern end of the Kara Sea with an

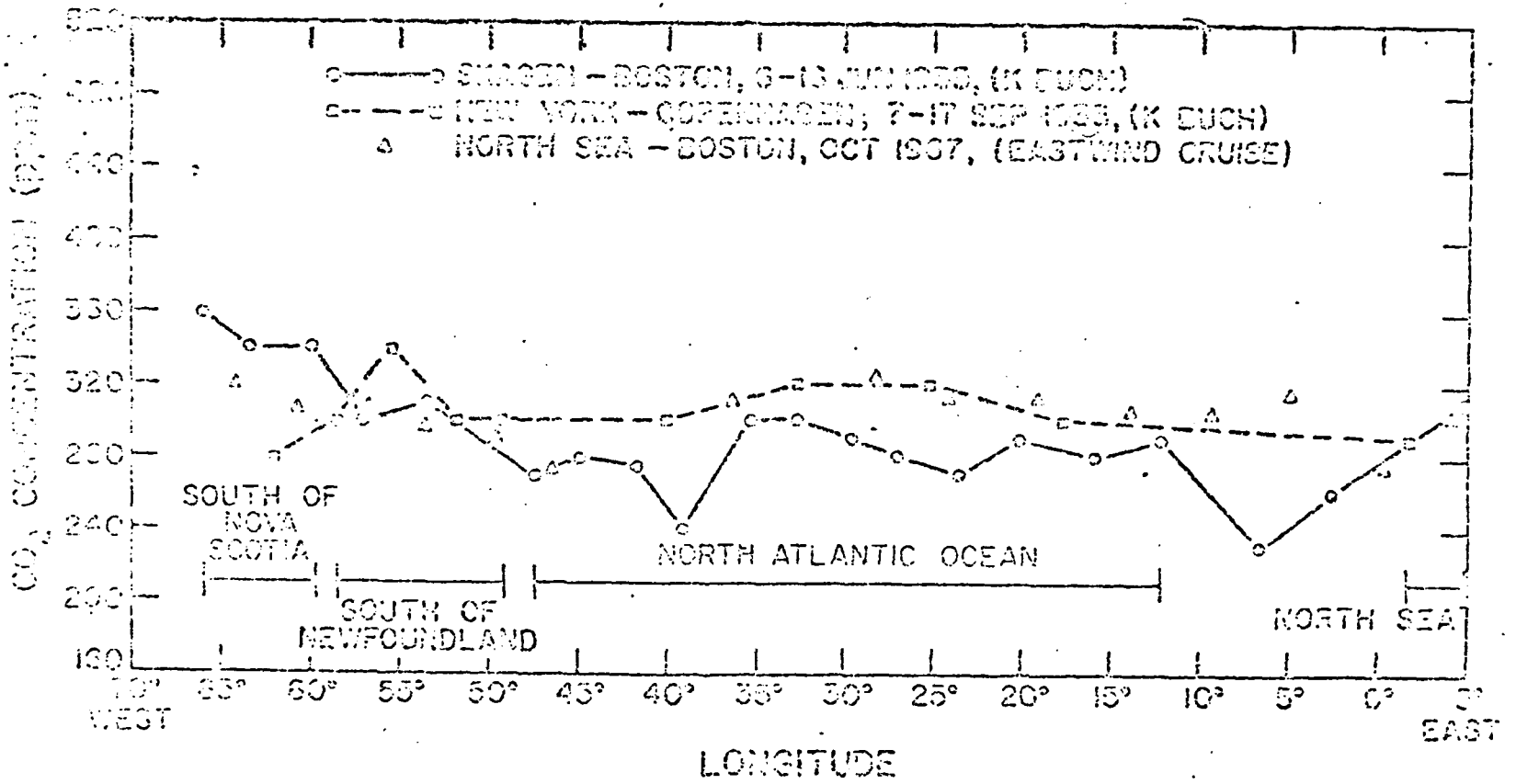

Figure 34. Equilibrium concentration of CO_2 in the north Atlantic Ocean.

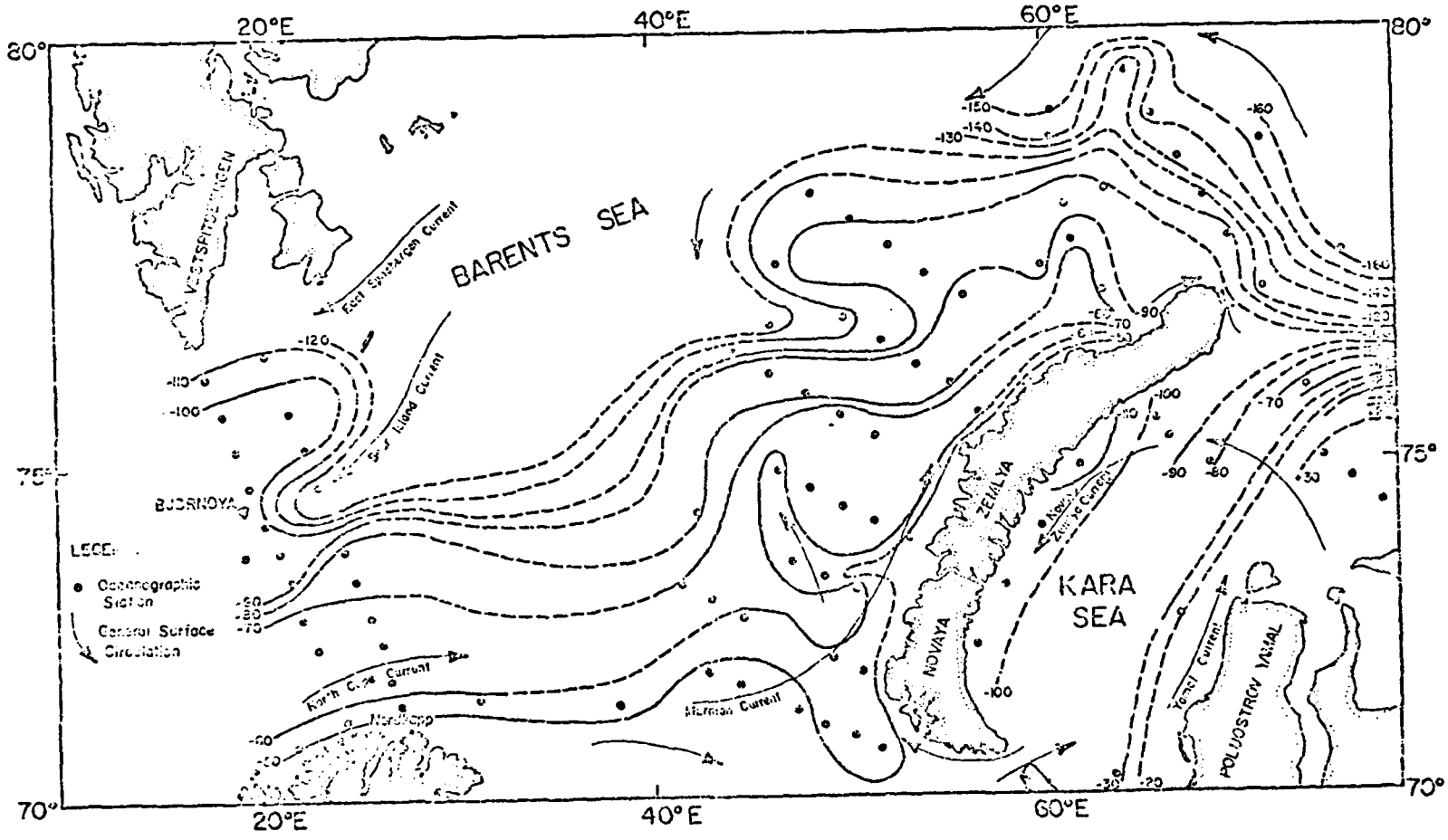

Figure 35. Equilibrium concentration of CO_2 and currents in the surface waters of the Barents and Kara Seas (*Eastwind* Cruise, 1967).

annual volume of 1500 km^3 (Zenkevitch, 1963). The Ob and the Yenisey mainly flow to the northeast along the coast of Teymyr. A portion of these waters turn north and northwest to the northern end of Novaya Zemlya and then partly turn west and southwest. A cyclonic rotation occurs in the southern part of the sea between Novaya Zemlya and Yamal (Figure 35). Atlantic waters of higher salinity enter the Kara Sea through the straits of Novaya Zemlya and sink below the much less saline surface waters. Both in the Barents and Kara Seas strong winds may temporarily modify the current regime and pattern of distribution of CO_2 in the surface waters. The surface sea water near the mouths of the Ob and Yenisey Rivers is supersaturated in CO_2 with respect to air. As the surface water cools in its flow north the CO_2 pressure falls. In the southern part of the sea a westward moving current cools and mixes with water from the Novaya Zemlya and Murman currents, which result in increasing undersaturation as the current moves toward Novaya Zemlya. As the water flows east it mixes with the lower salinity water from the Ob River, warms, and approaches near equilibrium of supersaturation conditions.

5.5 PCO_2 in the Surface Waters of the North Pacific Ocean and Eastern Bering Sea.

Kelley and Hood (1971) investigated the distribution of PCO_2 in the surface waters of the northwest Pacific Ocean and eastern Bering Sea aboard the NOAA vessel *Oceanographer*.

Two important factors of CO_2 concentration in surface sea water are; stability of the water column, and biological activity. CO_2 partial pressures depend on the exchange between the air and sea surface water, and from deep water, in which functions of photosynthesis and respiration occur.

CO_2 supersaturation with respect to air in the surface waters of the northeastern Pacific Ocean and Bering Sea are shown in Figure 36. As the coast was approached near Unimak Pass, undersaturation occurred. A condition thought to be due to high rates of photosynthesis accompanied by a highly stable water column. A belt of water that was slightly undersaturated with respect to air was observed in the western section of the northeastern Pacific Ocean, and corresponded generally with the southwestward flow of

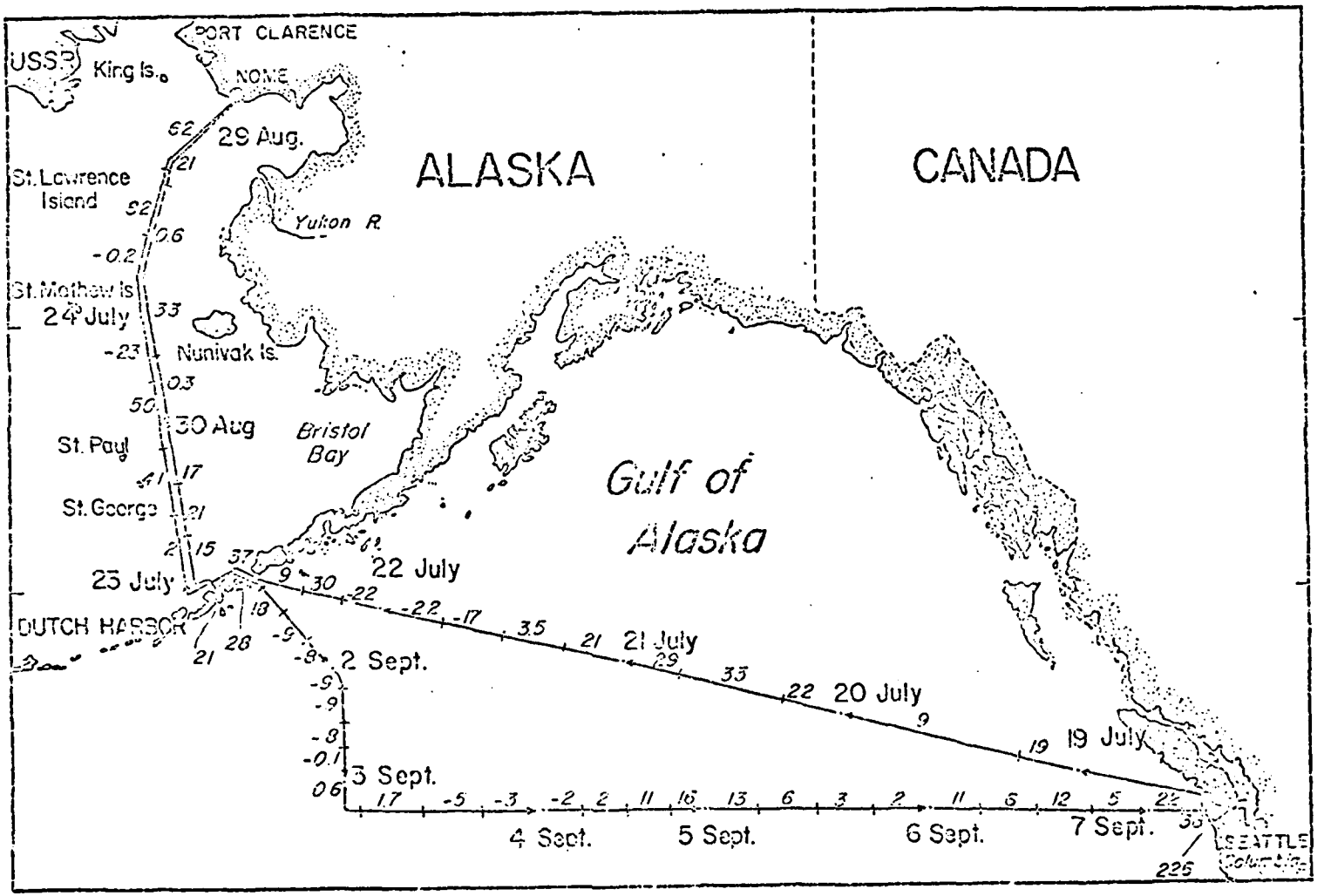

Figure 36. Equilibrium concentration of carbon dioxide in the surface waters of the Gulf of Alaska and eastern Bering Sea.

the Alaskan current. Another area of CO_2 undersaturation was observed east of St. Matthew's Island in the Bering Sea during July and August (see Figures 37 and 38).

Near-equilibrium conditions in CO_2 concentrations in the surface sea water with respect to air were observed between 43° and 49°N latitude and from 161° to 150°31'W longitude.

In the region close to the eastern shore of St. Lawrence Island, 63°03'N, 168°28'W (Figures 37, 38), local current-induced upwelling may be indicated by a high CO_2 concentration of 425 ppm in the surface waters and 317 ppm in the air (Figure 37), accompanied by an increase in salinity and lowering in temperature of surface water from an average of 9°C to 4.5°C. In this area, dissolved oxygen increased from 7 ml/ℓ, which is characteristic of the surface water oxygen solubility from approximately 56°N latitude (south of St. George Island), to 10 ml/ℓ off the eastern coast of St. Lawrence Island on the return trip from Nome to Seattle in late August. At this time, the maximum carbon dioxide concentration found in the sea was 370 ppm, against 312 ppm found in the air.

Near Unimak Pass (from about 54°N to 56°N), CO_2 concentrations varied appreciably, which could be attributed to the effect of the narrow pass in preventing the normal northward transport of water from the Alaskan stream. Deeper water may either be mixed upward to yield higher CO_2 concentrations in the surface or prevented from entering the pass by the sill. The water in the pass and north of it may be subject to processes of mixing with water arriving from the west near the continental shelf. CO_2 variations were accompanied by temperature, salinity, and oxygen solubility fluctuations that reflected the wide lateral east-west variations in surface water types along the transect to the north through Unimak Pass. Further evidence for upwelling, based on sea water nutrient concentrations near the margin of the continental shelf in the vicinity of Unalaska Island, Aleutian Islands, was suggested by Dugdale and Goering (1966). Sharp gradients in surface nutrients as determined by nitrate concentrations suggested the mixing of deep water to the surface. Nutrient concentrations varied from 15 µg-atoms/ℓ to undetectable levels between stations separated by less than 30 miles.

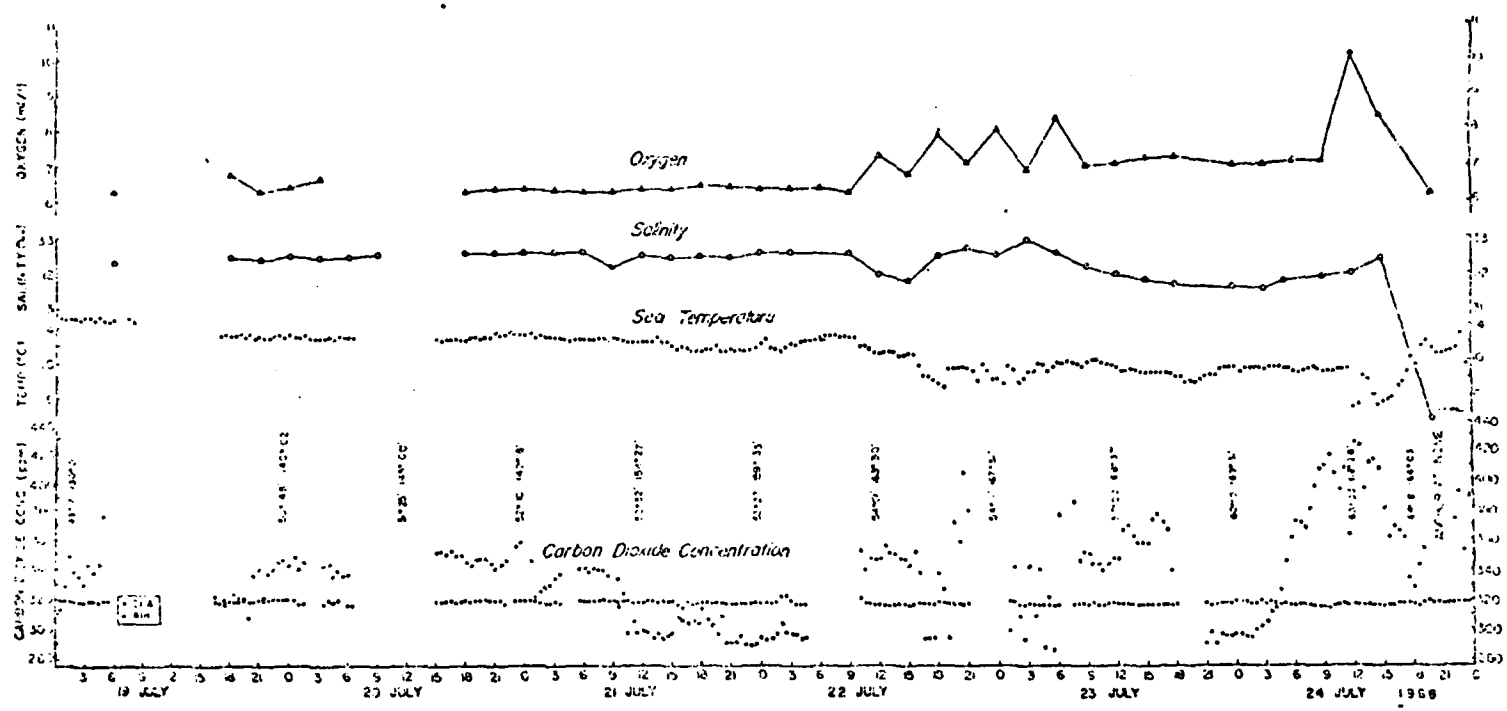

Figure 37. Carbon dioxide in the surface waters of the north Pacific Ocean and Bering Sea along a transect from the northwestern coast of the U.S. and Nome, Alaska.

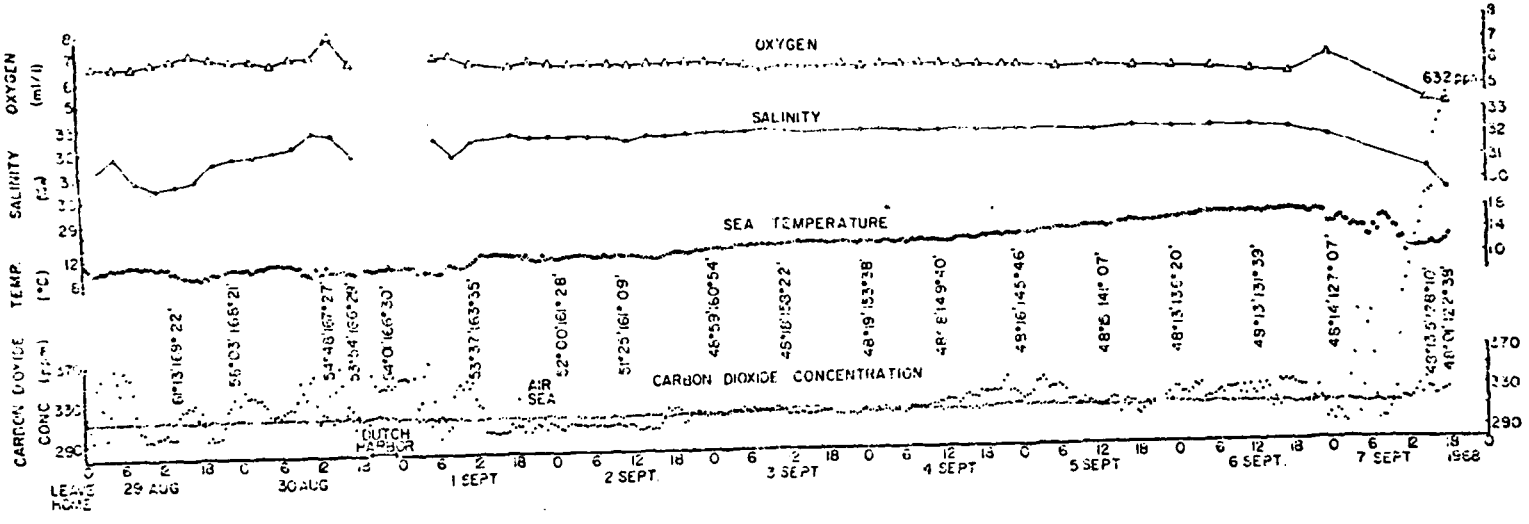

Figure 38. Carbon dioxide in the surface waters of the north Pacific Ocean and Bering Sea along a transect from Nome, Alaska to the Strait of Juan de Fuca.

High CO_2 concentrations may occur in an estuary where there is appreciable river inflow. For example, high concentrations of CO_2 for the Columbia River were reported by Park *et al.* (1969). The variation was explained as a combined effect of high concentrations of CO_2 in the source water such as soil water, biochemical oxidation *in situ*, and the rate of escape of CO_2 from the river to the atmosphere.

Within the coastal regions near Puget Sound, Washington, and Nome, Alaska, the CO_2 concentrations were supersaturated. This condition was associated with the fresh-water dilution attributable to river discharge into the sea. Near Nome, Alaska (Figure 37), coastal waters were influenced by flow from the Yukon River and by local discharges from the Nome River. CO_2 supersaturation in the sea with respect to air was as high as 390 ppm against values for air of 318 ppm. Fresh-water dilution was indicated by salinity decrease from $32°/_{oo}$ to $28°/_{oo}$.

Concurrent with the *Oceanographer* survey, Gordon *et al.* (1971) made a series of measurements in the subarctic Pacific Ocean and Bering Sea. From the combined data it was possible to extend Keeling's (1968) global chart northward and is presented in Gordon *et al.* (1973).

Principal features of the PCO_2 anomalies in the Bering Sea (Figure 39) are (Gordon *et al.*, 1973): an intense undersaturation of -100 ppm in the north central part (i.e., 100 ppm lower than the average ambient PCO_2 of near surface air, 312 ppm), general undersaturation of about -60 ppm in the western part, and supersaturation conditions in the eastern part during late summer (August-September). The principal features of the subarctic Pacific Ocean are: undersaturation of as much as -45 ppm in the western north Pacific Ocean with an indication of a complicated structure in the region of the subarctic boundary, near euilibrium in the Gulf of Alaska, and a belt of near-saturation water in the west ranging of supersaturation in the east, between the Pacific Ocean and Bering Sea, along the Aleutian Komandorskie Island Arc.

The data shown in Figure 39 do not include the effect of seasonal changes which may be very important for this region. Nearly all of the data for PCO_2 distribution in the surface waters of the world's oceans mostly reflect summer conditions. The results of the GEOSECS program,

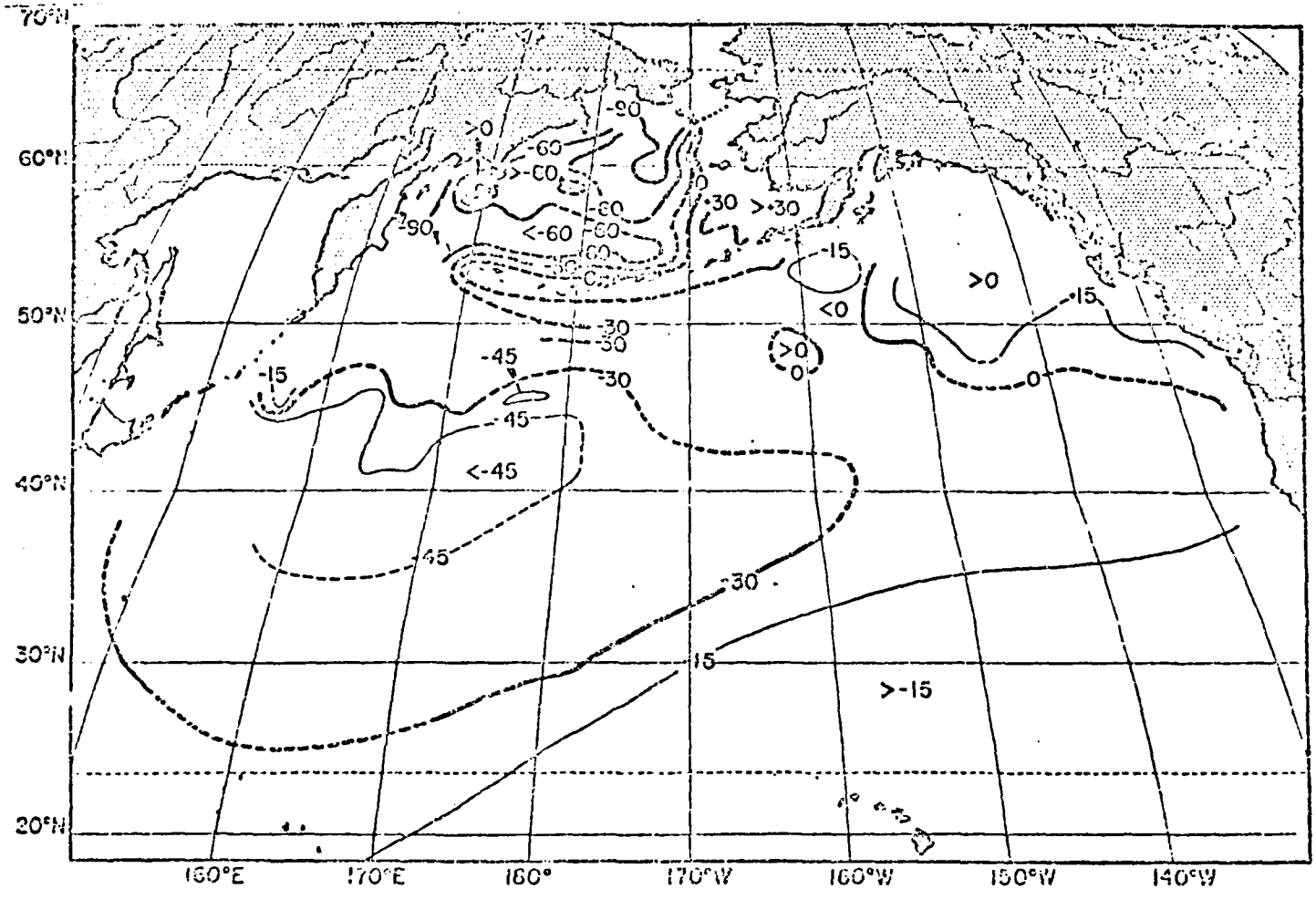

Figure 39. North Pacific and Bering Sea extension of the "Global Distribution" chart (Keeling, 1968) of surface seawater CO_2 anomaly contoured on an interval of 30 ppm are values of the sea surface PCO_2 minus atmospheric PCO_2(after Gordon *et al.*, 1973).

however, may offer more information on the seasonality of PCO_2 in ocean surface waters.

Further evidence for changes in the CO_2 content of seawater attributed to marine plant growth, was seen in the area near Izembek Lagoon, an embayment of the Bering Sea at the tip of the Alaska Peninsula. This lagoon is the largest and most important eelgrass (*Zostera marina L.*) area on the coast of Alaska (McRoy, 1968). Dilution in the lagoon was slight and limited to areas near streams. The salinity was generally the same as in the Bering Sea surface water. The seasonal range of values for CO_2 in the surface waters both inside and outside the lagoon are shown in Figure 40. The length of the line (Figure 40), showing the average concentration of CO_2 in the air, represents the length of time that analyses of CO_2 in the surface water were made. The vertical line represents the maximum and minimum range of concentrations of CO_2 in the surface water that was observed. Measurements made during June in the tidally flushed lagoon, yielded in all cases, conditions of CO_2 undersaturation with respect to air. CO_2 concentrations noted in September were nearly in equilibrium with air as measured in the seawater of the Bering Sea just outside Izembek Lagoon. October values for CO_2 in Izembek Lagoon exhibited supersaturation in the surface waters with respect to air. Gordon *et al.* (1971) also show that CO_2 in the surface waters of the subarctic Pacific Ocean varies seasonally.

5.6 PCO_2 Seawater in the Ice Covered Seas.

PCO_2 was invested in open leads and polyni of the ice covered northern seas. The U.S. Coast Guard icebreaker *Northwind*, during February 1970, provided an opportunity to cruise in the vicinity of the southern limit of the winter sea ice pack in the Bering Sea. The icebreaker was able to search out and select areas of open water in the constantly shifting pack. Oceanographic station selections were established (Figure 41) after the ship maneuvered into a lead or polynya and shut down its engines and overboard waste disposal to reduce contamination of the surface water.

The line showing the southern limit of the ice is based on the best information to be had at the time of the investigation from aircraft ice

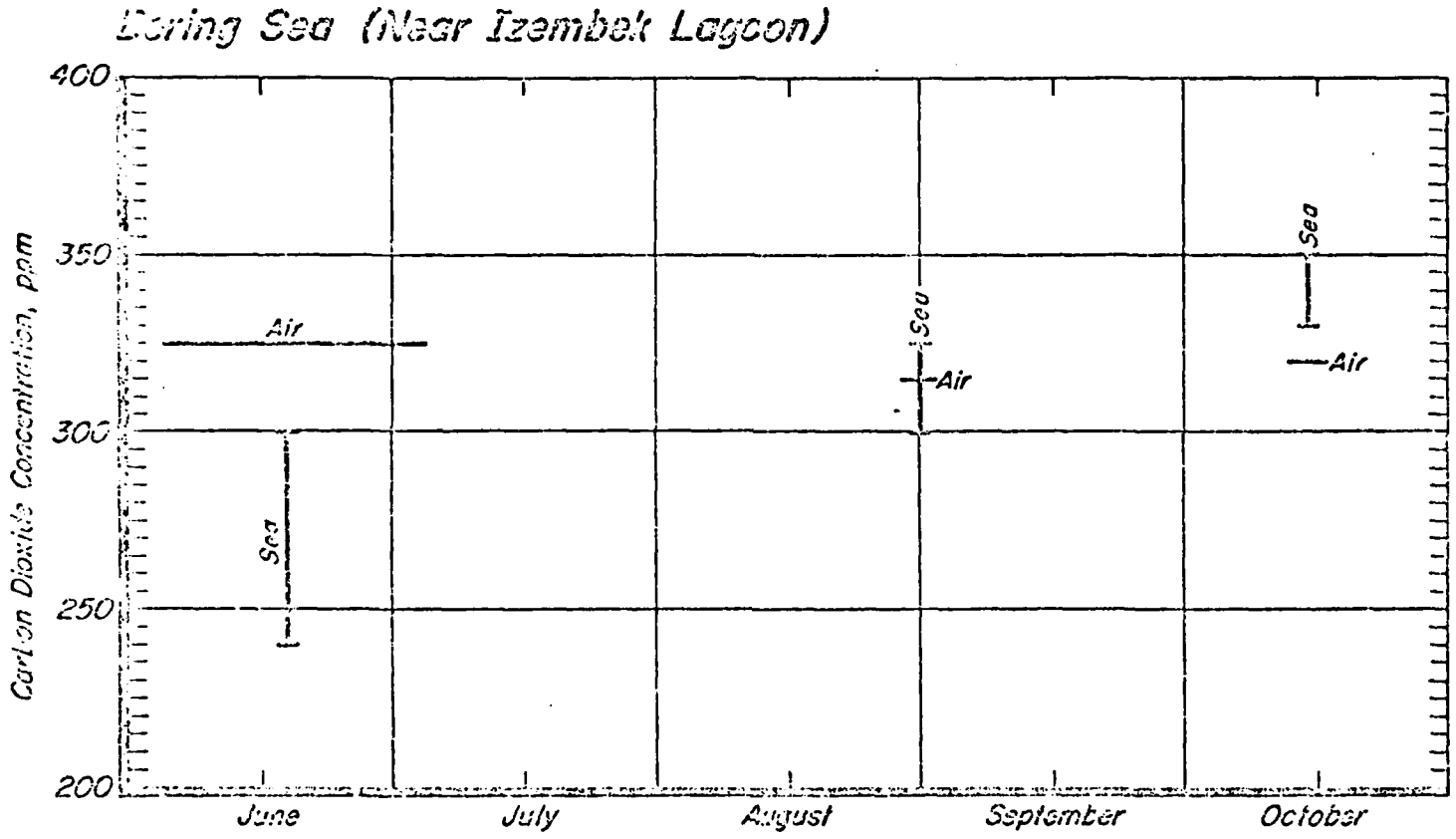

Figure 40. Seasonal (late spring and fall) variation of carbon dioxide in the surface sea water.

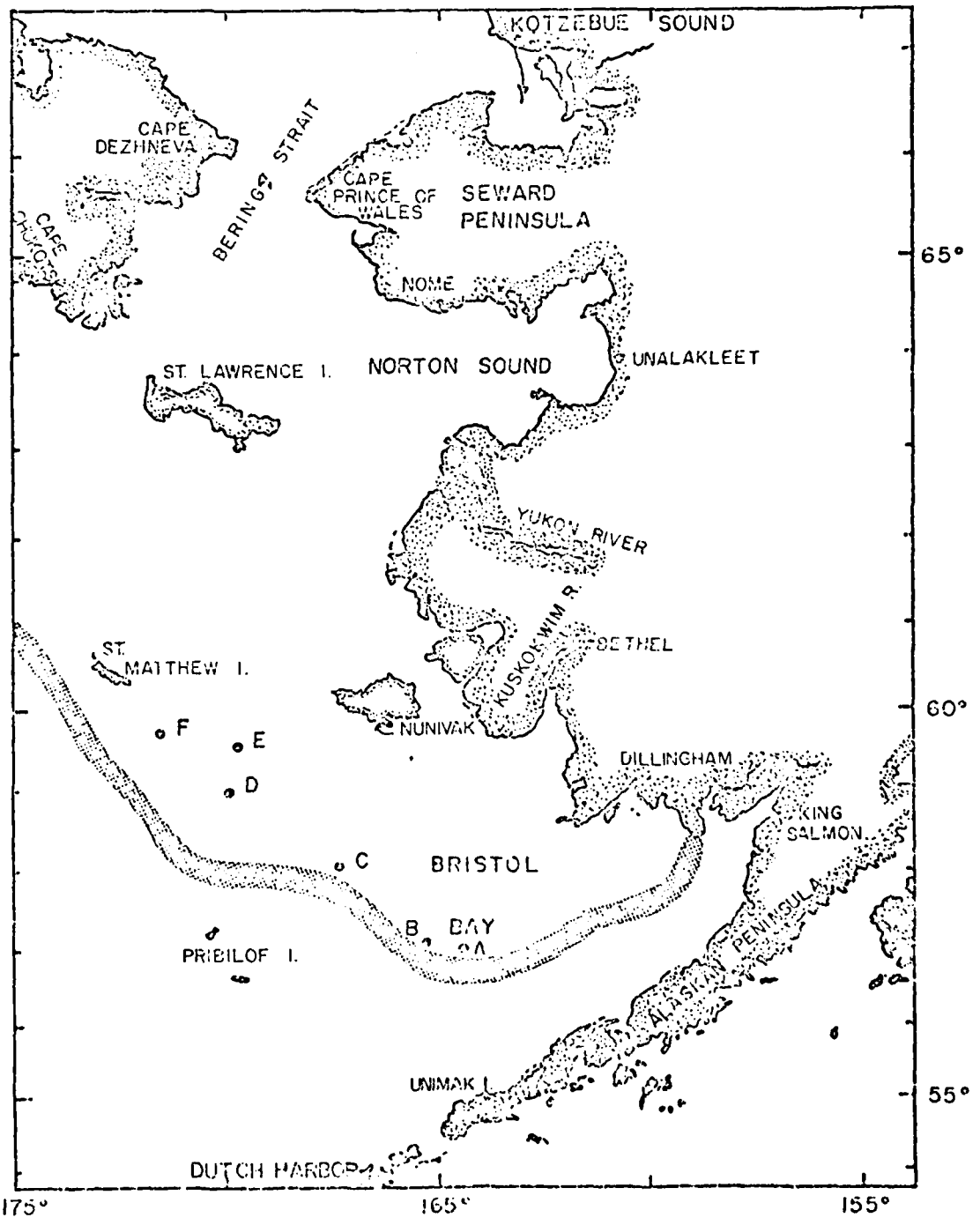

Figure 41. Survey stations for the measurement of PCO_2 under the sea ice. The hatched line gives the approximate southern limit of the ice.

reconnaissance reports. Several days prior to sampling, open water prevailed at Stations A and B (Figure 41). At the time that the observations were made, the ice had drifted south beyond the stations. The ice thickness at all of the sampling sites was less than 50 cm.

The concentration of CO_2 in the seawater restricted by leads and polyni in an ice covered sea showed that the water was supersaturated in CO_2 with respect to air, and that the magnitude of the supersaturation was less than 50 ppm over the air value at both locations in the Bering Sea and the central Arctic Ocean (Kelley, 1963a).

Open water in ice covered areas during the winter may be important in assessing the atmospheric inventory of CO_2 in the arctic. Unlike the summer, when autotrophic plant bloom on land and sea develop and provide a sink for CO_2, the northern arctic and subarctic regions are snow and ice covered for several months of the year and provide no biological sink for CO_2.

The importance of open water in the air-sea interactions, which may result in the transfer of CO_2 from the sea to the lower atmosphere, is emphasized by Whitman and Schule (1966), who estimate that the yearly variation of open water during the winter may be as much as 11% in the Eurasian Basin and 12% in the Canadian Basin. It has already been shown by Badgley (1966) that turbulent heat flux to the atmosphere increased about a hundredfold during the winter over an artificial open lead.

Like the northern part of the Eurasian Basin of the Arctic Ocean (Kelley, 1968a; Kelley and Hood, 1971a) the data for CO_2 in the southeastern Bering Sea suggest a potential source area for CO_2 in seawater. If the ice were removed for a significant period of time, as in leads or polyni, then CO_2 could be released from the seawater to the atmospheric reservoir.

5.7 PCO_2 in the Surface Waters of the Aleutian Island Passes

The pass areas of the Aleutian Islands became the subject of an intense investigation as a result of the observations noted in Section 5.5. High values of PCO_2, as well as high nutrient concentrations (Dugdale and Goering, 1966), indicated the possibility of the occurrence of extensive upwelling in these areas.

Unimak Pass (maximum sill depth of 55 m) is shallow and the most easterly of the major Aleutian passes. It is unique among the passes in that it opens north, directly onto the shallow shelf of Bristol Bay. Amukta and Samalga Passes, on the other hand, are of intermediate depth (maximum sill depth of 455 and 185 m, respectively), and open north into the deeper water of the southwestern Bering Sea. These passes showed major differences in CO_2 distribution. During June and September, Unimak Pass waters were undersaturated in CO_2 with respect to air, in contrast to high supersaturation conditions in surface waters of the Amukta and Samalga Passes farther west. Undersaturation of CO_2 in Unimak Pass is interpreted as being the result of utilization of CO_2 by autotrophic plants in the sea water. Previous surveys of this area showed it to be highly variable with undersaturation and supersaturation of CO_2 in the surface waters occurring in close proximity. These differences may be due to conditions of entrainment and tidal mixing. At no time, however, did local levels of supersaturation reach that seen in Amukta and Samalga Passes.

An explanation for the highly supersaturated surface water found in Amukta and Samalga Passes lies in the source of water to these areas. According to Arsenev (1967), the permanent and strong Alaska current flows in the Pacific Ocean from east to west along the southern side of the Aleutian Islands. The waters penetrate into the Bering Sea, primarily through the deep passes in the western Aleutians and then flow eastward north of the Aleutian Islands.

From Arsenev's current analyses, it is noted that Unimak Pass differs greatly from Amukta Pass, in that Unimak Pass is characterized by northward flow from the Pacific, while Amukta Pass is dominated by a cyclonic gyral north of the pass. Upwelling of Pacific waters entering the Bering Sea occurs in the gyrals of the Bering Sea. The deep waters of the Bering Sea, similar to the overlying intermediate and subsurface waters, rise gradually to the surface in the cyclonic gyrals while being gradually transformed and returned to the northern part of the Pacific Ocean as surface waters. The Bering Sea obtains its deep water from the Pacific, its surface waters migrating back to the Pacific.

Figure 42 describes the distribution of equilibrium CO_2, salinity, oxygen, and surface water temperature along a transect north of Samalga Pass during August 1970. The upwelled area is associated with CO_2 concentrations in the surface water in excess of 475 ppm, low sea surface temperatures, an increase in salinity, and a decrease in dissolved oxygen.

Observations of oxygen, CO_2, temperature, and salinity in the surface waters in the vicinity of Amukta Pass, are shown in Figure 43. Again, the same situation prevails as in the case of Samalga Pass. Two transects through the Amukta Pass area reveal CO_2 concentrations in the surface waters that rise from less than 200 ppm (undersaturation with respect to air) outside of the pass area, to more than 500 ppm (supersaturation) within and north of the pass.

Because of the decomposition of organisms, deep water contains large amounts of CO_2 and dissolved nutrients which must be released when the water contacts the atmosphere. Upwelling brings subsurface water to the surface layers, and induces horizontal anomalies in the distributions of physical and chemical properties that normally have marked vertical gradients.

During the June 1970 cruise, continuous flow nitrate-nitrogen analyses were run concurrently with the CO_2 determinations. The relationship between these nitrate-nitrogen and CO_2 values from the north Pacific Ocean, near the southwestern end of Unimak Island to the area north of Seguam Island, is shown in Figure 44. The NO_3-N concentration varied directly with increasing CO_2 concentration in the surface water. Low nitrate-nitrogen and low CO_2 values were associated with the surface water on the Pacific Ocean side of the islands, and high values of nitrate-nitrogen and CO_2 were associated within and north of Amukta Pass. These data suggested a similar situation in the Amukta Pass region as evidenced by Dugdale and Goering (1966) for the area north of Unalaska Island. It is presumed that nutrient and CO_2-rich deep water was brought to the surface by inertial type upwelling caused by deep easterly currents sliding up the continental slope with sufficient velocity to cause surface outcropping. Wind speeds and directions were observed where upwelling was noted (10 to 60 knots) during the June and September cruises. Variation of wind direction was

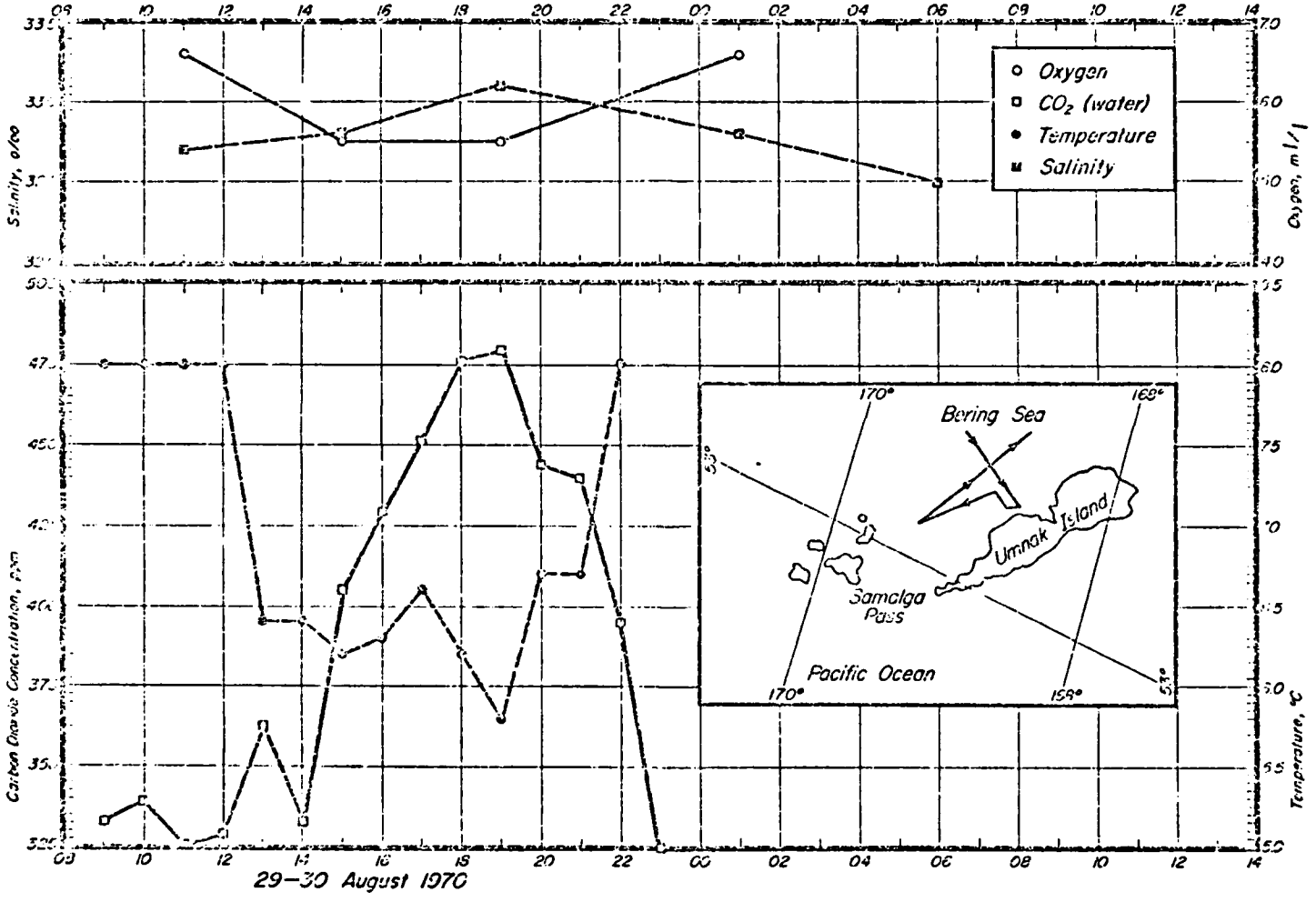

Figure 42. Carbon dioxide concentrations in the surface sea water north of Umnak Island and Samalga Pass.

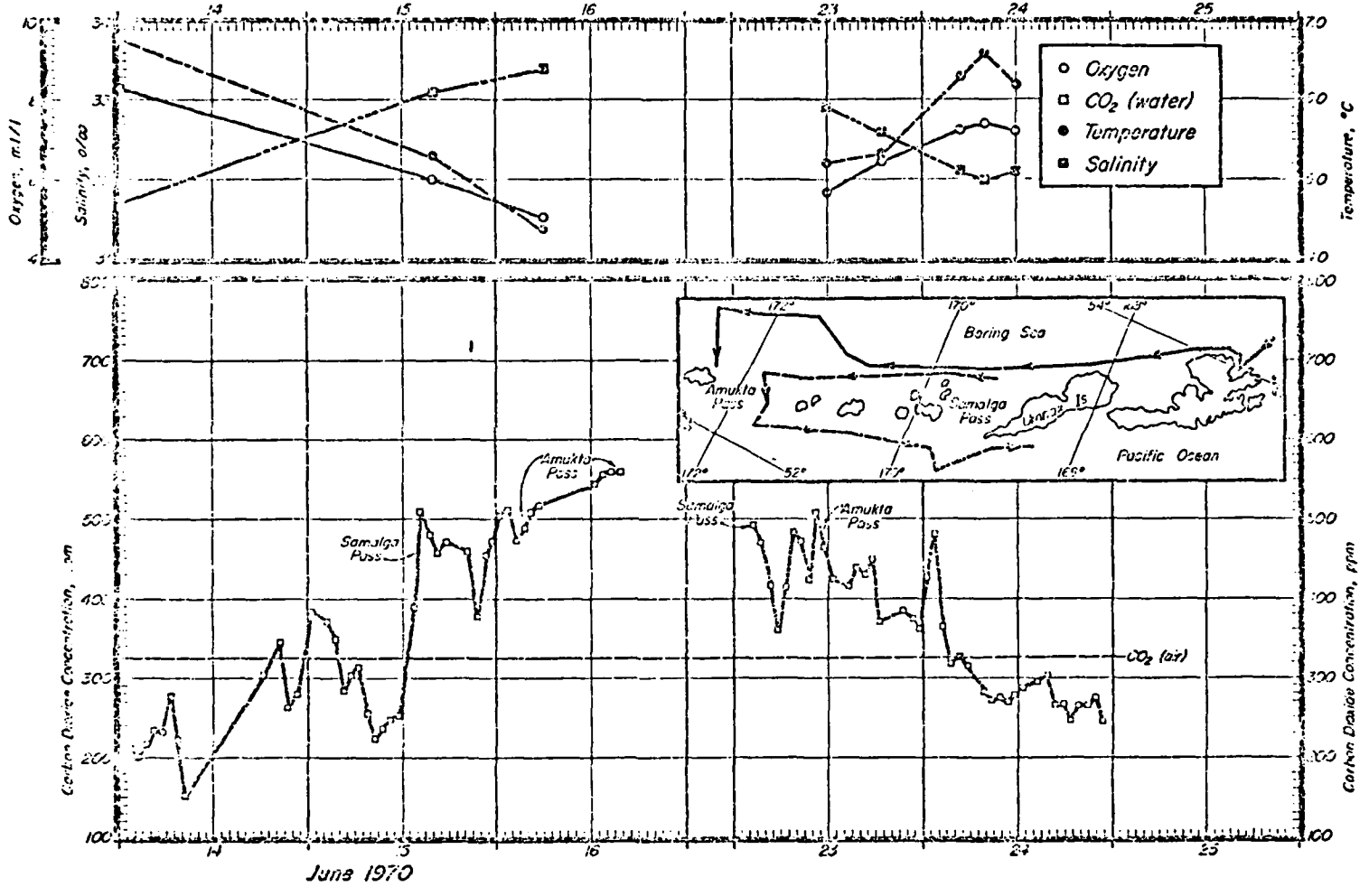

Figure 43. Carbon dioxide concentrations in the surface sea water north and south of the eastern Aleutian Islands.

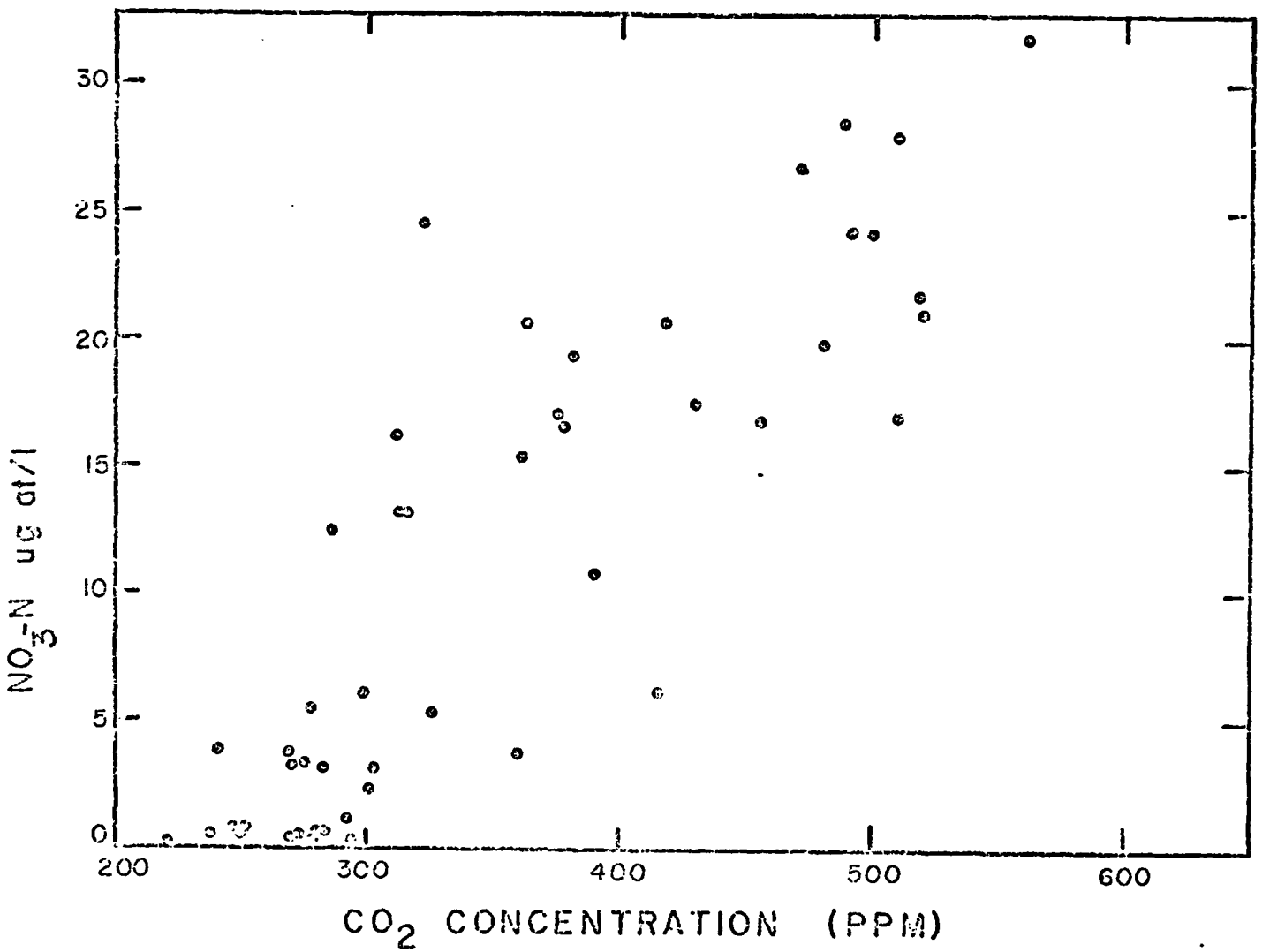

Figure 44. Carbon dioxide and nitrate-N concentrations in the surface sea water in the vicinity of Amukta Pass.

random over an area of consistent upwelling, showing that wind-driven upwelling does not appear to be a major factor here. A detailed discussion of the distribution of various chemical parameters associated with the currents and water masses of the Aleutian Island Passes is given in Kelley *et al.*, 1973, 1973a.

Maximum surface water PCO_2 values observed along the Aleutian Island Passes (Cruise 115, June-July 1971; Cruise 138, July 1972) were 611 ppm and 615 ppm respectively (Kelley *et al.*, 1973). These values occurred in the upwelled areas. The source depth for CO_2 in the depth at which a PCO_2 of 600 ppm occurs. The data of Alvarez-Borrego *et al.* (1972) were used to determine at what depth this level is reached. Near the longitude of the upwelled area this level is estimated to be at 200 m depth (Figure 45).

The horizontal distribution of PCO_2 in the coastal surface waters of the eastern Aleutian Islands and the southwest coast of Alaska reveals that these waters were undersaturated in PCO_2 with respect to air (air = 322 ppm) as shown by the PCO_2 anomaly in Figure 46.

PCO_2 undersaturation prevailed all along the coastal areas including Unimak Pass until the vicinity of Umnak Island and Samalga Pass; the latter being previously described as upwelled.

The undersaturated water is presumed to be the result of high primary productivity by autotrophic marine plankton under the influence of high nutrients which are turbulently mixed to the surface in the shallow coastal water. The strength of this oceanic sink for CO_2 has been shown to vary seasonally (Kelley *et al.*, 1971).

The PCO_2 anomaly is high within the whole Samalga Pass region (Figure 47). Surface nutrient distributions (nitrate, silicate, phosphate) were high in all cases: phosphate 1.25 to 2.50 µg-at P/ℓ; nitrate 15-20 µg-at N/ℓ; and silicate, 20-27 µg-at Si/ℓ.

In regions of the world's oceans where strong upwelling occurs in association with high nutrient concentrations, there exist higher concentrations of marine flora and fauna than in the surface waters of the more nutrient-depleted oceanic areas. Although we have no direct evidence at this time for relative amounts of biomass for the various Aleutian passes, it is interesting to note the observations of Murie (1959), who spent two

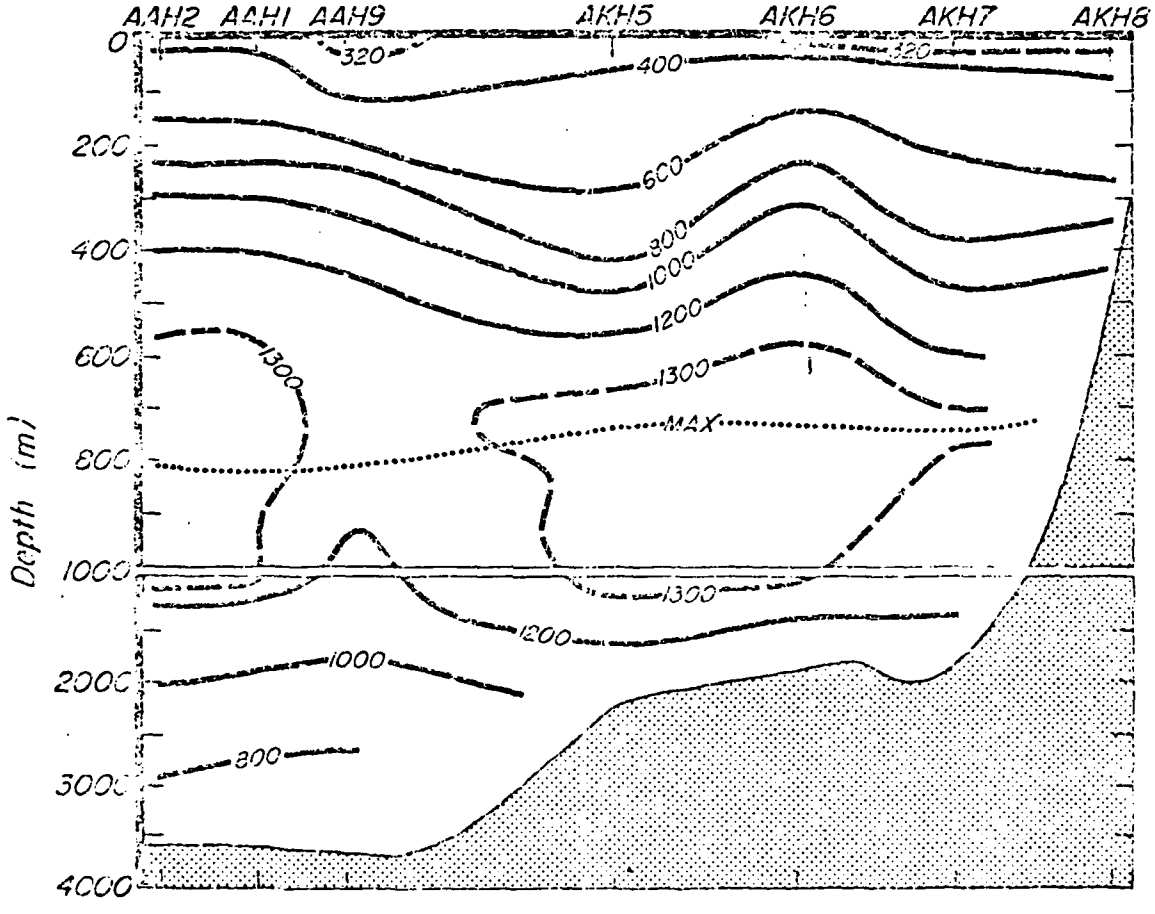

Figure 45. Vertical PCO_2 distribution (ppm) in the Bering Sea near the Aleutian Islands (after Alvarez-Borrego *et al.*, 1972).

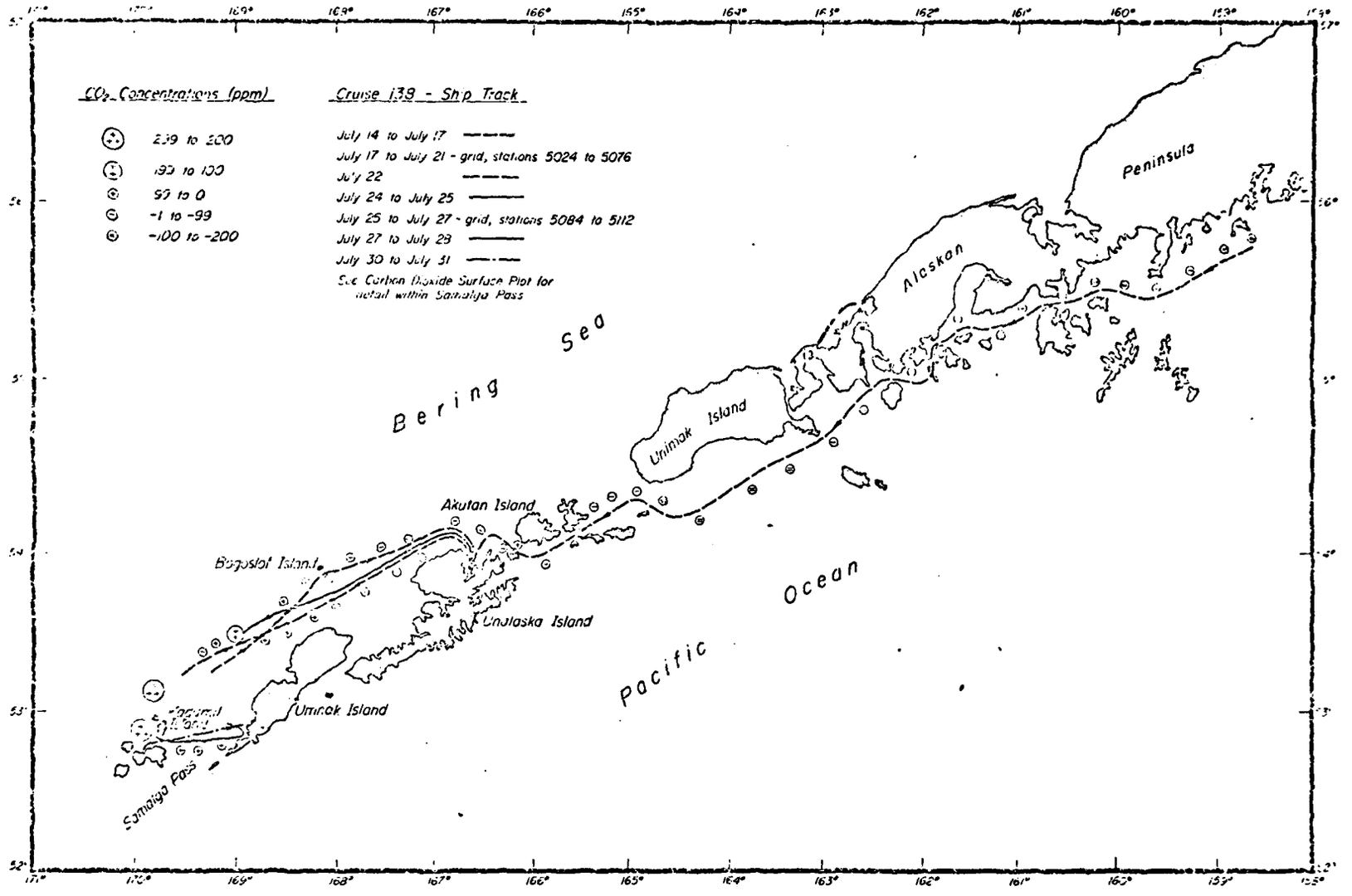

Figure 46. PCO_2 anomaly along the coastal areas of the eastern Aleutian Islands and southwest Alaska.

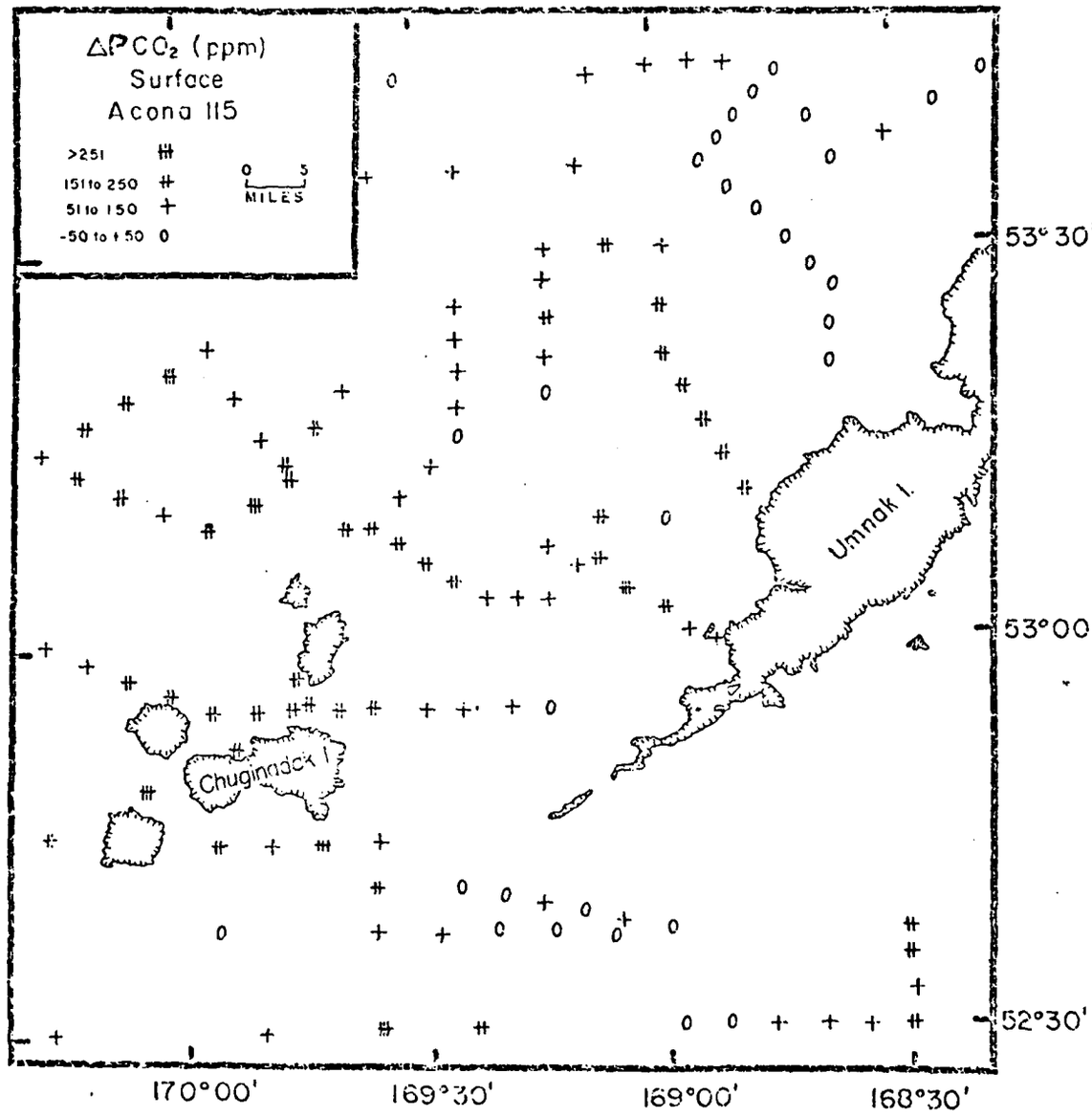

Figure 47. PCO_2 anomaly in the vicinity of Samalga Pass, July 1971.

seasons studying the fauna of nearly every Aleutian Island. He observed that the islands of Amukta and Chagulak have the largest and principal nesting colonies of fulmars (fish-eating petrel family) in the Aleutian Chain, a phenomenon which may be associated with the proximity of this area of high nutrients in the surface water.

CHAPTER 6

SUMMARY AND CONCLUSIONS

6.1 Atmospheric CO_2

Accurate analyses of CO_2 in the arctic atmosphere by infrared analysis have shown that there is a secular increase of about 0.8 ppm per year in the atmosphere which closely follows a similar increase in the tropics and in antarctica. The daily variation in CO_2 in the fall and winter and spring resembles the antarctic trend. There is, however, a distinct diurnal variation during the summer when the snow melts and the ice thaws. This variation is in response to uptake of CO_2 by the vegetation and release of CO_2 from the soil. A seasonal oscillation in atmospheric CO_2 is clearly evident. The seasonal variation is primarily a response to the use of CO_2 by vegetation in the northern hemisphere. The seasonal carbon dioxide amplitude is greatest in the arctic (12 ppm), and diminishes to 6.5 ppm in Hawaii, and approximately 0.5 ppm in the antarctic.

Although the period of observations was long (1961-1967), recent emphasis on environmental awareness and documentation of changes that occur in the atmosphere, indicate that more extensive monitoring for longer periods is required. In response to this need, the U.S. National Oceanographic and Atmospheric Administration (NOAA) has reinstated a CO_2 observation station at Barrow. Infrared techniques are used and reference is made to the same calibration system and analytical technique used in this investigation.

6.2 Subnivean CO_2

Arctic tundra soils are, in general, characterized by a seasonal freeze-thaw or active zone which overlays perennially frozen ground (permafrost). During the summer thaw period vascular plant roots and rhizomes, microbial decomposition, and animal respiration are continual sources of CO_2 to the soil environment. The CO_2, moving down its concentration gradient, escapes at the soil surface where it may be immediately refixed photosynthetically or mixed with the ambient atmosphere. Throughout the thaw season tundra soils represent a significant source for CO_2.

There is an increase in subnivean CO_2 over ambient CO_2 concentrations beginning a few days after the first snowfall. This increase continues into December, at which time CO_2 declines to relatively stable concentrations approaching, but still in excess of ambient air levels. Soil surface CO_2 increases from early May to late June when the snow melts.

CO_2 production during a portion of the fall and spring can be associated with biological activity when media temperatures are above the minimum physiological threshold approximately -7°C. Litter decomposition in these soils also ceases at about -7.5°C.

Carbon dioxide concentration profiles across the snowpack, monitored during spring of 1971, show that subnivean CO_2 was continually higher than ambient CO_2 throughout the period 1 May to 9 June. Twice during this period, subnivean concentrations at the ground surface, under the snow, increased rapidly reaching values greater than 800 and 2500 ppm respectively. These concentrations appeared to result from the release of gas pockets contained during fall freeze-up of the active soil layer.

Maximum concentration differentials of atmospheric CO_2 across the snowpack approached 2000 ppm with an average for the 40-day period greater than 150 ppm. Tundra soils of the arctic coastal plain of Alaska are apparently CO_2. Sources throughout the year even when temperatures are too low for significant biological activity. CO_2 from biological sources expressed by freezing the soil solution, evidently leaks to the subnivean environment throughout the winter months. In spring, thermally induced, physical processes may release the contained gases suddenly.

6.3 CO_2 in Tundra Surface Waters

Seasonal changes in the CO_2 partial pressure (PCO_2) regime were measured for an arctic tundra fresh water pond and lake. PCO_2 was measured by infrared gas analysis by determining the CO_2 concentration of air in equilibrium with the water. These arctic waters were generally supersaturated in CO_2 with respect to air throughout the period of open water, and indicate a CO_2 source to the arctic atmosphere. Meltwater standing on the bottomfast ice of the lake in spring and water beneath the newly formed ice in fall, also had CO_2 partial pressure greater than ambient air.

The seasonal mean CO_2 partial pressure gradient between the water and the ambient air was 397 ± 185 ppm for the pond and 115 ± 83 ppm for the lake. PCO_2 was inversely related to wind speed and water temperature, but directly related to sediment temperature. Evasion rate coefficients calculated for the lake based on *in situ* rate experiments, indicated an average transfer of 0.34 ± 0.17 mg CO_2/cm^2-atm-min to the atmosphere.

6.4 CO_2 in Sea Surface Waters

Prior to this study little was known about the distribution of the CO_2 in arctic ocean surface waters. Measurements of PCO_2 with respect to air in the Kara, Barents, and Norwegian Seas, during the late summer, show general undersaturation, with a PCO_2 anomaly (PCO_2-PCO_2) as low as -160 ppm north of Novaya Zemlya, USSR. Positive PCO_2 anomalies (supersaturation) occur in the Kara Sea near the mouth of Ob and Yenisey Rivers. The north Atlantic Ocean during late summer is slightly undersaturated, except for limited areas such as the North Sea, an area south of Nova Scotia, and within the Gulf Stream where conditions of supersaturation are found. Observations across the north Atlantic Ocean from the North Sea to Massachusetts Bay agree closely with the results of K. Buch from a similar track in 1935.

Principal features of the PCO_2 anomalies in the Bering Sea are: an intense undersaturation of -100 ppm in the north central part, a general undersaturation of -60 ppm in the western part; and supersaturation in the eastern part. The principal features of the subarctic Pacific are: a general undersaturation of as much as -45 ppm in the western north Pacific Ocean, near equilibrium in the Gulf of Alaska, and a belt of near saturation water in the west, ranging to supersaturation in the east, between the Pacific Ocean and Bering Sea, along the Aleutian Komondorskie Arc.

6.5 CO_2 in the Seawater Under Ice

The surface waters of the Bering Sea and central Arctic Ocean show that these waters are slightly supersaturated in CO_2 with respect to air. Open water during the winter in the form of leads and polyni, may amount

to as much as 11%, and could be important in the air-sea transfer of CO_2 in the Arctic. If the ice were removed for a significant period of time, as in leads or polyni, then CO_2 could be released from the seawater to the atmospheric reservoir.

6.6 Upwelling

Samalga and Amukta Passes in the eastern Aleutian Islands showed conditions of high positive PCO_2 anomalies indicative of upwelling. Supporting evidence in the upwelled areas show high nutrient content high salinities and low sea surface temperatures and low dissolved oxygen. Based on maximum recorded CO_2 concentrations in excess of 600 ppm the source of the upwelled water was estimated to be from 200 m depth.

6.7 Environmental Effects

It has been shown that carbon dioxide has been steadily rising in the world's atmosphere presumably as a direct result of industrialization over the past century. The observed rise in CO_2 is not to be taken as a calamitous one because CO_2 is a non-toxic gas. In fact, an increase in CO_2 in the atmosphere may be beneficial to the growth of vegetation. What is important is that as a consequence of increasing atmospheric CO_2 concurrent with an efflux of gases and particulate matter from other sources, there may occur alterations in our environment of considerable biological, and economic consequence within the foreseeable future. It seems certain that a continuing rise in the amount of CO_2 in the atmosphere is likely to be accompanied by a significant warming of the surface of the earth. The rate at which this warming might occur is at the present time somewhat speculative because of the complexity of the problem.

The effects of a rising CO_2 content in the atmosphere have been shown to be world-wide. They will be significant not only to us but to future generations. The consumption and many uses of fossil fuels has increased to such proportions that the effect on our atmosphere is cause for the investigation and development of new sources of future power and energy.

This research on the dynamics of carbon dioxide in the atmosphere, oceans and terrestrial components of the arctic regions, which occupy a

small but important area of our planet, are consequential to understanding future changes which may occur there. The role and importance of CO_2 exchange in the biosphere is less well understood than the magnitude and distribution of CO_2 in the atmosphere and the oceans. The marine phytoplankton are postulated to be stable in size and probably affected to a lesser degree than the terrestrial biota to increases in CO_2. Terrestrial plant productivity may be rising with the increase in CO_2 although there are far too few ecological data to support this claim. If true, this could have an effect in reducing the amount of CO_2 by incorporating it in the trunks of trees. This situation may be unlikely because of the increased requirement for wood products. Cultivation of new land would also add to the atmospheric CO_2 inventory. Although the treeless tundra and the taiga regions may be somewhat diminished in importance, since they are highly undeveloped regions, recent attention to development in the tropics may prove to be consequential to atmospheric modification.

Long term consequences as a result of an increase in atmospheric CO_2 and temperatures should be a noticeable warming of the ocean surface accompanied by higher absolute humidity and cloudiness which could have the effect of reducing the amount of the temperature increase. It might be speculated that early stages of a world-wide temperature increase might be accompanied by increases in upland glacier snowfields and retreat of low altitude glaciers.

Though there are numerous effects on the environment that may occur as a consequence of an increase in CO_2, there are also numerous compensating factors in nature. However, any sudden and persistent changes brought about by man may serve to overwhelm the buffering mechanisms that have been operational in the past.

BIBLIOGRAPHY

Akiyama, T. 1968. Partial pressure of carbon dioxide in the atmosphere and in sea water over the western north Pacific Ocean. *The Oceanographical Magazine* 20(2): 133-146.

Akiyama, T. 1969a. Carbon dioxide in the atmosphere and in seawater over the western north Pacific Ocean. *The Oceanographical Magazine* 21(2): 129-135.

Akiyama, T. 1969b. Carbon dioxide in the atmosphere and in seawater in the Pacific Ocean east of Japan. *The Oceanographical Magazine* 21(2): 121-127.

Akiyama, T., T. Sagi and T. Yura. 1968. On the distribution of pH *in situ* and total alkalinity in the western north Pacific Ocean. *The Oceanographical Magazine* 29(1):1-8.

Alvarez-Borrego, S., L. I. Gordon, L. B. Jones, P. K. Park, and R. M. Pytkowicz. 1972. Oxigen-carbon dioxide-nutrients relationships in the southeastern region of the Bering Sea. *J. of the Oceanog. Soc. of Japan* 28(2):71-93.

Arrhenius, S. 1896. On the influence of carbonic acid in the air upon the temperature of the ground. *Phil. Mag.* 41:237-296.

Arrhenius, S. 1903. Lehrbuch der Kosmischen Physik 2. Leipzig, Hirzel.

Arsenev, V. S. 1967. The currents and water masses of the Bering Sea. *Izdatel'stvo Nauka*, Moscow, 135 pp.

Badgley, F. I. 1966. Proceedings of the Sumposium on the Arctic Heat Budget and Atmospheric Circulation, Memorandum RM5233NSF, 267-277.

Bainbridge, A. E. 1971. Atmospheric carbon dioxide variations. *Trans. Am. Geophys. Un.* 52:222.

Bate, G. C., A. D'Aoust and D. T. Canvin. 1969. Calibration of infra-red CO_2 gas analyzers. *Plant Physiol.* 44:1122-1126.

Benson, C. S. 1969. The seasonal snow cover of Arctic Alaska. *Arctic Inst. N. Amer. Res.* Paper 51, 1-47.

Benoit, R. E., W. B. Campbell and R. W. Harris. 1972. Decomposition of organic matter in the wet meadow tundra, Barrow; a revised world model. *In* J. Brown (Coord.), *Proc. 1972 Tundra Biome Symposium*, Tundra Biome Center, University of Alaska, Fairbanks, 111-115.

Billings, W. D., K. M. Peterson, G. R. Shaver and A. W. Trent. 1973. Effect of temperature on root growth and respiration in a tundra ecosystem, Barrow, Alaska. *In* J. K. Marshall (ed.), *The below ground ecosystem: A synthesis of plant-associated processes.* U.S. IBP Synthesis Volume. Grassland Biome, Ft. Collins, Co. In Press.

Bohr, C. 1899. Definition und Method zur Bestimmung der Invasions und Evasions - Coeffizienten bei der Auflösung von Gases in Flussingkeiten. Werthe der genannter Constanten sowie der Absorptioncoefficienten der Kohlensäure bei Auflosung in Wasser und in Chlornaturium-lösungen. *Ann. Physk.* Lpz. 304 (N.F.), 68:500-525.

Bolin, B. and W. Bischof. 1970. Variations of the carbon dioxide content of the atmosphere in the northern hemisphere. *Tellus* 22:431-442.

Bolin, B. and E. Eriksson. 1959. Changes in the carbon dioxide content of the atmosphere and the sea due to fossil fuel combustion. *In* B. Bolin (ed.), *The Atmosphere and the Sea in Motion, Rossby Memorial Volume*, Rockerfeller Institute Press, New York, 130-142.

Bolin, B. and C. D. Keeling. 1963. Large-scale atmospheric mixing as deduced from the seasonal and meridional variations of carbon dioxide. *J. Geophys. Res.* 68(13):3899-3920.

Bray, J. R. 1959. A analysis of the possible recent change in atmospheric carbon dioxide concentrations. *Tellus* 11:220-230.

Britton, M. E. 1967. Vegetation of the arctic tundra. *In* H. P. Hansen (ed.), *Arctic Biology*. Oregon State University Press, Corvallis. 67-130.

Brooks, C. E. P. 1951. Geological and historical aspects of climatic change. *Comp. of Meteor.*, Boston, Mass. 1004-1018.

Brown, C. W. and C. D. Keeling. 1965. The concentration of atmospheric carbon dioxide in Antarctica. *J. Geophys. Res.* 70(24):6077-6085.

Brown, J. and G. West. 1970. The structure and function of cold-dominated ecosystems. U.S. Tundra Biome Rept. 70-1. Tundra Biome Center, Univ. of Alaska, Fairbanks. 148 pp.

Burevich, S. V. and S. W. Liutsarev. 1961. On the CO_2 content of the atmosphere over the Pacific and Indian Oceans, also over the regions of the Black Sea. *Doklady ANSSSR*. 136 pp.

Buch, K. 1934. Beobachtung über chemische factoren in der Nordsee, zwischen Nordsee und Island, sowie auf dem schelfgebiete Nördich von Island. *Conseil. Perm. Intern. p. l'Explorat. de la Mer.* Rapp. et proc. verb. 89:13.

Buch, K. 1939a. Kohlensäure in Atmosphäre und Meer an der Grenze zum Arcticum. *Acta Acad. Aboens. Mat. et Phys.* 11:12.

Buch, K. 1939b. Beobachtunger über dar kohlensaurengleichgewicht und über den kohlensaureaustausch zwischen Atmosphere und Meer im Nördatlandischen Ozean. *Acta. Acad. Aboen. Mat. et Phys.* 11(9): 3-32.

Buch, K. 1951. Das Kohlensäure gleichgewichtssystem im Meerwasser. *Havsforsknigs Institutets Skrift*, Helsingfors. No. 151, 3-18.

Buchen, M. 1971. Ergebnisse der CO_2-Konzentrationmessung in der oceannahen Luftschicht und im Oberflächenwasser wärend der Atlantischen Expedition 1969. *"Meteor" Forsch. Ergbnisse*. B:7, 55-70.

Callendar, G. S. 1938. The artificial production of carbon dioxide and its influence on temperature. *Quart. J. Roy. Met. Soc.* 64: 223-227.

Callendar, G. S. 1940. Variations in the amounts of carbon dioxide in different air currents. *Quart. J. Roy. Met. Soc.* 66:395.

Callendar, G. S. 1949. Can carbon dioxide influence climate? *Weather* 4:310.

Callendar, G. S. 1958. On the amount of carbon dioxide in the atmosphere. *Tellus* 10:243-248.

Chamberlin, T. C. 1897. A group of hypotheses bearing on climatic changes. *J. of Geol.* 5:653-683.

Chamberlin, T. C. 1898. The influence of the great epochs of limestone formation upon the constitution of the atmosphere. *J. of Geol.* 6:609-621.

Chamberlin, T. C. 1899. An attempt to frame a working hypothesis of the cause of glacial periods on an atmospheric basis. *J. of Geol.* 7:545-584.

Cook, F. A. 1955. Near surface soil temperature measurements at Resolute Bay, Northwest Territories. *Arctic* 8:237-249.

Coyne, P. I. and J. J. Kelley. 1971. Release of carbon cioxide from frozen soil to the arctic atmosphere. *Nature* 234(5329):407-408.

Coyne, P. I. and J. J. Kelley. 1973. Variations of carbon dioxide across an arctic snowpack during spring. *J. Geophys. Res.* In Press.

Coyne, P. I. and J. J. Kelley. 1973a. Equilibrium partial pressure of CO_2 in arctic surface waters. *Limnol. and Oceanog.* Submitted for Publication.

Coyne, P. I. and J. J. Kelley. 1973b. CO_2 exchange over the Alaskan arctic tundra: Meteorological assessment by an aerodynamic method. In preparation.

Dugdale, R. C. and J. J. Goering. 1966. Dynamics of nitrogen cycles in the sea. Inst. Mar. Sci. Report R-66-2, Univ. of Alaska, College. 23 pp.

Eriksson, E. 1954. Report on an informal conference in atmospheric chemistry held at the Meteorological Institute, University of Stockholm, May 24-26, 1954. *Tellus* 6:302.

Flanagan, P. W. and A. Scarborough. 1972. Laboratory and field studies on decomposition of plant material in Alaskan tundra areas. *In* J. Brown (ed.), *Tundra Biome Center*, Univ. of Alaska, Fairbanks. 310 pp.

Fonselius, S. and F. Koroleff, 1955. Microdetermination of CO_2 in air, with current data for Scandinavia. *Tellus* 7(2):258-265.

Fonselius, S., F. Koroleff and K-E. Wärme. 1956. Carbon dioxide variations in the atmosphere. *Tellus* 8(2):176-183.

Gleukauf, E. 1951. The composition of atmospheric air. *Comp. of Meteor.* American Meteorological Society, Boston. 3-10.

Gordon, L. I. 1973. A study of carbon dioxide partial pressures in surface waters of the Pacific Ocean. Ph.D. Dissertation. Department of Oceanography, University of Oregon, Corvallis. 216 pp.

Gordon, L. I., P. K. Park, S. W. Hager and T. R. Parsons. 1971. Carbon dioxide partial pressures in northern Pacific waters - time variations. *J. Oceanog. Soc. of Japan* 27(3):81-90.

Gordon, L. I. and L. B. Jones. 1973. The effect of temperature on carbon dioxide partial pressures in seawater. In Press.

Gordon, L. I., P. K. Park, J. J. Kelley and D. W. Hood. 1973. Carbon dioxide partial pressures in North Pacific surface waters, 2. General late summer distribution. *Mar. Chem.* 1:191-198.

Harvey, H. W. 1960. The Chemistry and Fertility of Sea Waters. 2nd ed. Cambridge University Press, London. 240 pp.

Hobbie, J., R. barsdate, V. Alexander, D. Stanley, C. McRoy, R. Stross, D. Bierle, R. Dillon, M. Miller, P. Coyne and J. Kelley. 1972. Carbon Flux Through a Tundra Pond Ecosystem at Barrow, Alaska. U.S. Tundra Biome Report, 72-1. Tundra Biome Center, University of Alaska, Fairbanks. 28 pp.

Hood, D. W. D. Berkshire, I. Supernaw and R. Adams. 1963. Calcium carbonate saturation level of the ocean from latitudes of North America to Antarctica and other chemical oceanographic studies during cruise III of the USNS *Eltanin*. Data Report for the National Science Foundation, Texas A&M University, College Station, Texas.

Hutchinson, G. E. 1954. The biochemistry of the terrestrial atmosphere. *In* G. P. Kuiper (ed.), *The Earth as a Planet*. University of Chicago Press, Chicago. 371-433.

Ibert, E. W. 1963. An investigation of carbon dioxide between the atmosphere and the sea. Ph.D. Dissertation, Texas A&M University, College Station, Texas. 131 pp.

Ibert, E. R. and D. W. Hood. 1963. The distribution of carbon dioxide between the atmosphere and the sea. Tech. Rept. 63, Texas A&M University, College Station, Texas. 131 pp.

Johnson, P. L. and J. J. Kelley. 1970. Dynamics of carbon dioxide and productivity in an arctic biosphere. *Ecology* 51(1):73-80.

Junge, C. and G. Czeplak. 1968. Some aspects of the seasonal variation of carbon dioxide and ozone. *Tellus* 20:422-424.

Kanwisher, J. 1960. pCO_2 in sea water and its effects on the movement of CO_2 in nature. *Tellus* 12(2):209-215.

Kanwisher, J. 1963. On the exchange of gases between the atmosphere and the sea. *Deep-Sea Res.* 10:195-207.

Kaplan, L. D. 1960. The influence of carbon dioxide variations on the atmospheric heat balance. *Tellus* 12:204-208.

Keeling, C. D. 1958. The concentration and isotopic abundances of atmospheric carbon dioxide in rural areas. *Geochim. et Cosmochim. Acta* 13:322-334.

Keeling, C. D. 1960. The concentration and isotopic abundance of carbon dioxide in the atmosphere. *Tellus* 7(2):200-203.

Keeling, C. D. 1968. Carbon dioxide in surface ocean waters, 4. Global distribution. *J. Geophys. Res.* 73(14):4543-4553.

Keeling, C. D. and J. C. Pales. 1965. Mauna Loa carbon dioxide, Report 3. Scripps Institution of Oceanography, La Jolla, California. 180 pp.

Kelling, C. D., N. W. Rakestraw and L. S. Waterman. 1965. Carbon dioxide in surface waters of the Pacific Ocean, 1. Measurement of the distribution. *J. Geophys. Res.* 70:6087-6097.

Keeling, C. D. and L. S. Waterman. 1968. Carbon dioxide in surface ocean waters, 3. Measurements on LUSIAD expedition, 1962-1963. *J. Geophys. Res.* 73:4529-4541.

Keeling, C. D., T. B. Harris and E. M. Eilkins. 1968. Concentration of atmospheric carbon dioxide at 500 and 700 millibars. *J. Geophys. Res.* 73(14):4511-4541.

Keeling, C. D., R. B. Bacastour, A. E. Bainbrifge, C. A. Ekdahl, Jr., P. R. Guenther, J. S. Chim and L. S. Waterman. 1976. Atmospheric carbon dioxide variations at Mauna Loa Observatory, Hawaii. *Tellus* 28:538-551.

Keeling, C. D., J. A. Adams, Jr., C. A. Ekdahl and P. R. Guenther. 1976. Atmospheric carbon dioxide variations at the South Pole. *Tellus* 28: 552-564.

Kelley, J. J. 1968. Carbon dioxide and ozone studies in the arctic atmosphere. *In* J. E. Sater (coord.), *Arctic Drifting Stations* (156-165). Arctic Institute of North America, Washington, D.C. 475 pp.

Kelley, J. J. 1968a. Carbon dioxide in the seawater under the arctic ice. *Nature* 318(5144):1-5.

Kelley, J. J. 1969. An analysis of carbon dioxide in the arctic atmosphere near Barrow, Alaska - 1961 to 1967. Scientific Report 3. Department of Atmospheric Sciences, University of Washington, Seattle. 172 pp.

Kelley, J. J. 1969a. Observations of carbon dioxide in the atmosphere over the western United States. *J. Geophys. Res.* 74(6):1688-1693.

Kelley, J. J. 1969b. Investigations of atmospheric trace gases and particulate matter on Mount Olympus, Washington. *J. Geophys. Res.* 74(2):435-443.

Kelley, J. J. 1970. Carbon dioxide in the surface waters of the North Atlantic ocean and the Barents and Kara seas. *Limnol. and Oceanog.* 15(1):80-87.

Kelley, J. J. 1973. Baseline observations of atmospheric trace gases in the arctic atmosphere of North America. Proc. of the TECOMAP Conference. Sponsored by the U.N.-WMO/WHO, Helsinki, Finland, August 1973. In Press.

Kelley, J. J. 1973a. Surface ozone in the arctic atmosphere. *Pure and Applied Geophys.* In Press.

Kelley, J. J. and D. F. Weaver. 1966. Carbon dioxide and ozone in the arctic atmosphere. Proc. of the 16th Alaskan Science Conf. College, Alaska. 151-167.

Kelley, J. J., D. F. Weaver and B. P. Smith. 1968. The variations of carbon dioxide under the snow in the arctic. *Ecology* 49(2):358-361.

Kelley, J. J. and D. F. Weaver. 1969. Physical processes at the surface of the arctic tundra. *Arctic* 22(4):425-437.

Kelley, J. J. and D. W. Hood. 1971. Carbon dioxide in the Pacific Ocean and Bering Sea: Upwelling and mixing. *J. Geophys. Res.* 76(3):745-752.

Kelley, J. J. and D. W. Hood. 1971a. Carbon dioxide in the surface water of the ice covered Bering Sea. *Nature* 229(5279):37-39.

Kelley, J. J., L. L. Longerich and D. W. Hood. 1971. Effect of upwelling, mixing, and high primary productivity on CO_2 concentrations in the surface waters of the Bering Sea. *J. Geophys. Res.* 76(36):8687-8693.

Kelley, J. J. and P. I. Coyne. 1973. A case for comparison and standardization of carbon dioxide reference gases. *In: Terrestrial Primary Production*, Proc. of the Interbiome Workshop on Gaseous Exchange Methodology, Oak Ridge National Laboratory, April 13-14, 1972. 163-181.

Kelley, J. J., D. W. Hood, L. L. Longerich and J. Groves. 1973. Oceanography of the Bering Sea. Phase 2. Turbulent upwelling and water mass identification in the vicinity of Samalga Pass, Eastern Aleutian Islands. Vol. 2, Part 1. Final Report to the National Science Foundation, Inst. Mar. Sci., Univ. of Alaska. 118 pp.

Kelley, J. J., D. W. Hood, J. J. Goering, R. Barsdate, M. Nebert, L. L. Longerich, J. Groves and C. Patton. 1973a. Oceanography of the Bering Sea. Phase 2. Turbulent upwelling and water mass identification in the vicinity of Samalga Pass, Eastern Aleutian Islands. Vol. 2, Part 2. Final Report to the National Science Foundation, Inst. Mar. Sci., Univ. of Alaska. 263 pp.

Krogh, A. 1904. On the tension of carbonic acid in natural waters and especially in the sea. *Medd. Groenland.* 26:231-342.

Krogh, A. and P. Brandt-Rehbert. 1929. CO_2-Bestimmungen in der atmosphärischen luft durch mikrotitration. *Biochemische Zeitschr.* 205:205-265.

Li, Y. H., T. T. Takahashi and W. S. Broeker. 1969. Degree of saturation of $CaCO_3$ in the oceans. *J. Geophys. Res.* 74(23):5507-5525.

Liutsarev, S. V. and S. V. Bruevich. 1964. Carbon dioxide content of the atmosphere above the Pacific and Indian Oceans and above the northern regions of the Black Sea. *Trudy Institut Okeanologii. AN SSSR* 67:7-40.

Lyman, J. 1956. Buffer mechanism of sea water. Doctoral dissertation. La Jolla, University of California, Los Angeles. 196 pp.

Manabe, S. and R. F. Strickler. 1964. Thermal equilibrium of the atmosphere with convective adjustment. *J. Atm. Sci.* 21:361-385.

Manabe, S. and R. T. Wetherald. 1967. Thermal equlibrium of the atmosphere with a given distribution of relative humidity. *J. Atm. Sci.* 24:241-259.

Maykut, G. A. and P. E. Church. 1973. Radiation climate of Barrow, Alaska. *J. Appl. Meteo.* 12(4):620-628.

McCarthy, G. R. 1952. Geothermal investigations on the arctic north slope. *Trans. Amer. Geophys. Un.* 33:589-593.

McRoy, C. P. 1968. The distribution and biogeography of *Zostera marina* (eelgrass) in Alaska. *Pacific Sci.* 22:507-513.

Miyake, Y. and Y. Sugimura. 1969. Carbon dioxide in the surface water and the atmosphere in the Pacific Ocean, the Indian Ocean and the Antarctic Ocean areas. *Records of Oceanographic Works in Japan* 10(1): 23-28.

Monteith, J. L. 1973. *Principles of Environmental Physics*. Edward Arnold (Publ.), Ltd. London. 241 pp.

Möller, F. 1963. On the influence of changes in the CO_2 concentration in air on the radiation balance of the earth's surface and on the climate. *J. Geophys. Res.* 68(13):3877-3885.

Muller, S. W. 1947. *Permafrost, or permanently frozen ground and related engineering problems.* Edwards Bros. (Publ.), Ann Arbor, Mich. 231 pp.

Murie, O. J. 1959. Fauna of the Aleutian Islands and Alaska Peninsula. *U.S. Fish and Wildlife Publication 61.* 405 pp.

Namias, J. 1970. Macroscale variations in sea-surface temperatures in the North Pacific. *J. Geophys. Res.* 73(3):565-582.

Nansen, R. 1915. Spitzbergen waters. Oceanographic observations during the cruise of the *Veslemoy* to Spitzbergen in 1912. Norsk Videnskaps-Academi, Oslo, *Naturvidenskapelig Klasse*, Skirifter, No. 2.

N.B.S. Special Publication 260. 1970. Catalog of Standard Reference Materials, U.S. Department of Commerce, National Bureau of Standards, Washington, D.C. 77 pp.

Pales, J. C. and C. D. Keeling. 1965. The concentration of atmospheric carbon dioxide in Hawaii. *J. Geophys. Res.* 70(24):6053-6076.

Park, P. K., L. I. Gordon, S. W. Hager and M. C. Cissell. 1969. Carbon dioxide partial pressure in the Columbia river. *Science* 166(3907): 867-868.

Pitelka, F. A. 1972. Cyclic pattern in lemming populations near Barrow, Alaska. *In: Proc. 1972 Tundra Biome Symposium*, J. Brown (coord.), Tundra Biome Center, University of Alaska, Fairbanks. 132-135.

Plass, G. N. 1956. The carbon dioxide theory of climatic change. *Tellus* 8(2):140-153.

Rasool, S. I. and S. H. Schneider. 1971. Atmospheric carbon dioxide and aerosols: effects of large increases on global climate. *Science* 173:138-141.

Revelle, R. and H. E. Suess. 1957. Carbon dioxide exchange between atmosphere and ocean and the question of an increase of atmospheric CO_2 during the past decades. *Tellus* 9:18-27.

Riley, J. P. and G. Skirrow. 1965. *Chemical Oceanography*. Vol. 1. Academic Press, New York. 712 pp.

Rodin, L. E. and N. I. Basilević. 1968. World distribution of plant biomass. *In* F. E. Eckhardt (ed.), *Functioning of Terrestrial Ecosystems. Proc. of the Copenhagen Symp., July 24-30, 1965.* UNESCO, Paris. 45-51.

Rudolf, W. 1971. Eine Methode zur kontinwierlichen Analyse des CO_2-Partialdrukes im Meerwasser. *"Meteor" Forsch.-Ergebnisse* B(6): 12-36.

SCEP Report. 1970. Man's Impact on the Global Environment. Assessment and Recommendations for Action. Report of the Study of Critical Environmental Problems. The MIT Press, Cambridge, Mass. 319 pp.

Schloesing, Th. 1872. Sur la dissolution du carbonate de chaux dans l'acide carbonique. *C. R. Acad. Sci.* 74-1552.

Schloesing, Th. 1880. Sur la constance de la proportion de l'acide carbonique dans l'air. *C. R. Acad. Sci.* 90:1.

Skujins, J. J. 1907. Enzymes in soil. *In* A. D. McLaren and G. H. Peterson (eds.), *Soil Biochemistry*, Marcel Dekker, Inc. 371-414.

Slocum, G. 1955. Has the amount of carbon dioxide in the atmosphere changed significantly since the beginning of the twentieth century. *Monthly Weather Rev.* 83:225-231.

Smith, V. N. 1953. A recording infrared analyzer. *Instruments* 26: 421-427.

Stepanova, N. A. 1952. A selective annotated bibliography on carbon dioxide in the atmosphere. *Meteor. Ads. Bibl.* 3:137-170.

Sterns, S. R. 1966. Permafrost (Perennially Frozen Ground). U.S. Army Cold Regions Research and Engineering Laboratory. *Cold Regions Science and Engineering. Part 1. Section A2.* 84 pp.

Sugimura, Y. and Y. Hirao. 1970. Carbon dioxide in the atmosphere and in surface sea water. *In* Y. Horibe (ed.), *Preliminary Report of the Hakuho Maru Cruise KH-68-4 (Southern Cross Cruise)*, Tokyo, Ocean Research Institute, University of Tokyo, Japan. 67-80.

Sugiura, Y., E. R. Ibert and D. W. Hood. 1963. Mass transfer of carbon dioxide across sea surfaces. *J. Mar. Res.* 21(1):11-21.

Takahashi, T. 1961. Carbon dioxide in the atmosphere and in Atlantic Ocean water. *J. Geophys. Res.* 66:477-494.

Takahashi, T., R. F. Weiss, C. H. Culberson, J. M. Edmond, D. E. Hammond, C. S. Wong, Y. Li and A. E. Bainbridge. 1970. A carbonate chemistry at the 1969 GEOSECS intercalibration station in the eastern Pacific Ocean. *J. Geophys. Res.* 75(36):7648-7666.

Teal, J. M. and J. Kanwisher. 1966. The use of pCO_2 for the calculation of biological production with examples from waters off Massachusetts. *J. Mar. Res.* 24:4-14.

Tyndall, J. 1861. On the absorption and radiation of gases and vapours, and on the physical connection of radiation, absorption, and conduction. *Phil. Mag.* 22(ser. 4):169-194.

Wattenberg, H. 1933. Kalzium karbonal und Kohlensäuregehald des Meerwassers, *Wissenschaftliche Ergebnisse der Deutschen Atlantischen Expedition*, 1925-1927, Vol. 8, Walter de Gryter, Berlin. 233-331.

Weller, G. and C. S. Benson. 1971. The micro- and regional climates of the Alaskan arctic tundra. *In* J. Brown (ed.), *The Structure and Function of the Tundra Ecosystem*, Vol. 1. Tundra Biome Center, Univ. of Alaska. 181-193.

Weller, G., S. Cubley, S. Parker, D. Trabant and C. S. Benson. 1972. The tundra microclimate during snow-melt at Barrow, Alaska. *Arctic* 25(4):291-300.

Whitman, W. I. and J. J. Schule, Jr. 1966. Proceedings of the Arctic heat Budget and atmospheric circulation. Memorandum RM5233NSF, The Rand Corporation, California. 217.

Wiggins, I. L. 1951. The distribution of vascular plants near Point Barrow, Alaska. *Contrib. Dudley Herbarium.* Natural History Museum of Stanford University, California. 56 pp.

Yen, Y-C. 1965. Effective thermal conductivity and water vapor diffusivity of natural compacted snow. *J. Geophys. Res.* 70(8):1821-1825.

Zenkevitch, L. 1963. *Biology of the Seas of the U.S.S.R.* Interscience, New York. 955 pp.